NREL
NATIONAL RENEWABLE ENERGY LABORATORY





"Quantifying Optical Loss of High-Voltage Degradation Modes in PV Modules Using Spectral Analysis"

David C. Miller, Katherine Hurst, Archana Sinha, Joanna Bomber, Jiadong Qian, Stephanie L. Moffitt, Soňa Uličná, Laura T. Schelhas, Peter Hacke

Presentation Format/Supplementary Information

Motivation and Method for Optical Transfer Function Analysis

Goals:

(1) accurate quantification to estimate absolute UV dose in weathering for UVID;

(2) F/A of aged positive voltage ionization specimens for qualitative degradation mode diagnosis;

(3) compare Δoptical performance packaging components to Δmodule performance (quantitative) for positive voltage ionization.

-What is the extent of optical and electrical damage?

-Can we identify degradation modes we didn't previously know about?

-Can method be used for field diagnosis (UV blocking vs. transmitting EVA)?

For (1):

$$F_t[\lambda] = \prod_{i=1}^{n}\left(1-\frac{\rho_{2i}}{100}\right)\left(1-\frac{\alpha_{2i+1}}{100}\right)\Bigg|_{\lambda} \qquad E_{cell} = E_{AM1.5G}[\lambda]F_t[\lambda]$$

Also, for (2) & (3):

$$F_r[\lambda] = \sum_{i=0}^{m}\prod_{j=0}^{i-1}\left(1-\frac{\rho_{2j}}{100}\right)^2\left(1-\frac{\alpha_{2j+1}}{100}\right)^2\left(\frac{\rho_{2i}}{100}\right)\Bigg|_{\lambda} \qquad J = q\int \frac{\lambda}{hc}E_{AM1.5G}[\lambda]Q_{ext}[\lambda]F_t[\lambda]d\lambda$$

For all: Considering initial pass of incident light (no subsequent optical events)

Optics: The Behavior and Measurement of Interfaces & Materials

- The *enabling optical modes* are reflectance (ρ) at interfaces and absorptance (α) in the bulk .

- We can *measure* the *modes* of transmittance (τ) and ρ.

- 100 {%} = $\rho + \alpha + \tau$.

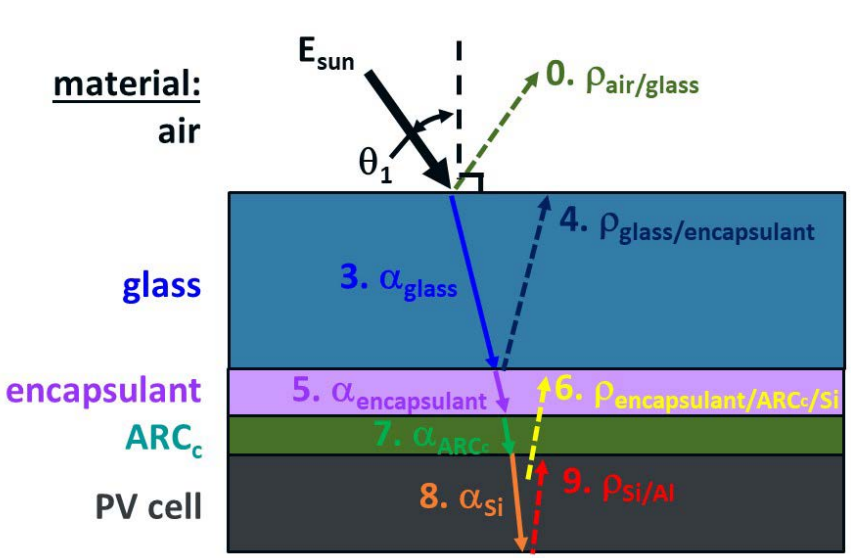

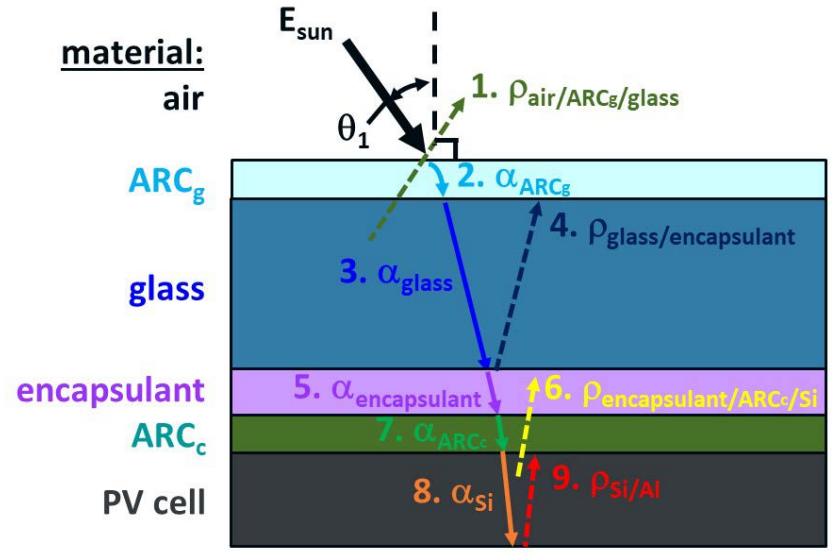

Cross-sectional schematic and taxonomy for PV *mini-module (left) and module (right)* in normal operation.

Optical Transfer Function Analysis For "Bulk" Materials

Method:

Apply method from analysis of CPV optical components to FP-PV.

Miller et. al., Opt. Eng., 50 (1), 2011, 013003. (DOI: 10.1117/1.3530092).

Glass:

(1) τ_h (measured); *n* (literature); ρ_h (estimated) $\rightarrow$ k (estimated)

(2) τ_h, ρ_h (measured); *n, k* (literature, estimated) $\rightarrow$ *n, k* (analysis$_1$)

Encapsulant

(3) τ_h (measured coupon); τ_h (glass) $\rightarrow$ τ_h, *k* (encapsulant only)

Glass:

(4) τ_h (measured); *n* (analysis$_1$); ρ_h (estimated) $\rightarrow$ k (analysis$_2$)

(5) τ_h, ρ_h (measured); *n, k* (analysis$_1$, analysis$_2$) $\rightarrow$ *n, k* (analysis$_3$)

(6) τ_h (measured); *n* (analysis$_3$); ρ_h (estimated) $\rightarrow$ k (analysis$_4$)

(7) τ_h, ρ_h (measured); *n, k* (analysis$_3$, analysis$_4$) $\rightarrow$ *n, k* (analysis$_5$)

The Bulk/Thin Film/Bulk Model For Reflectance

- A special situation occurs where AR layers (destructive interference), may be modeled using a bulk/thin film/bulk representation.

- No line-,surface-, or volume-integrals, just mathematical operations of complex numbers!
- The thin film may consist of multiple layers of material (Si_xN_y, Si_xO_y, black Si, …) of different thickness and/or refractive index.
- Model can account for non-perpendicular angle of initial incidence.
- Polarization inherent to reflection, treated with averaging (for now).

- The thin film may also have an absorptance (model using Beer's law).

bulk: air or encapsulant | **thin film: AR_g or AR_c** | **bulk: glass or Si**

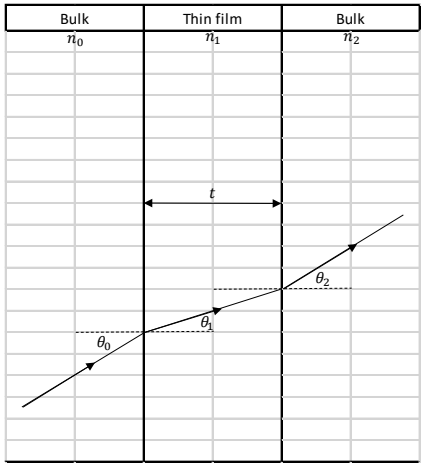

- Single-layer ARC under normal incidence:

$$R = \frac{(n_0 - n_s)^2 + \left(\frac{n_0 n_s}{n_1} - n_1\right)^2 \tan^2(\delta)}{(n_0 + n_s)^2 + \left(\frac{n_0 n_s}{n_1} + n_1\right)^2 \tan^2(\delta)}$$

$$\delta = \frac{2\pi}{\lambda} n_1 t \cos\theta_1$$

- Single-layer ARC under non-normal incidence; TE polarization:

$$R = \frac{[n_0\cos(\theta_0) - n_s\cos(\theta_s)]^2 + \left[\frac{n_0 n_s}{n_1}\cdot\frac{\cos(\theta_0)\cos(\theta_s)}{\cos(\theta_1)} - n_1\cos(\theta_1)\right]^2 \tan^2(\delta)}{[n_0\cos(\theta_0) + n_s\cos(\theta_s)]^2 + \left[\frac{n_0 n_s}{n_1}\cdot\frac{\cos(\theta_0)\cos(\theta_s)}{\cos(\theta_1)} + n_1\cos(\theta_1)\right]^2 \tan^2(\delta)}$$

- Single-layer ARC under non-normal incidence; TM polarization:

$$R = \frac{[n_0\cos(\theta_0) - n_s\cos(\theta_s)]^2 + \left[\frac{n_0 n_s}{n_1}\cdot\cos(\theta_0)\cos(\theta_1)\cos(\theta_s) - \frac{n_1}{\cos(\theta_1)}\right]^2 \tan^2(\delta)}{[n_0\cos(\theta_0) + n_s\cos(\theta_s)]^2 + \left[\frac{n_0 n_s}{n_1}\cdot\cos(\theta_0)\cos(\theta_1)\cos(\theta_s) + \frac{n_1}{\cos(\theta_1)}\right]^2 \tan^2(\delta)}$$

From S. Al-Turk, "Analytic Optimization Modeling of Antireflection Coatings for Solar Cells", MS Thesis, McMaster Univ., 2011.

What is the Optical Effect of the Interfaces & Materials in a PV MiMo? (1: Keeping It Real, Keeping It Old School)

- 4% reflectance at air/glass ⇒ use AR coating.
- Reflectance at glass/encapsulant interface is **minimal**!
- UV absorbing and transmitting encapsulants distinguished below 400 nm. (for $\lambda > 400$ nm: different products shown).
- 3% reflectance at encapsulant/Si_xN_y (shown for bulk) ⇒ use thin film (destructive interference) Si_xN_y coating.

- 2% reflectance loss air/water (or air/ice).
- 3% reflectance at air/encapsulant ⇒ notable loss possible for delamination from glass
- Si highly reflective in air (delamination) ⇒ use AR coating (hopefully AR_c does not corrode).
- 12% reflectance at air/Si_xN_y (result shown for bulk) ⇒ large loss possible for delamination

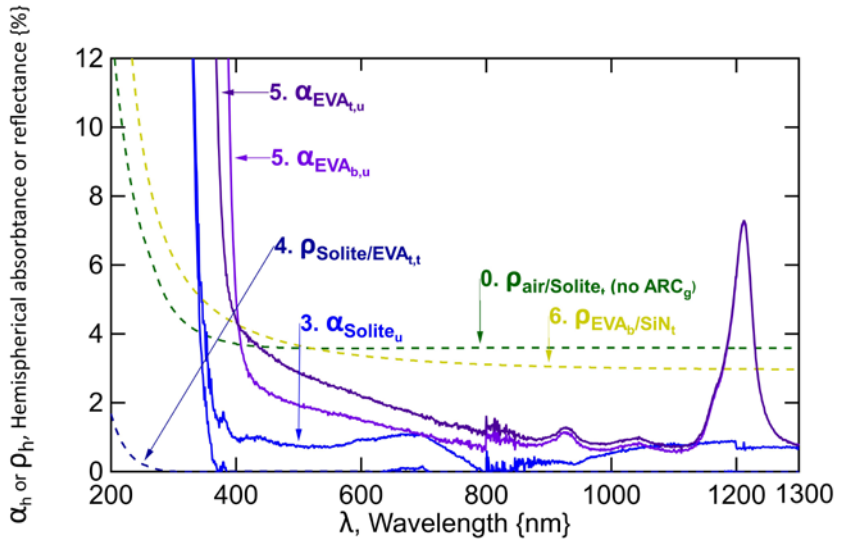

Results for (top) representative unaged and affected (bottom)PV packaging and common research components (real refractive index only).

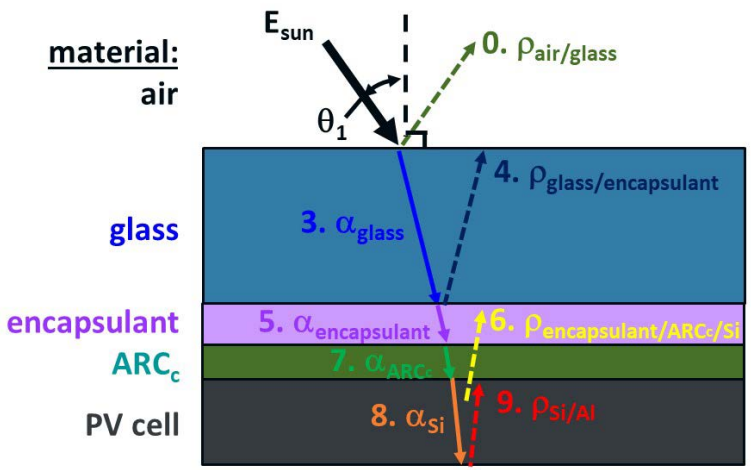

$$\alpha_i = -measured-$$

$$\rho_i = \frac{(n_1 - n_2)^2}{(n_1 + n_2)^2}$$

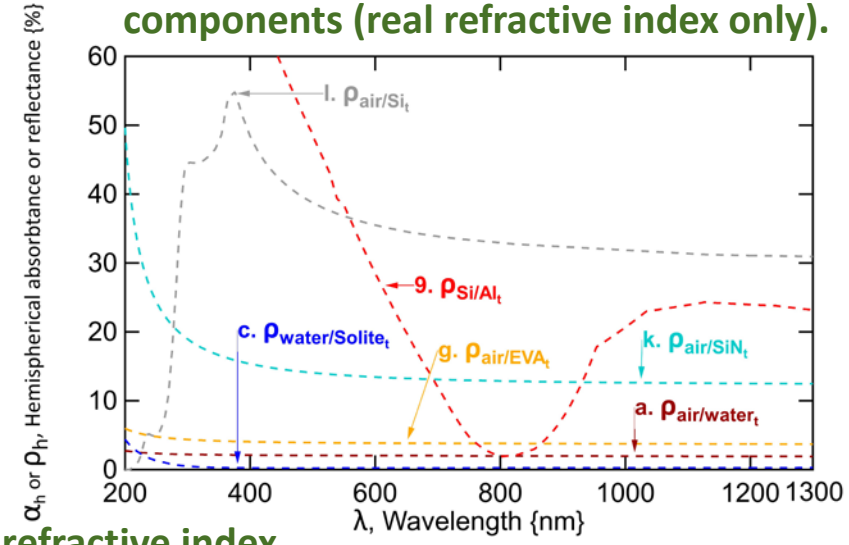

Comparison of interfaces and bulk materials for –real only- refractive index.

What is the Optical Effect of the Interfaces & Materials in a PV MiMo? (2: Including Complex)

- Absorptance of glass is less than encapsulant (EVA here).
- Goal: keep F_t high, F_r low, so EQE is high.

$$\rho_i = \frac{(n_1 - n_2)^2 + \hat{\imath}(k_1 - k_2)^2}{(n_1 + n_2)^2 + \hat{\imath}(k_1 + k_2)^2}$$

$$\alpha_i = 1 - e^{-h_i A_i}$$

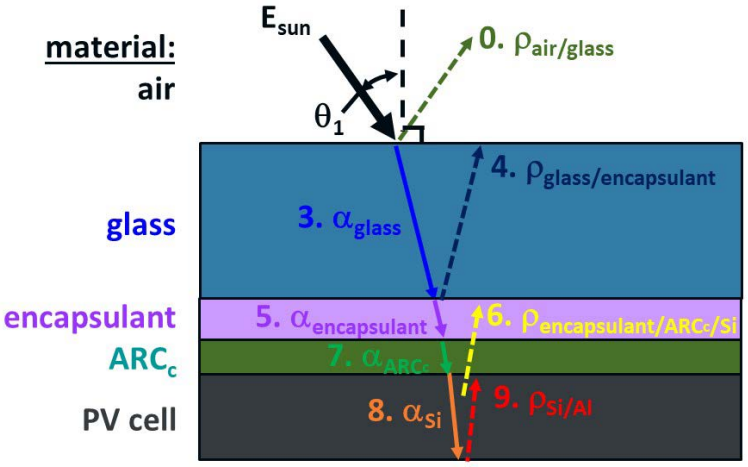

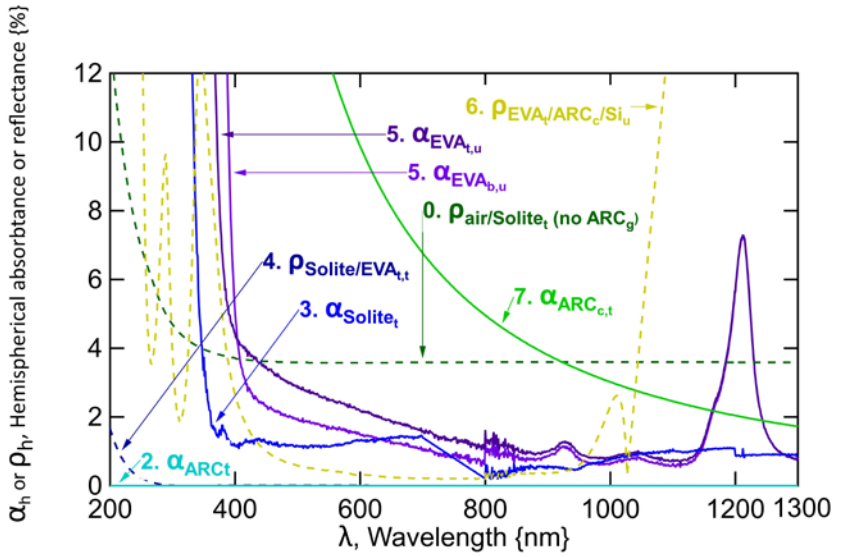

Results for (top) representative unaged and affected (bottom)PV packaging and common research components (complex refractive index).

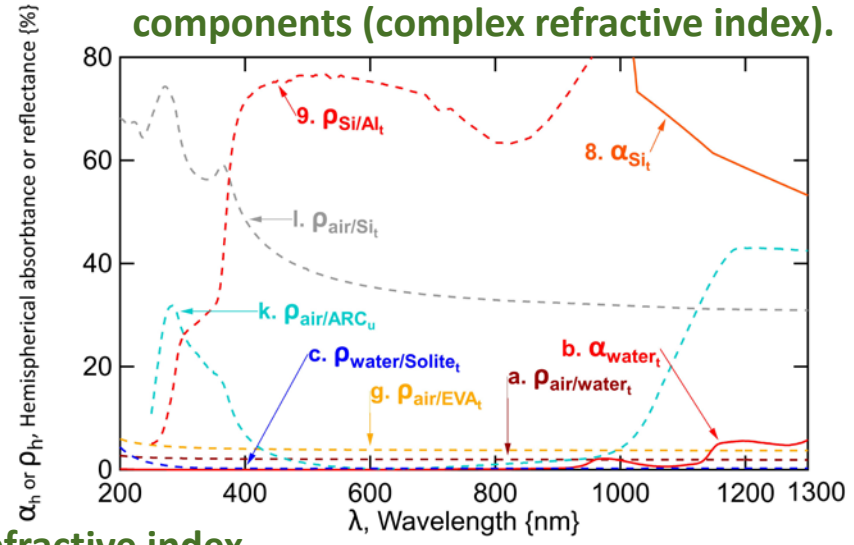

Comparison of interfaces and bulk materials for complex refractive index.

What is the Optical Effect of the Interfaces & Materials in a PV Module? (2: Including Complex)

- PS AR_g coatings presently popular, benefit VIS & NIR.
- Absorptance of glass is less than encapsulant (EVA here).
- Goal: keep F_t high, F_r low, so EQE is high.

$$\rho_i = \frac{(n_1 - n_2)^2 + \hat{\imath}(k_1 - k_2)^2}{(n_1 + n_2)^2 + \hat{\imath}(k_1 + k_2)^2}$$

$$\alpha_i = 1 - e^{-h_i A_i}$$

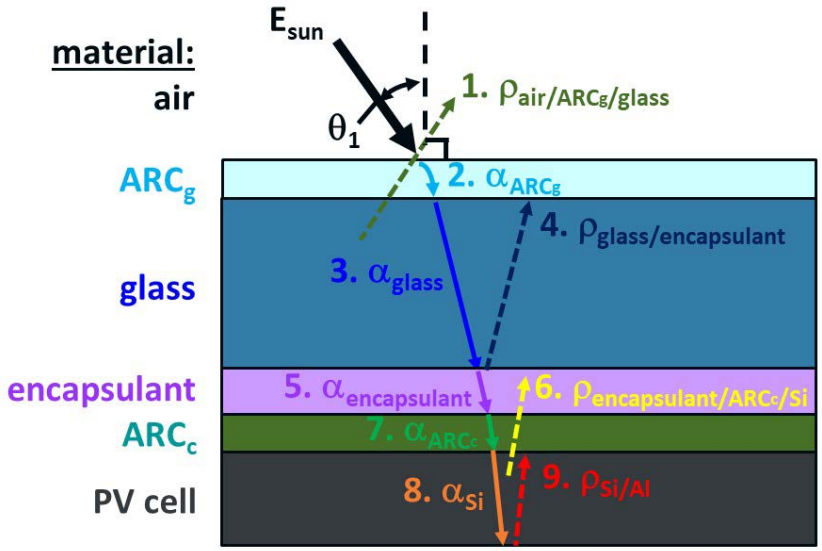

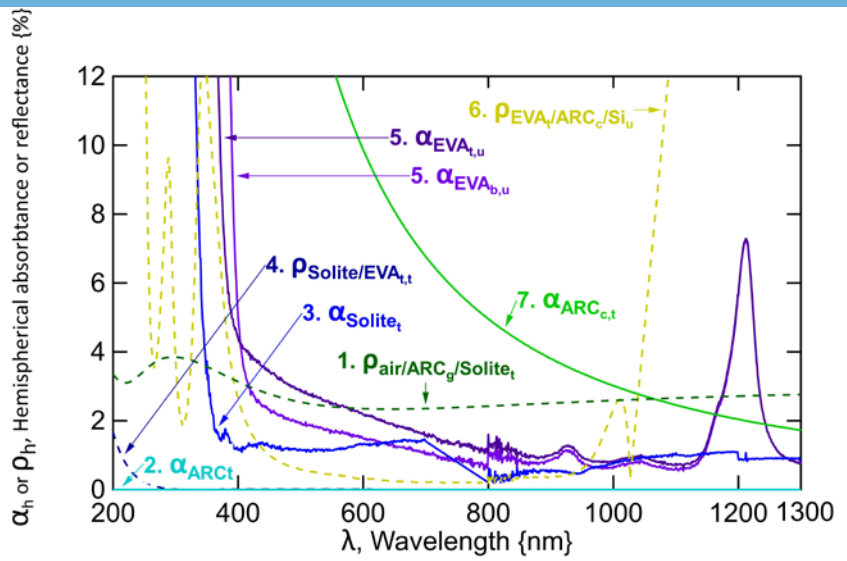

Results for (top) representative unaged and affected (bottom)PV packaging and common research components (complex refractive index).

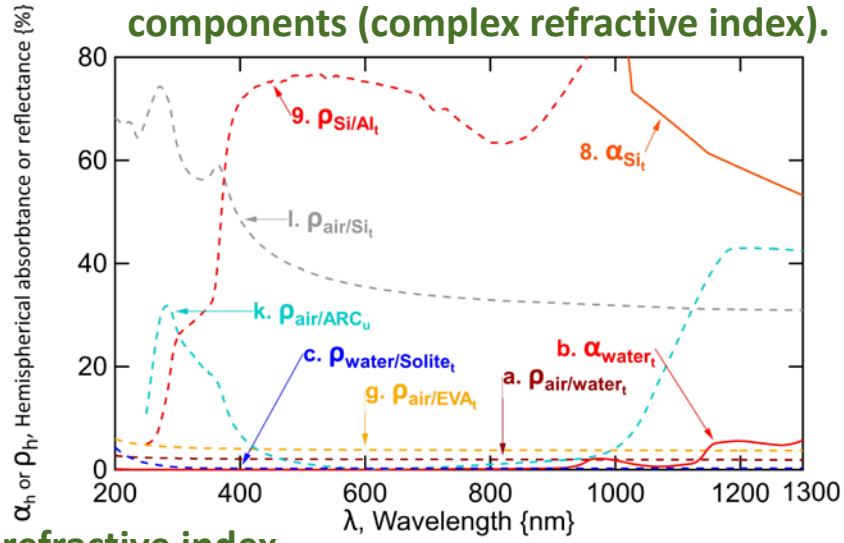

Comparison of interfaces and bulk materials for –real only- refractive index.

Comparing the Real Refractive Index

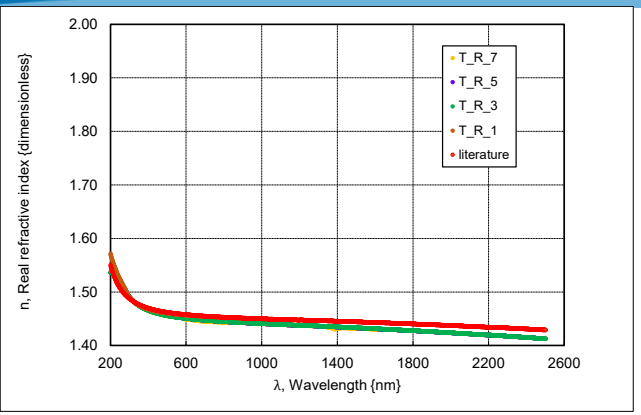

Silica

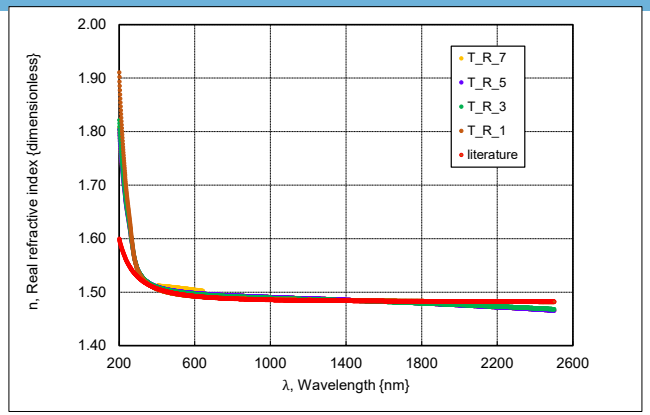

SG7.1

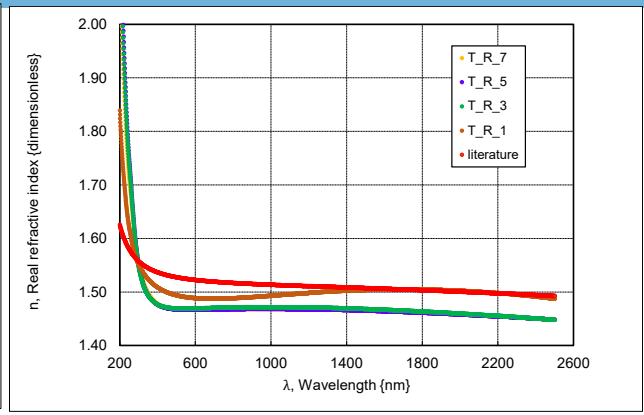

Solite

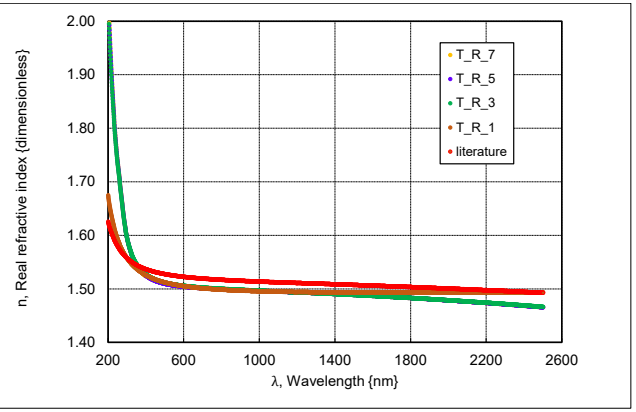

Diamant

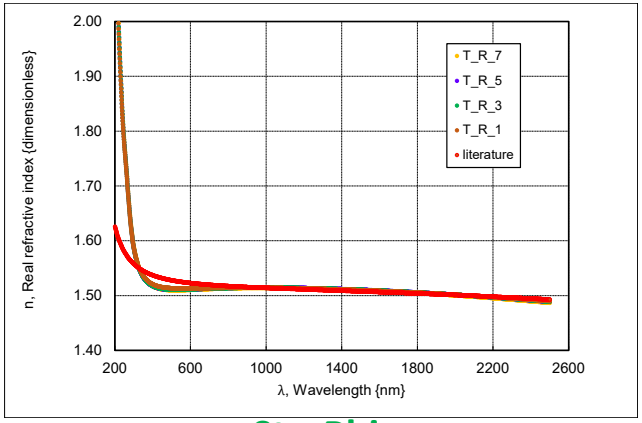

StarPhire

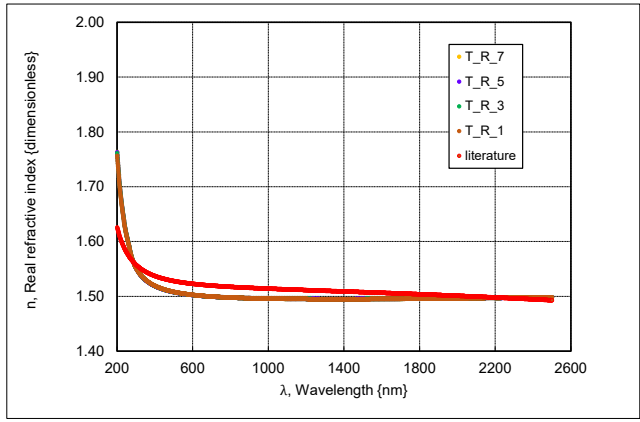

Avalanche

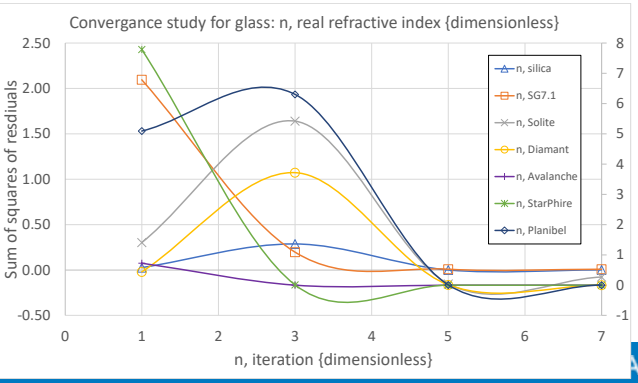

- Solite, Diamant snap to a solution after step (2).
- SG7.1 rebounds similar manufacturer's data.

Comparing the Imaginary Refractive Index

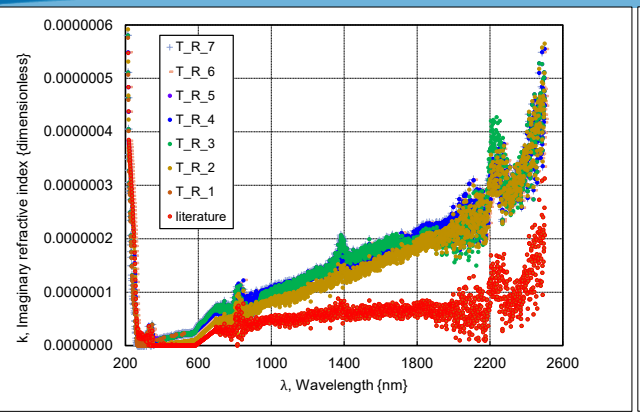

Silica

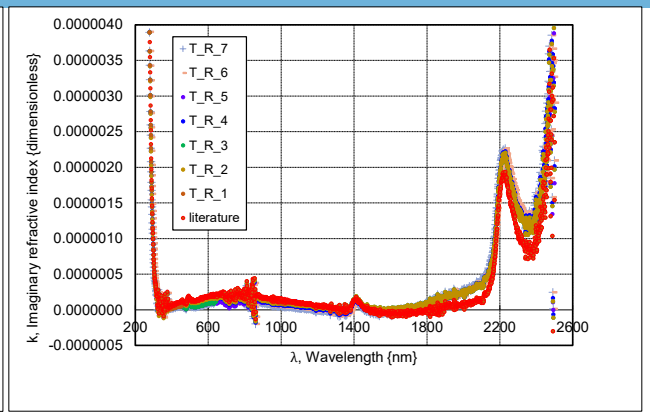

SG7.1

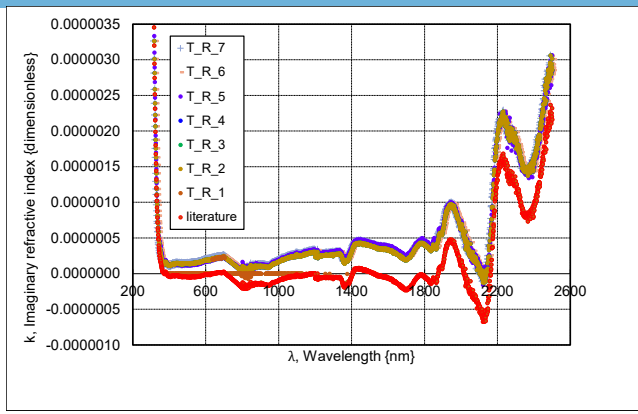

Solite

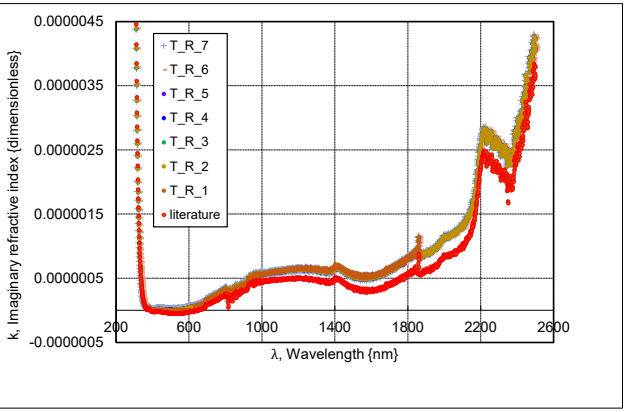

Diamant

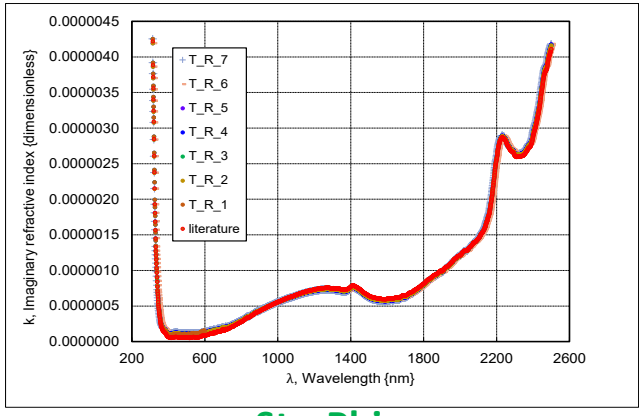

StarPhire

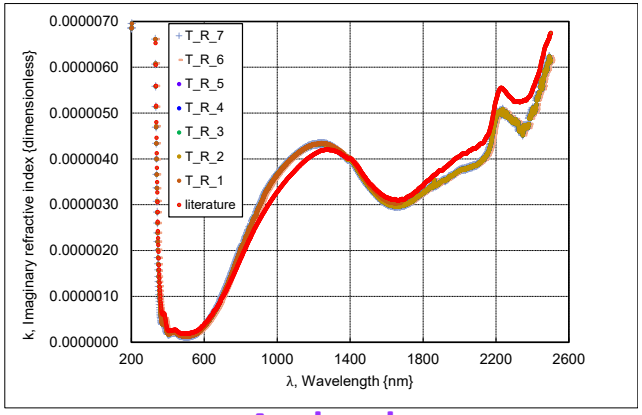

Avalanche

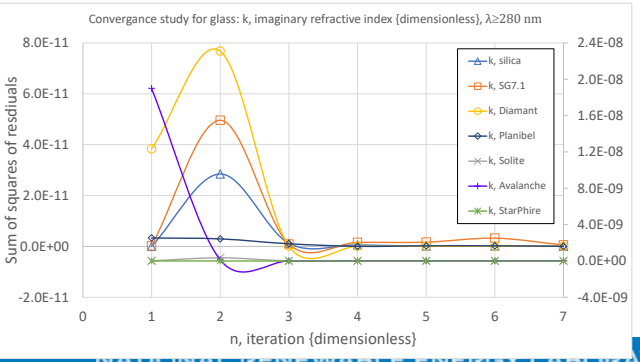

- Initial estimate:
  (a) limited (all materials).
  (b) negative values observed (SG7.1, Solite).

Comparing the Absorption Coefficient

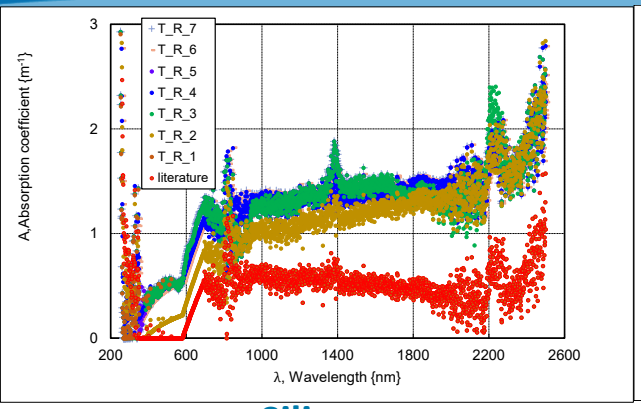

Silica

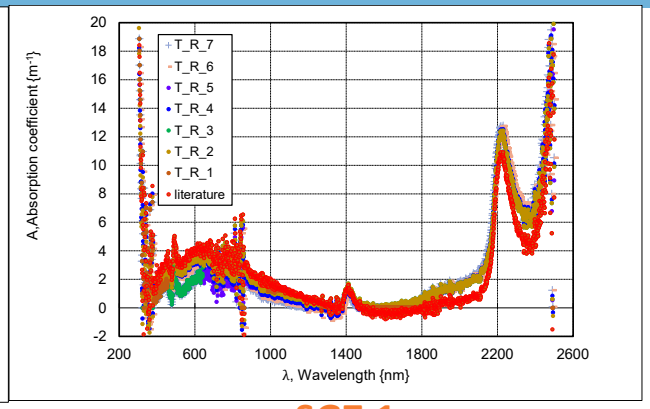

SG7.1

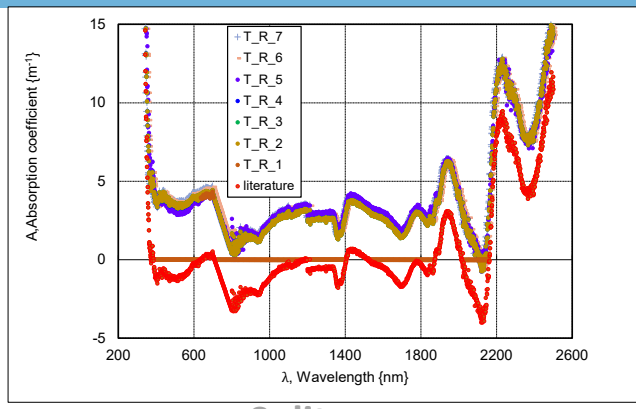

Solite

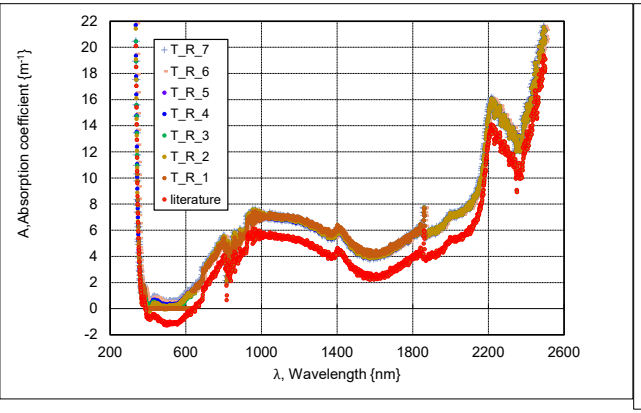

Diamant

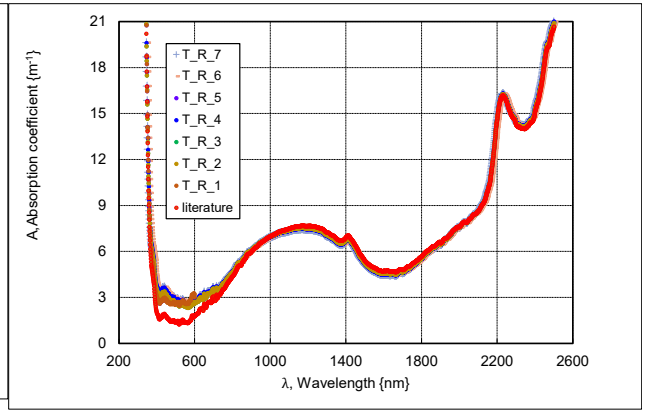

StarPhire

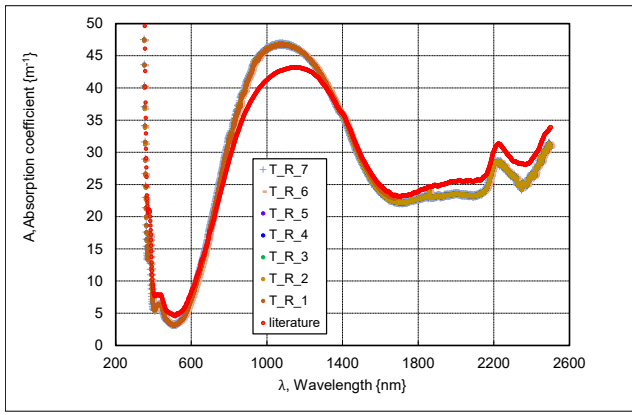

Avalanche

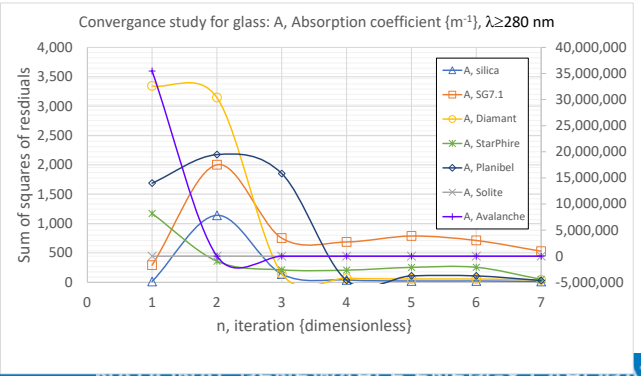

$$A = \frac{4\pi k}{\lambda}$$

- Initial estimate:

(a) limited (all materials).

(b) negative values observed (SG7.1, Solite).

Improvement of (Real) Refractive Index

- Minor improvement observed for real refractive index of silica.
(high quality glass should not vary greatly between products and manufacturers).

- Modest improvement of index observed for other (e.g., textured) glass.
-3rd or 4th significant figure can affect interfacial ρ or bulk α.
-estimate for bulk α notably improved for Solite.
-Refractive index may vary with density of glass.
-low-iron glass may even subtly vary in composition between fabrication batches.

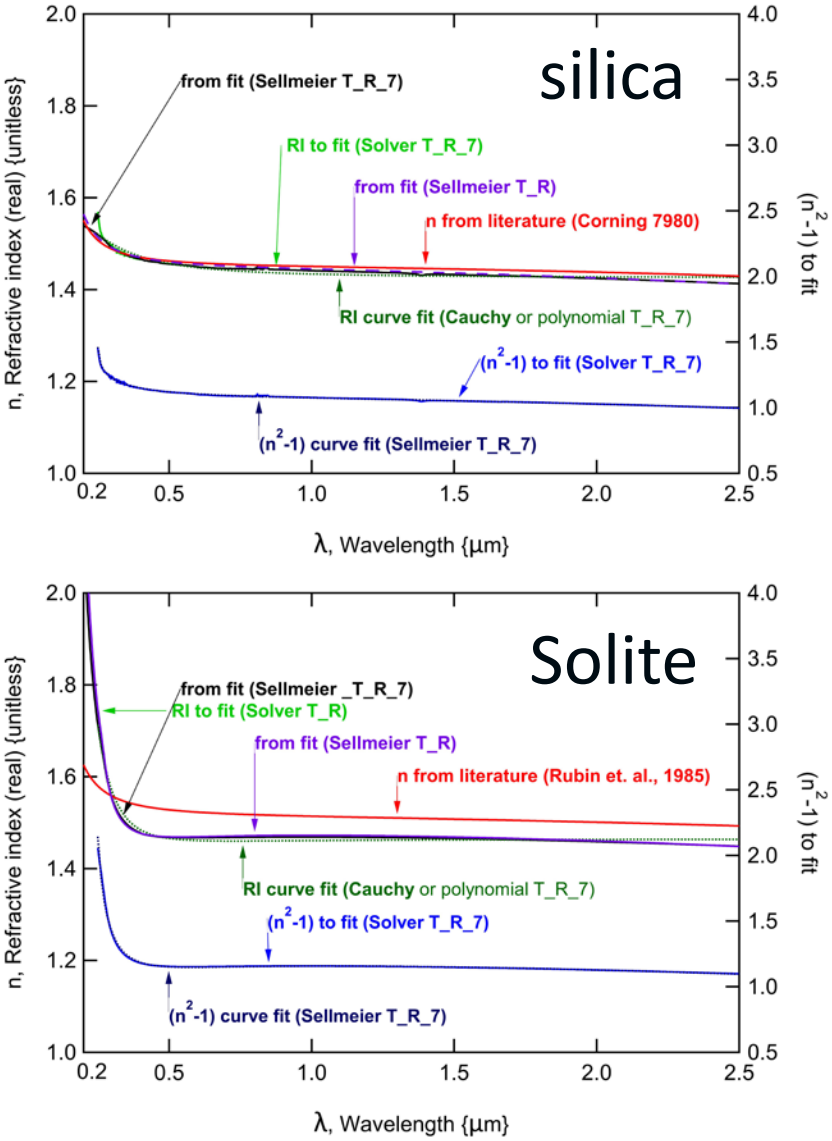

Fitting of real refractive index for: (top) silica used in the experiment, (bottom) Solite glass (AGC).

Comparison of Glass Used in PV and PV Research

- α was estimated from real complex refractive index for the 4 glass types.
  - silica (G.M. Associates) is UV transmitting and will not corrode
  - SG7.1 (Corning) is a lower cost alternate (UV transmitting)
  - Solite (AGC) is a textured glass (similar to PV module)
  - Diamant (S-G) is solarization and corrosion resistant (Xe 1000h, DH 2000h).
  - StarPhire (PPG) is an alternate low-Fe, soda-lime float glass.
  - Avalanche (Architectural Concepts) is a window glass. Fe peak at ~1100 nm.
- Each material gives a different performance (know which glass you are using)!

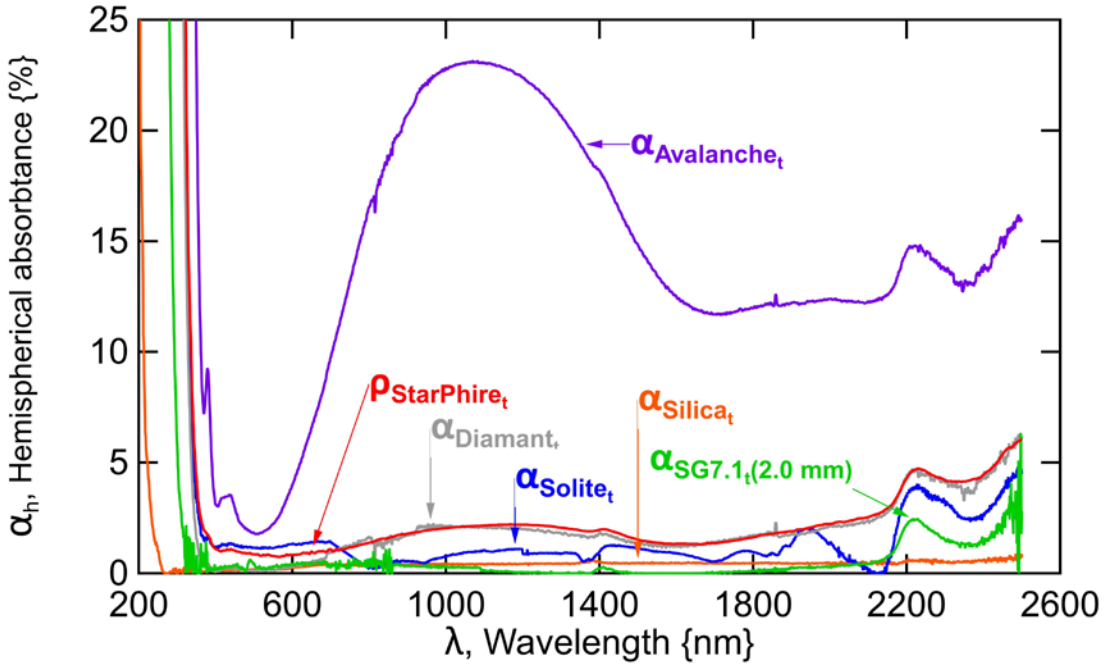

Absorptance spectra for the glass materials examined (typically shown for h = 3.2 mm, except where noted)

Damp Heat Weathering of Solite Glass

- τ_{rsw} increases through 1000 h, followed by a more substantive decrease as DH continues to 8000 h.
- ρ_{rsw} decreases from its initial value through 500 h, remaining relatively steady through 8000 h.
- α_{rsw} increases with DH at a steady rate through 8000 h.

- τ, ρ, α spectra shifted to longer wavelengths with DH.

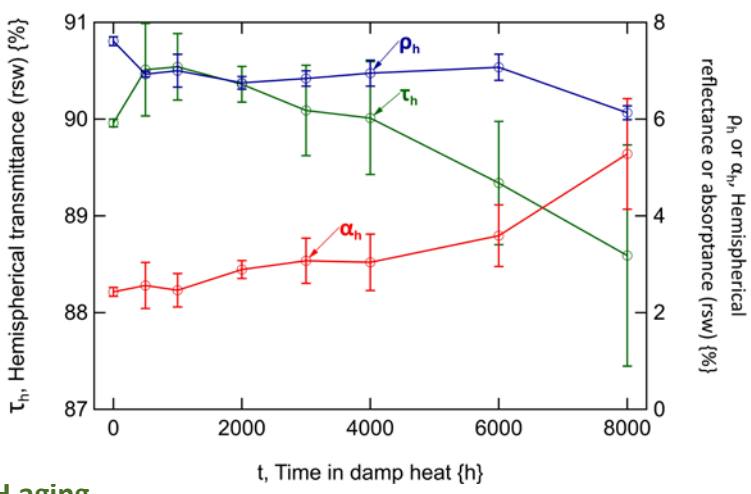

Optical performance (representative solar weighted-transmittance, -reflectance, and -absorptance) and corresponding spectra for monolithic textured Solite glass through DH aging.

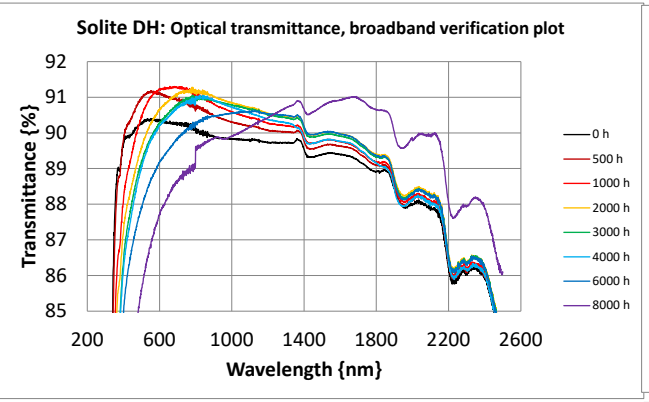

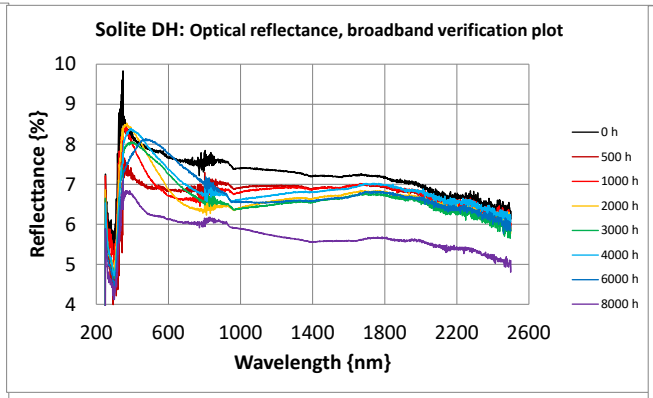

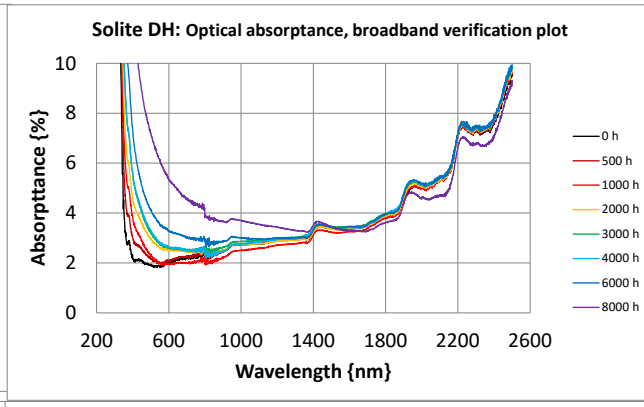

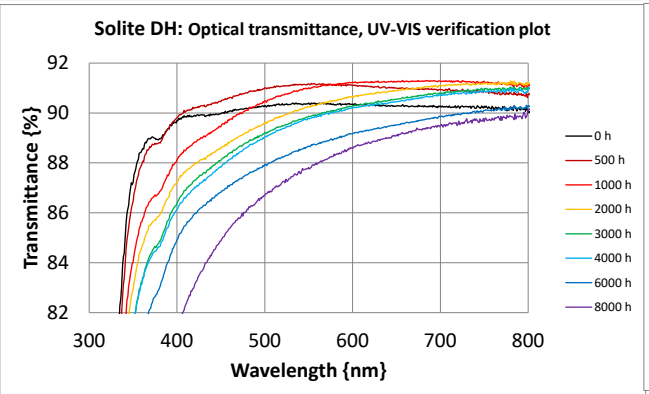

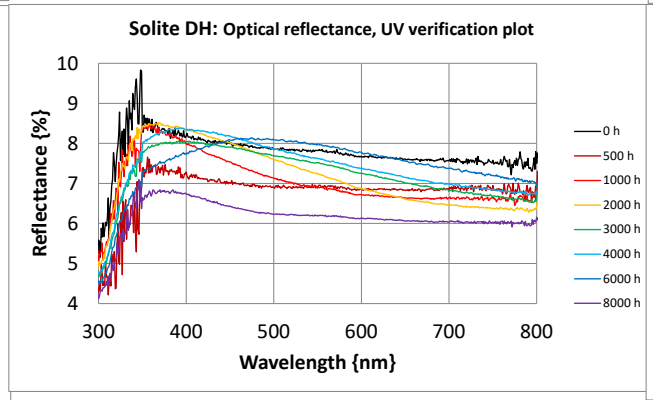

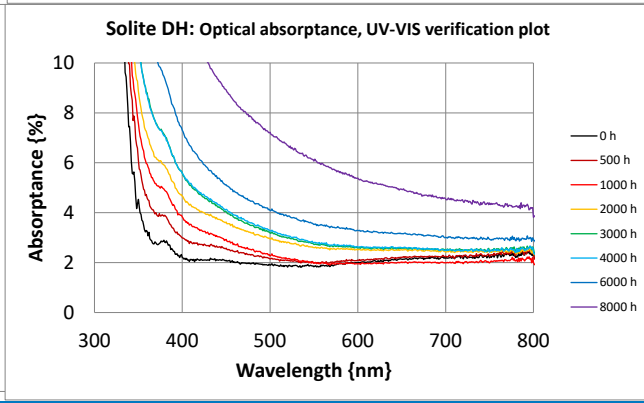

Damp Heat Weathering of Diamant Glass

Optical performance (representative solar weighted-transmittance, -reflectance, and -absorptance) and corresponding spectra for monolithic float Diamant glass through DH aging.

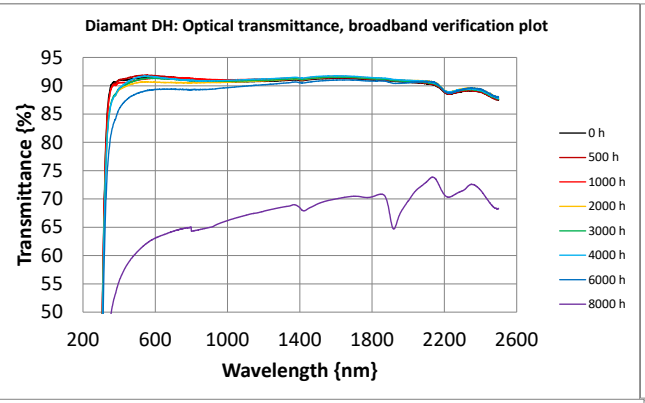

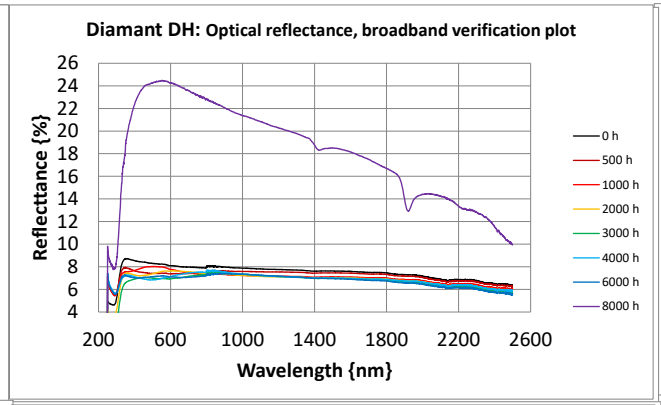

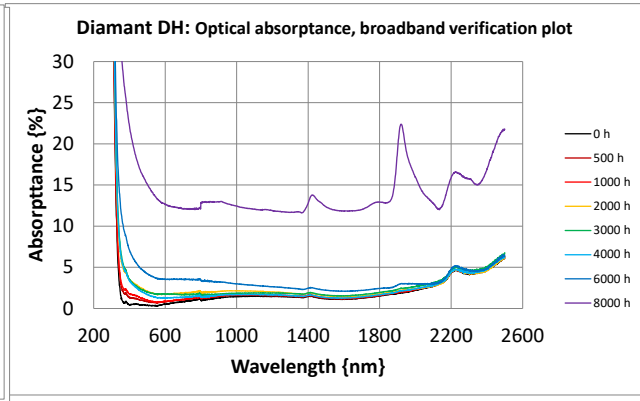

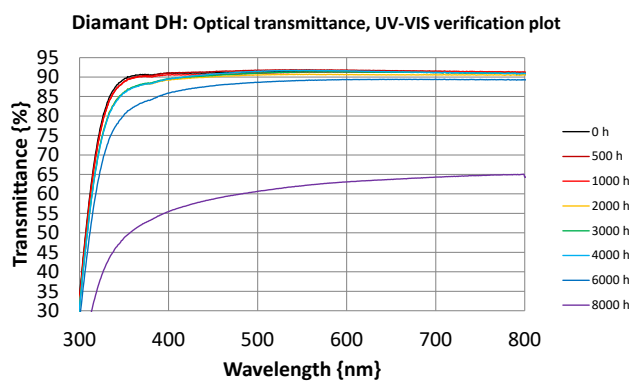

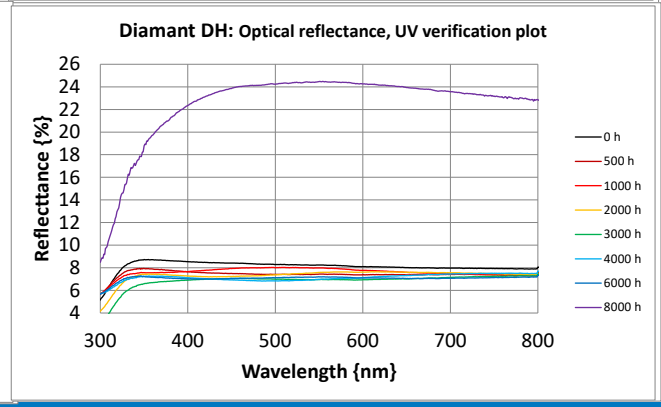

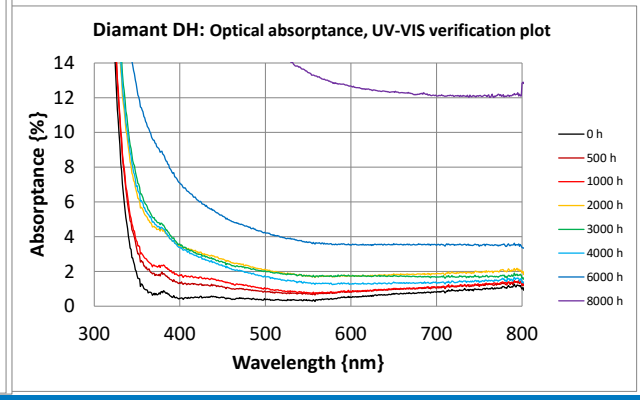

Damp Heat Weathering of StarPhire Glass

Optical performance (representative solar weighted-transmittance, -reflectance, and -absorptance) and corresponding spectra for monolithic float StarPhire glass through DH aging.

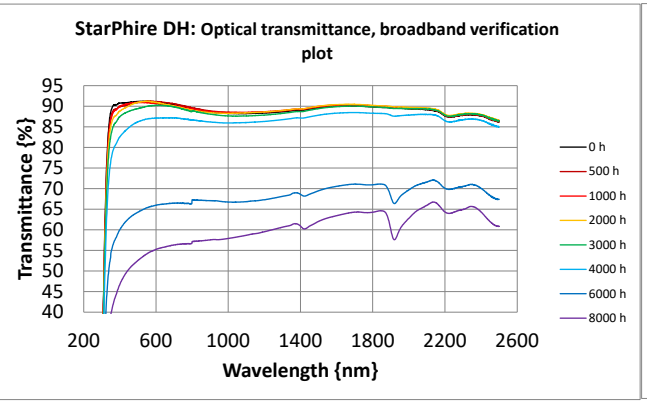

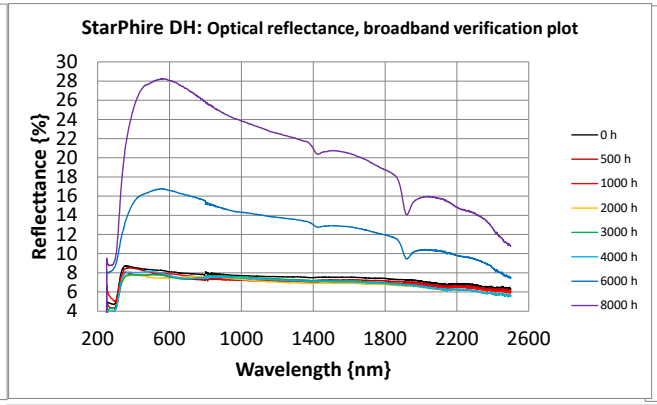

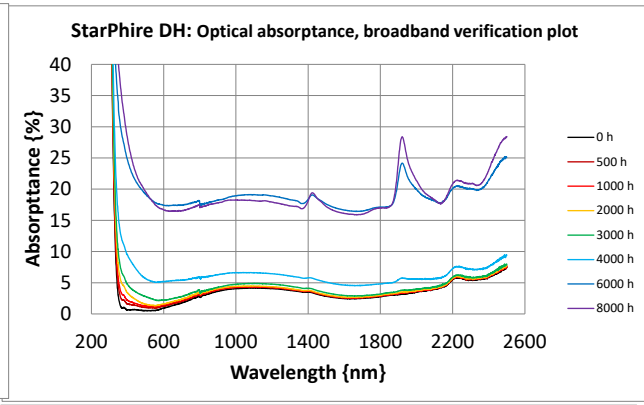

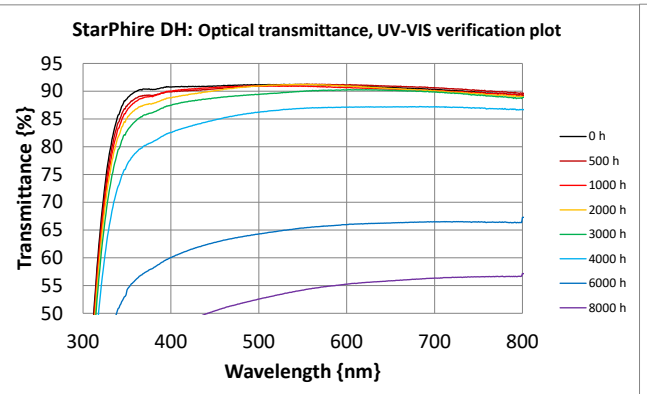

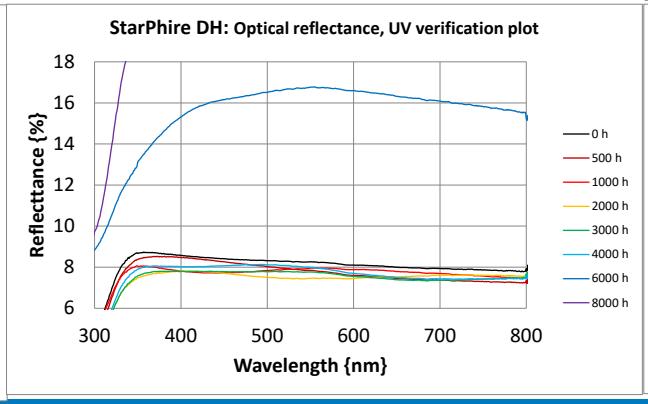

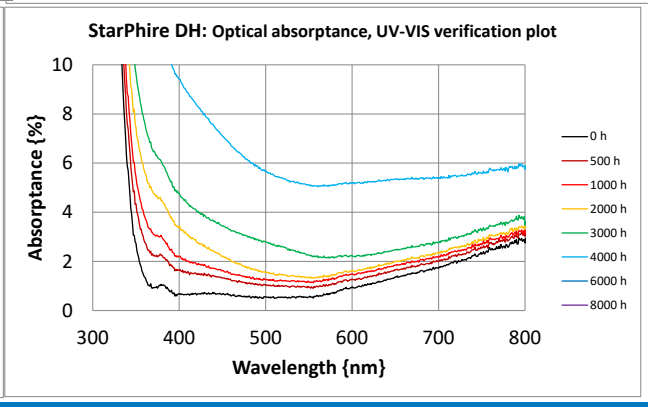

Damp Heat Weathering of Glass

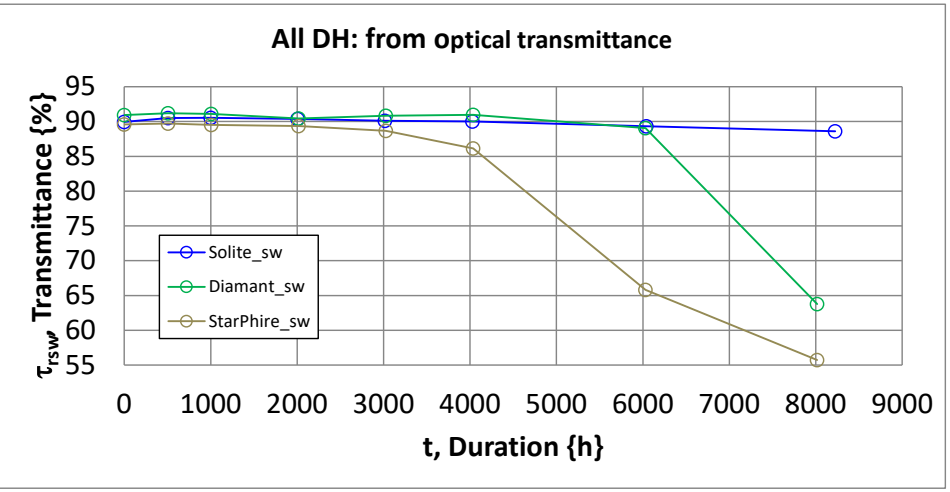

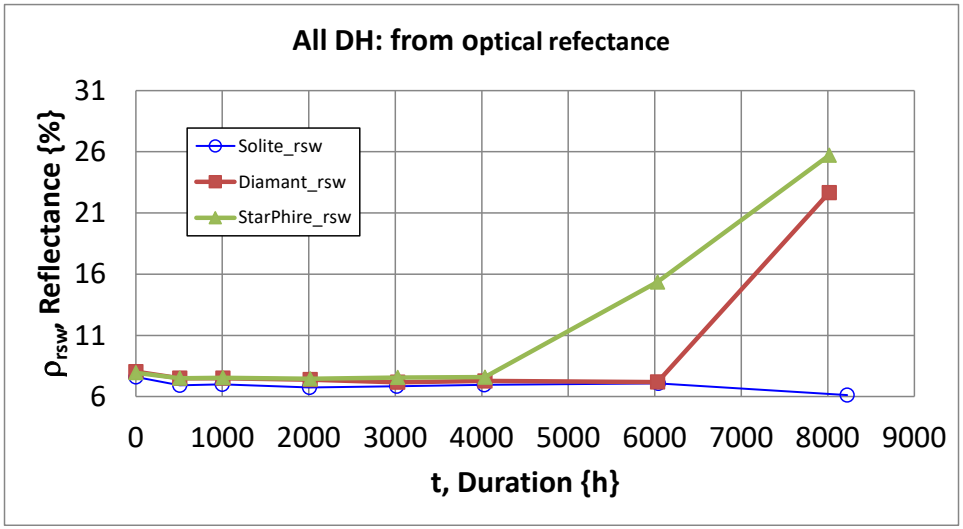

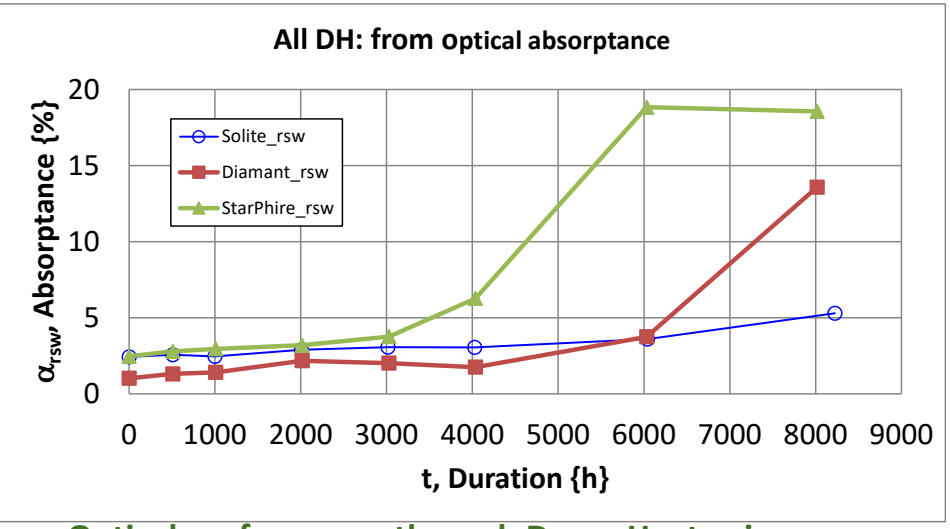

Optical performance through Damp Heat aging.

Damp Heat Weathering Glass

- YI from τ_h is increased with DH.
- YI from ρ_h is decreased through 2000 h, followed by a gradual increase approaching its original value.
- Increase in λ_{cUV} in the order of 3 nm was observed for the τ_{rsw} of Solite through DH.

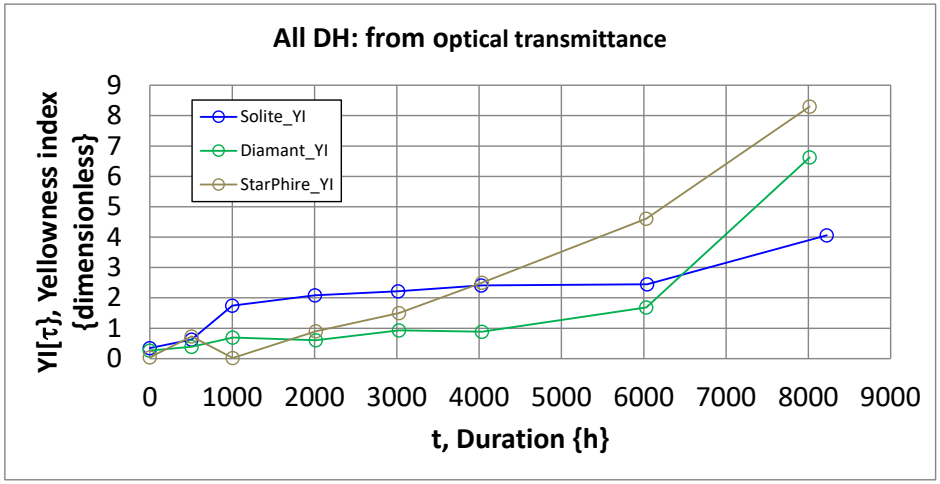

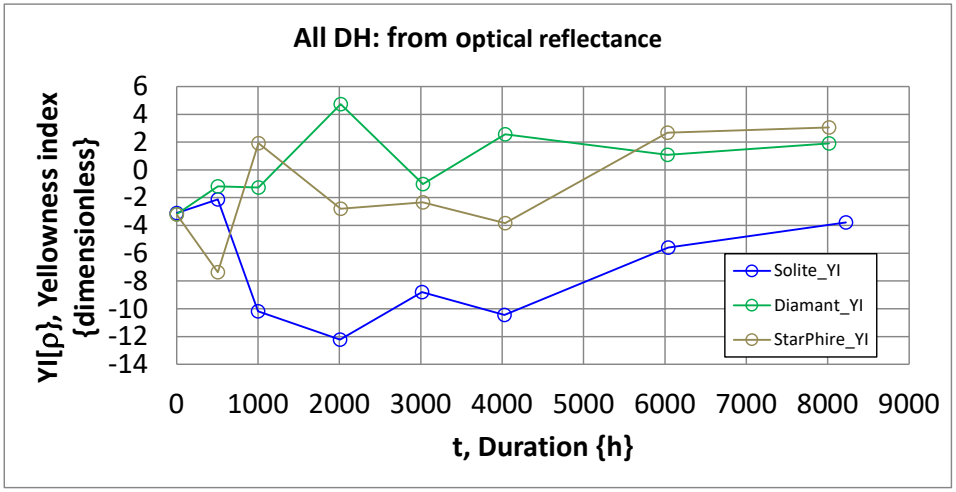

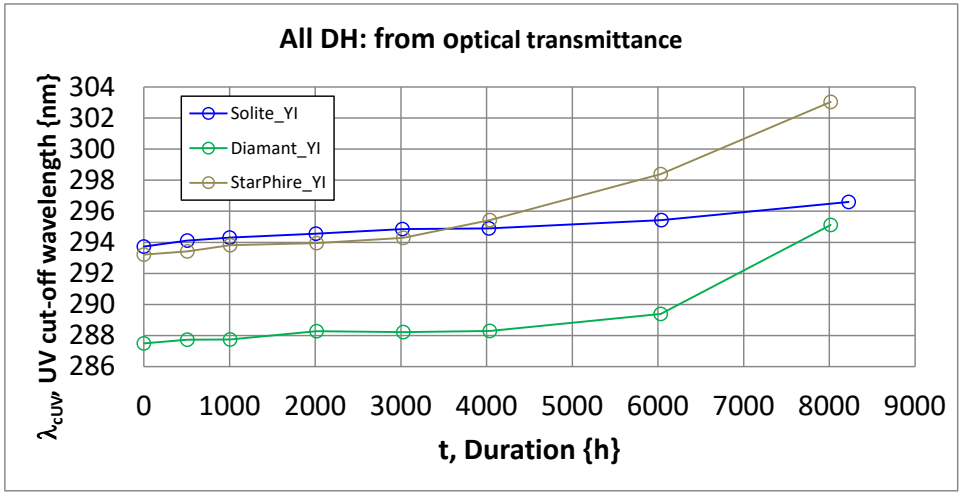

- Net increase in YI for both τ_h and ρ_h reminds that optical scattering occurs in both transmittance and reflectance, even if the magnitude of F_t exceeds F_r for the glass.
- Increase in λ_{cUV} and the shift in the peak of the τ_h and ρ_h spectra to longer wavelengths is consistent with roughening of the surface towards larger average feature sizes.

Optical performance through Damp Heat aging, from hemispherical optical performance measurements.

The Optical Effect of Degradation Modes

- Reflectance (ρ) at interfaces and absorptance (α) in the bulk are indicated for common degradation modes. They also apply to PV degradation!
- There are a greater # of events that could occur than in normal operation.

Cross-sectional schematic and taxonomy of optical events for PV module subject to degradation (all possible modes).

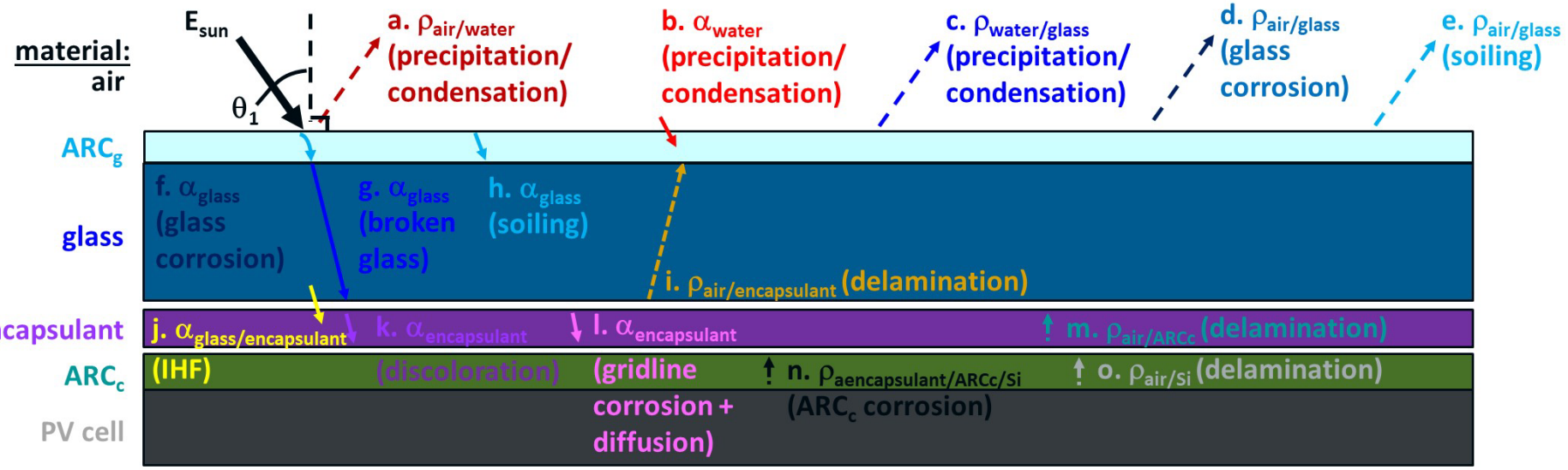

Photos of DH Specimens (Glass Only, Black Background)

- Solite not as overtly affected as float glass. Was anti-corrosion processing of the surface performed during manufacture?
- Float glass: more overt damage to Sn-poor than Sn-rich surface.
- Float glass: visibly overt damage ≥ 6000 h.
- Float glass: damage can be very localized.
  (?from stochastic degradation?)

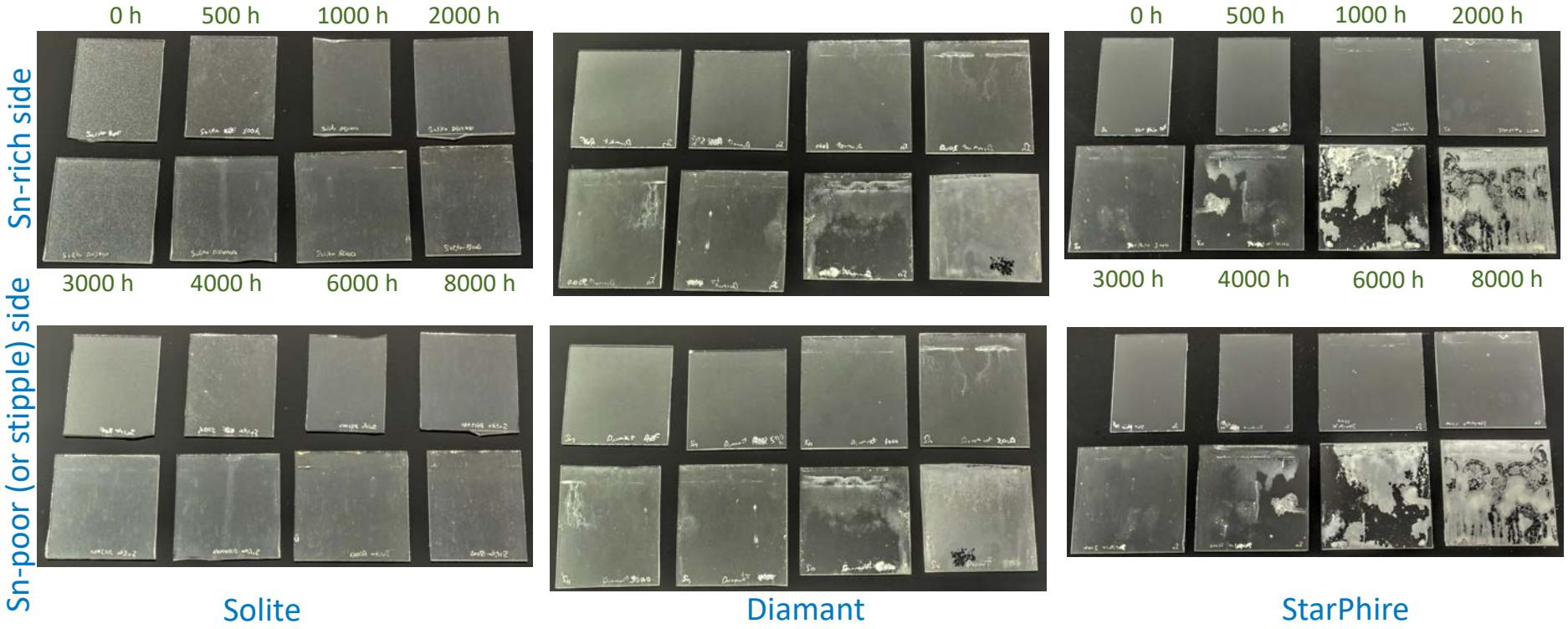

Photos of DH Specimens (Glass Only, White Background)

- Glass corrosion gives a (yellow) discoloration.

Keyence:

- StarPhire, Diamant: little, localized damage on Sn-rich side.
- Diamant: crystalline structure to corroded surface, Sn-rich & Sn-poor
- Solite: yellow/brown color often seen with localized corrosion. Difficult to image stipple surface.

Microscopy of DH –Glass Only- Specimens (DH 8000h, @30x)

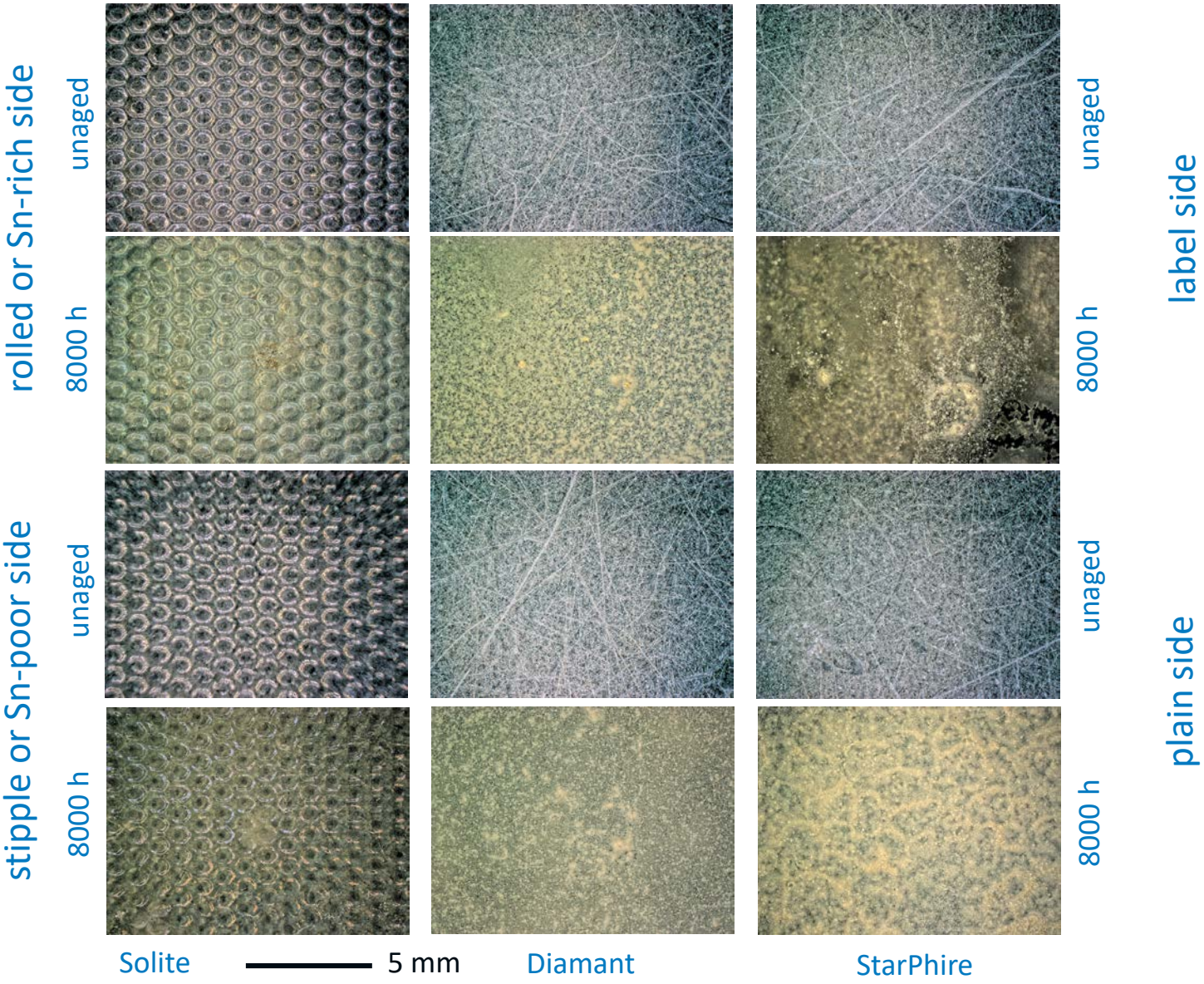

Microscopy of DH –Glass Only- Specimens (DH 8000h, @200x)

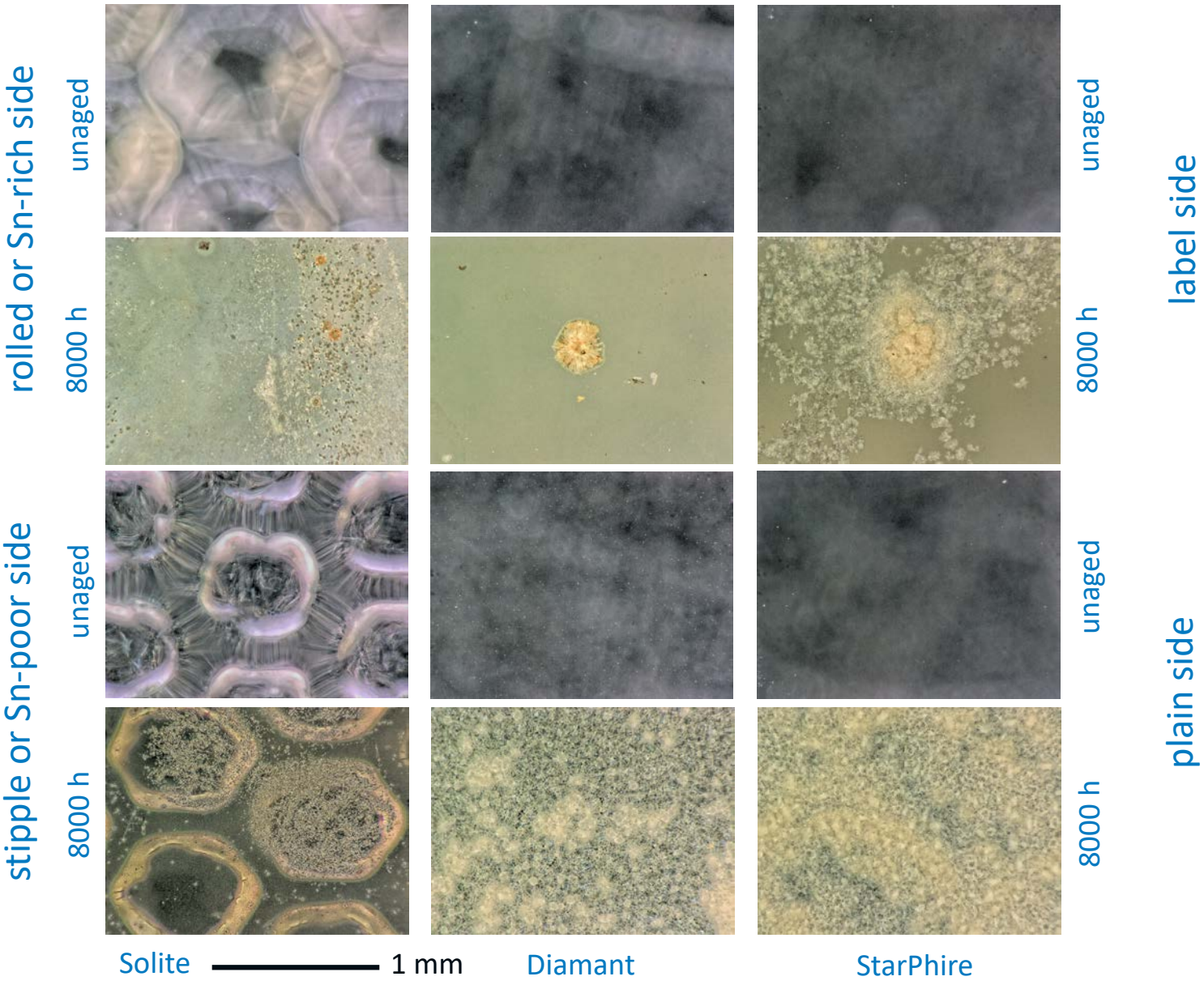

SEMs of DH Specimens (100x)

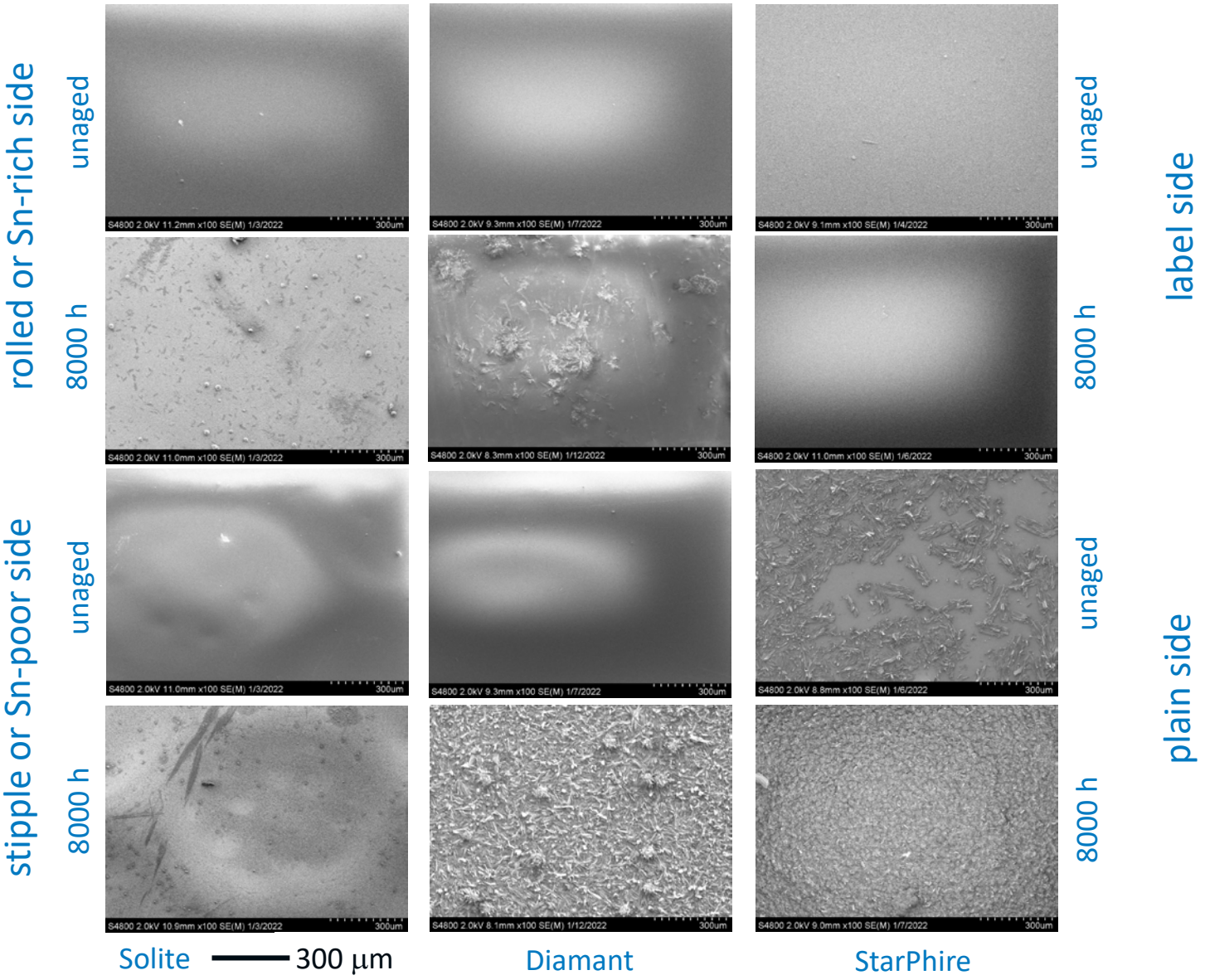

SEMs of DH Specimens (500x)

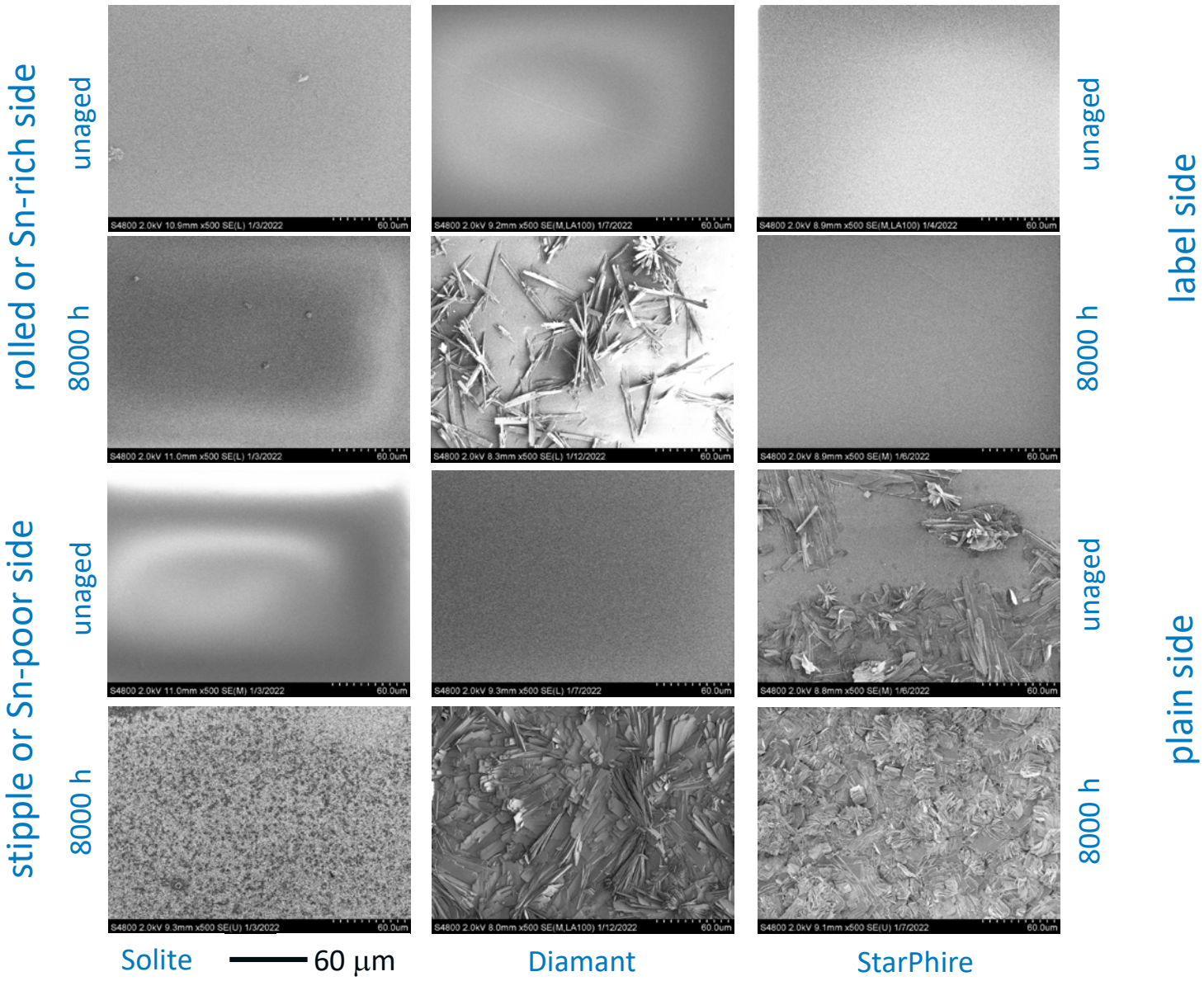

SEMs of DH Specimens (2kx)

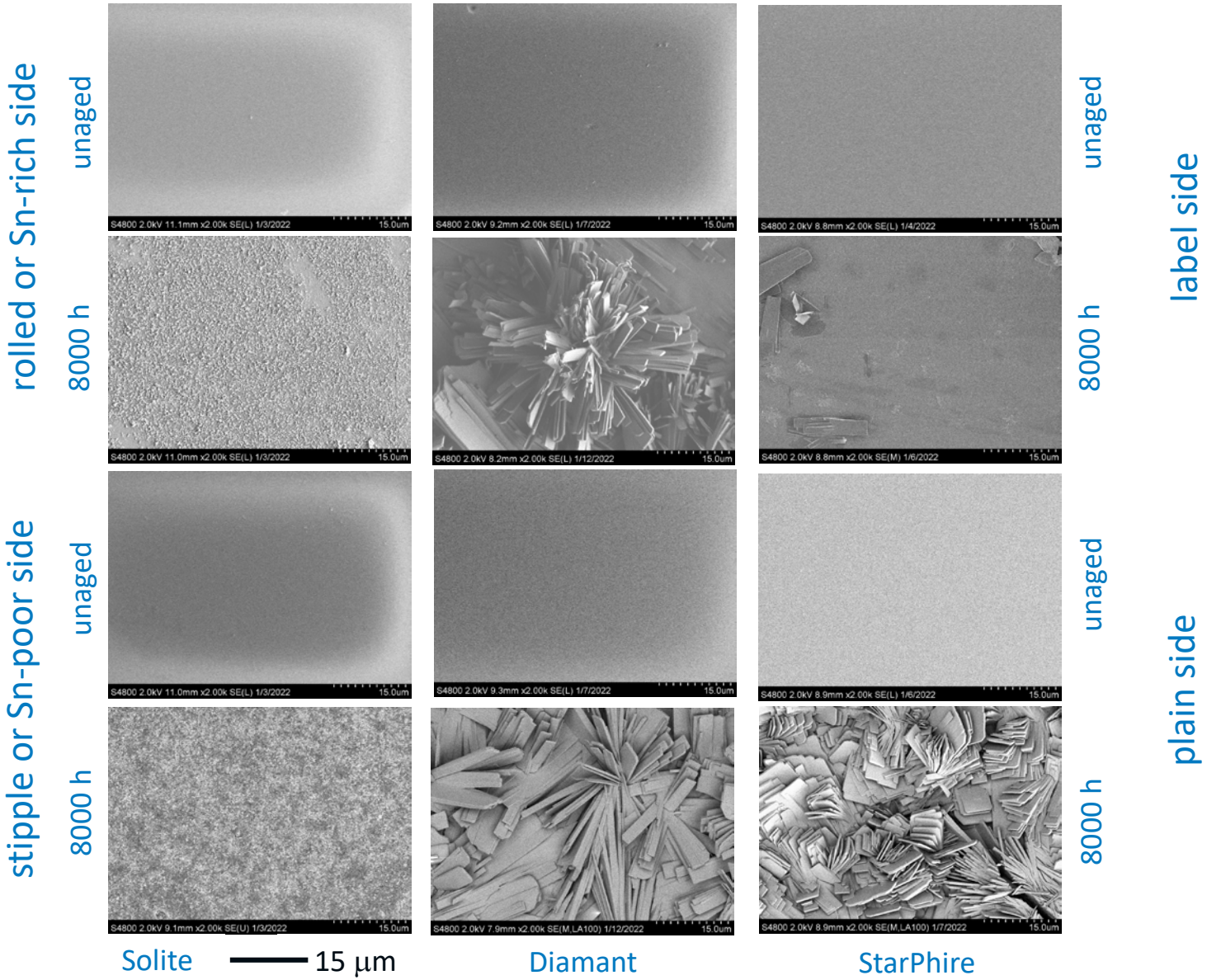

SEMs of DH Specimens (10kx)

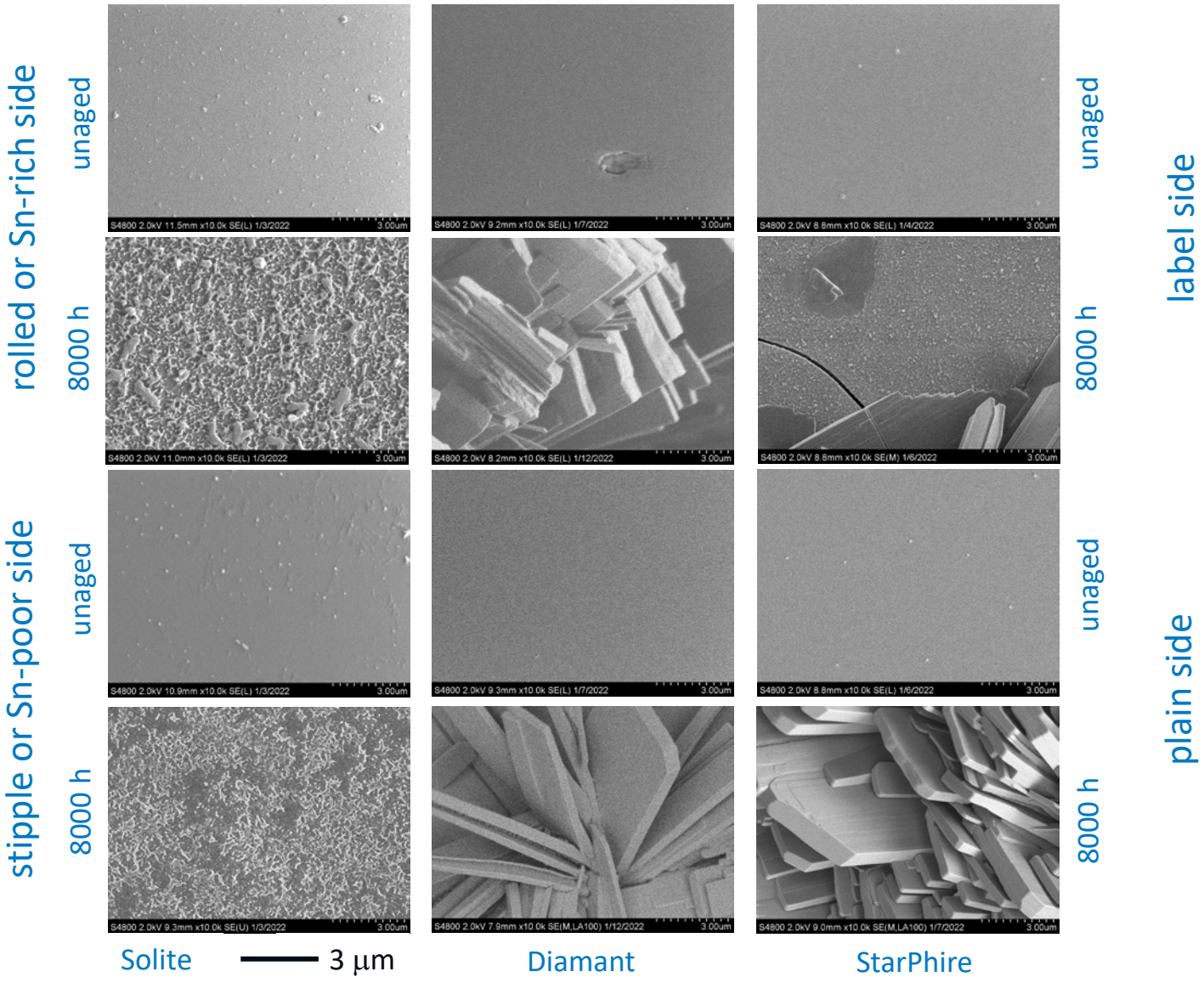

SEMs of DH Specimens (50kx)

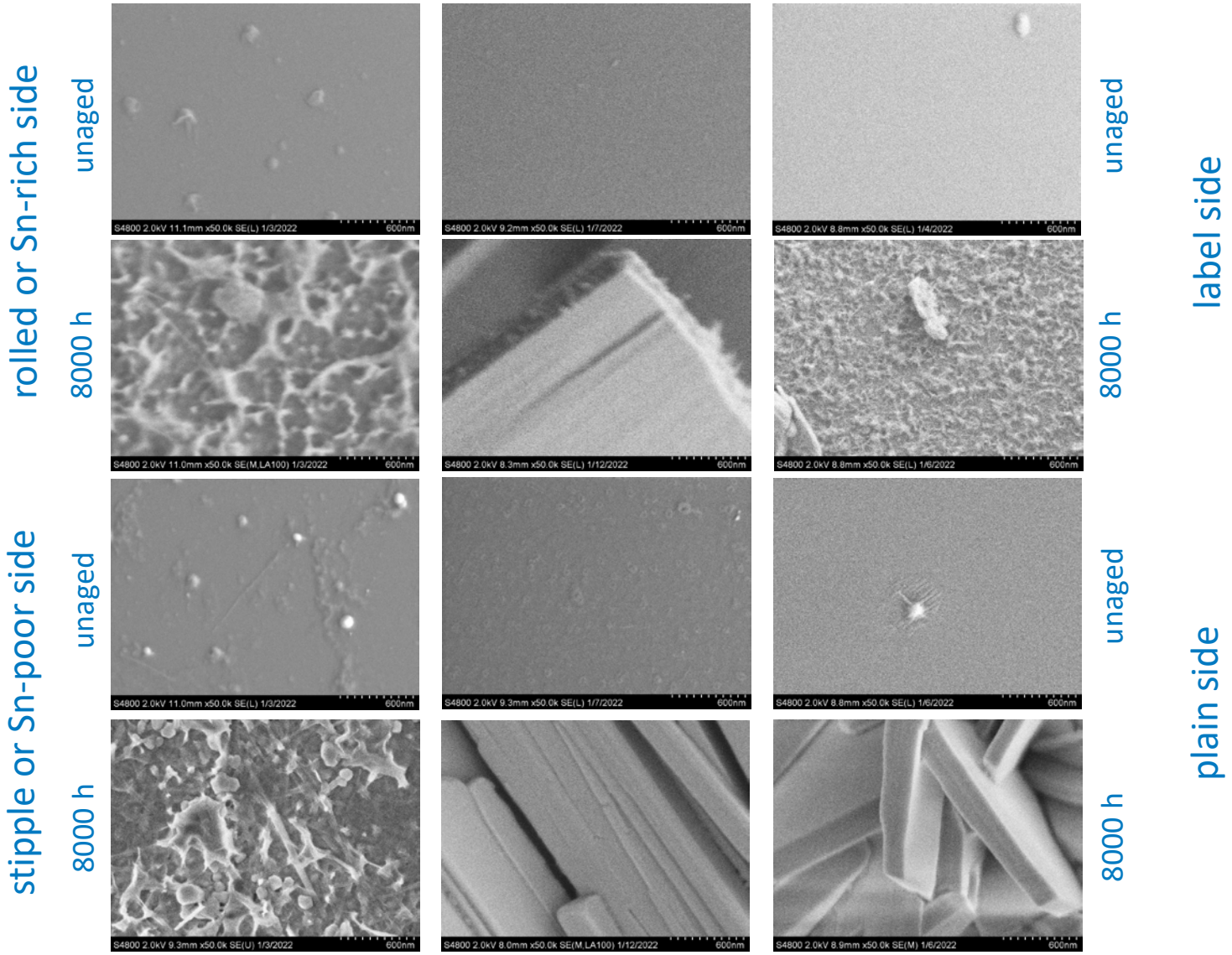

Damp Heat Weathering (Textured S-L Glass)

- DH weathering gave loss of transmittance and increased YI.
- From appearance, YI results from optical scattering: samples are –*unexpectedly*- not yellow in appearance.
- Transmittance is decreased through the experiment more significantly than only external glass corrosion, suggesting a different degradation mode.
- Initially suspected interaction at glass/encapsulant interface between basic glass corrosion and deacetylation of EVA, occurring in addition to glass corrosion on external surfaces of glass.
- Precipitate formation may enable IHF.
- Acetic acid (neutralized) would have catalyzed EVA discoloration.
- Consider 5% loss of performance → fails IEC 61215.
- While not widely documented, degradation mode expected to occur in DH tests of modules.
- Rate & extent of glass corrosion may be additionally affected in DH by external voltage bias.

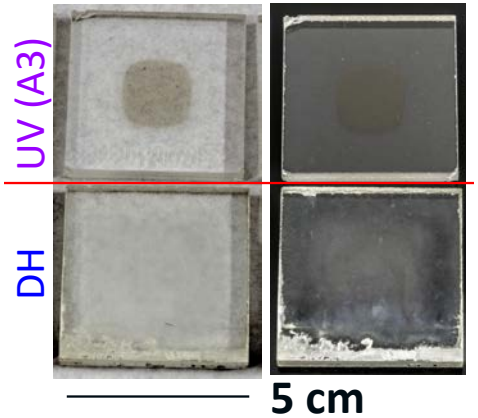

Representative images of EVA-A after 4000 h of: UV weathering (top) and Damp Heat (bottom) on white (left) and black (right) background.

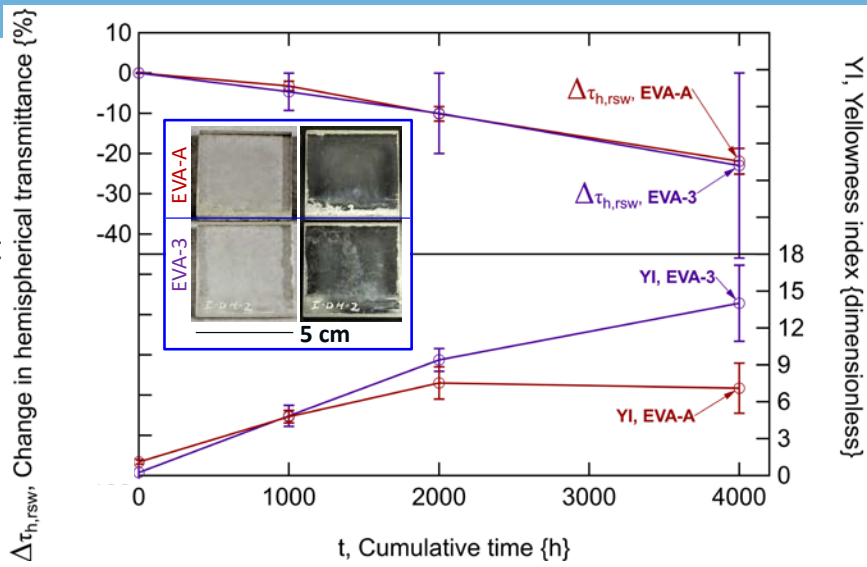

Yellowness index through 4000 h of Damp Heat for EVA-A and EVA-3. A representative image of the specimens at the end of the experiment is shown in the inset, including on a white background (left) and a black background (right).

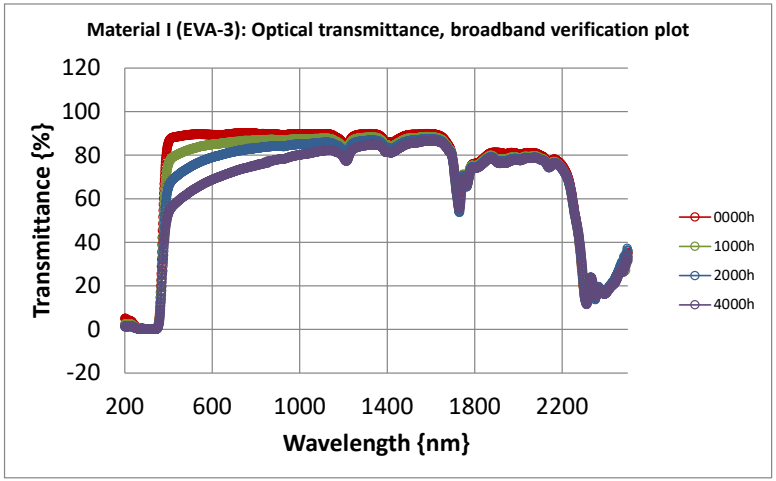

Representative τ_h spectra through the Damp Heat test for EVA-3.

Damp Heat Weathering (Other Samples)

Follow-on experiment (from 2020/4/29):

- Samples:

-silica/EVA-3/silica (produces acetic acid, non-alkali glass).

-Solite/TPO-3/Solite (no acetic acid, soda-lime glass).

-unaged replicates available (all samples).

- Read points: 0, 1000, 2000, 3000, 4000h
- More uniform, haze observed for EVA-3 (silica) at 1000h! Size of affected region reduces over time. Absorbed water?
- Heterogeneous surface haze observed for TPO-3 (Solite). Consistent with external surface glass corrosion.

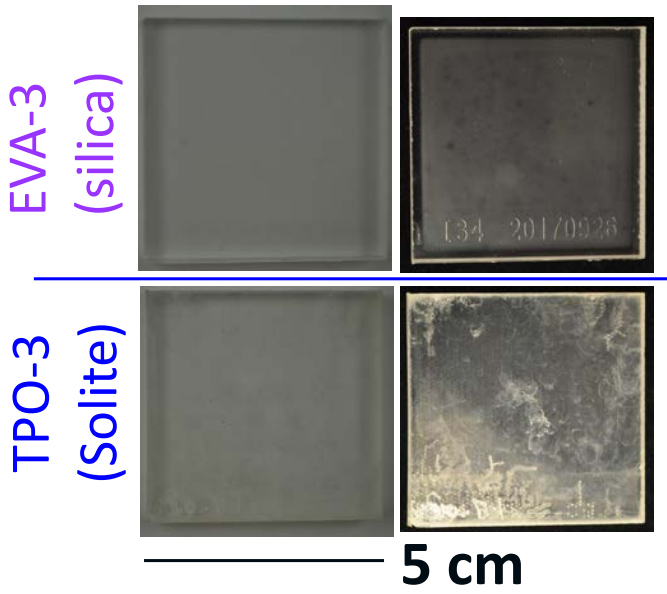

Representative images of after 1000 h of Damp Heat on white (left) and black (right) background.

Additonal characterizations:

- Optical mapping of original; DH samples.
- Keyence (microscope) image the surface to document external glass corrosion. Clean samples. Reimage.
- Water jet dice into 1" or ½" samples to facilitate F/A?
- Composition analysis of encapsulant/ near glass interface.
  - FTIR?
  - XPS? Silica glass too?

			CONCENTRATION {% atomic}								
GLASS	SURFACE	DEPTH {nm}	Al	C	Ca	Fe	Mg	Na	O	Si	Sn
silica		AVG[50-70] ±2 S.D.	unverified								
Solite	sun (rolled smooth)	AVG[50-70] ±2 S.D.	0.7±0.2	0.0±0.0	2.4±0.1	0.0±0.0	0.8±0.1	2.2±0.2	56.3±0.6	37.6±0.8	0.0±0.0
Solite	cell (stipple)	AVG[50-70] ±2 S.D.	1.4±0.2	0.0±0.0	3.1±0.1	0.0±0.1	1.2±0.1	2.9±0.2	37.6±0.4	53.7±0.4	0.0±0.0

Composition of glass used in study.

Damp Heat Weathering (Additional Samples)

•TPO-3 (Solite glass) gives external glass corrosion, with very limited evidence of internal haze formation.
-Solite is a soda-lime glass that will corrode in Damp Heat.
-PO has no acetate side groups: no acetic acid (internal to coupons).
-Effect reduced for TPO relative to EVA (Solite).
-Slight halo observed adjacent to periphery.
-Transmittance initially increased, consistent with external glass corrosion.

•EVA-3 (silica glass) gives internal haze formation, with no evidence of external glass corrosion.
-No glass corrosion would be expected for silica (no Ca, Na, or Mg).
-EVA can still produce acetic acid (internal to coupons).
-Effect reduced for EVA-3 (silica) relative to EVA-3 (Solite).
-Less affected periphery from ready egress of water?

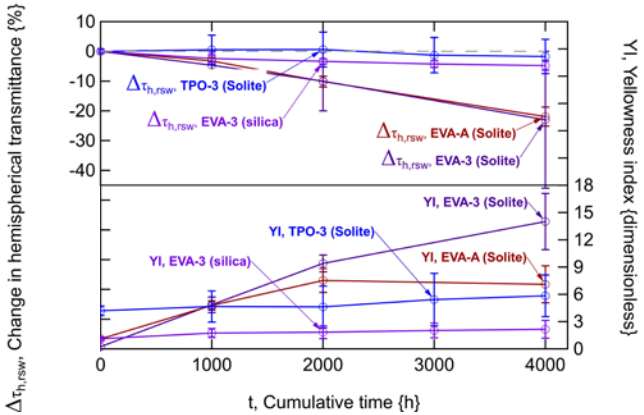

Comparison of transmittance and yellowness index through 4000 h of Damp Heat (85 °C/85%ChRH) for EVA-A, EVA-3, and TPO-3. The results are compared between laminated glass/encapsulant/glass coupon samples constructed using Solite or silica glass.

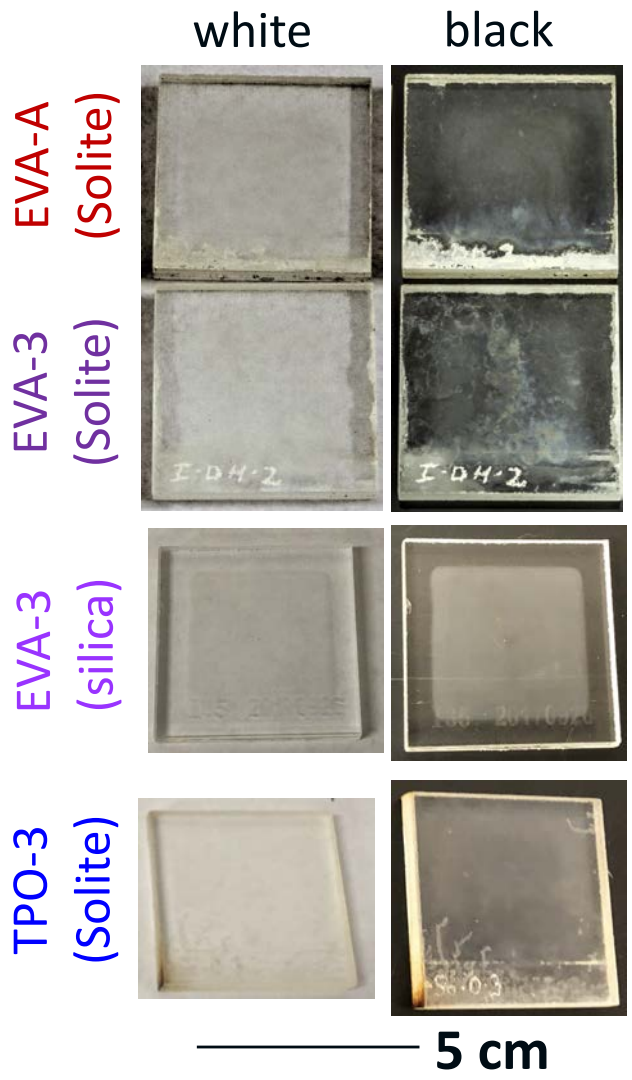

Representative images of the EVA-A, EVA-3, and TPO-3 coupons after 4000 h of Damp Heat, including on a white background (left) and a black background (right).

Failure Analysis of DH4000: Optical Microscopy (Solite & EVA-A, 30x)

- Samples examined in 3 locations on scribed & plain surfaces.
- Samples examined as aged, cleaned, or unaged (cleaned).
- Aged & cleaned samples not re-examined in same exact location.
- Cleaning: Liquinox detergent + DI, scrub vigorously with Twillx 1622 (Berkshire Corp.) cloth cleanroom wipe → DI rinse → blow dry.

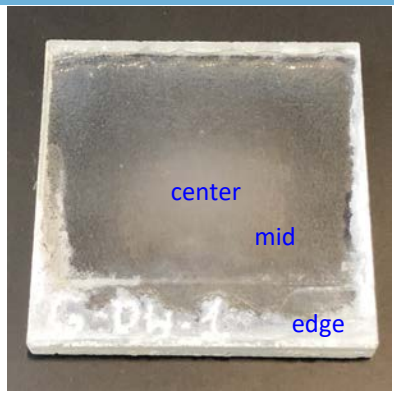

Example image locations shown for scribed (label) sample surface.

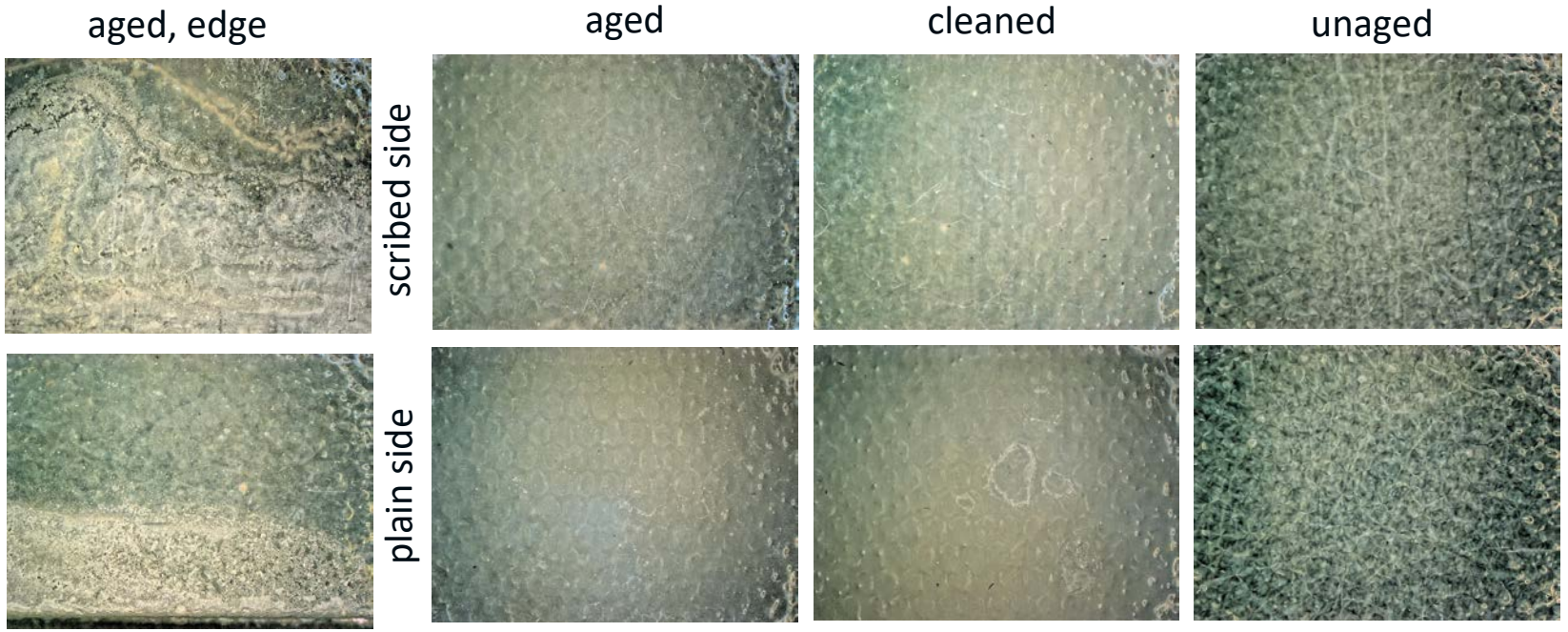

Representative microscope images, typically from the "mid" location.

Failure Analysis of DH4000: Optical Microscopy (Solite & EVA-A, 200x)

- External glass corrosion is confirmed on both external surfaces of coupons, from features including: micro-scale flaking/spalling and cracking of the surface.
- Corrosion is not dense or uniform.

  How many performance measurements would be required to give an effective result?
- Cleaning did not remove much of the spalled glass.

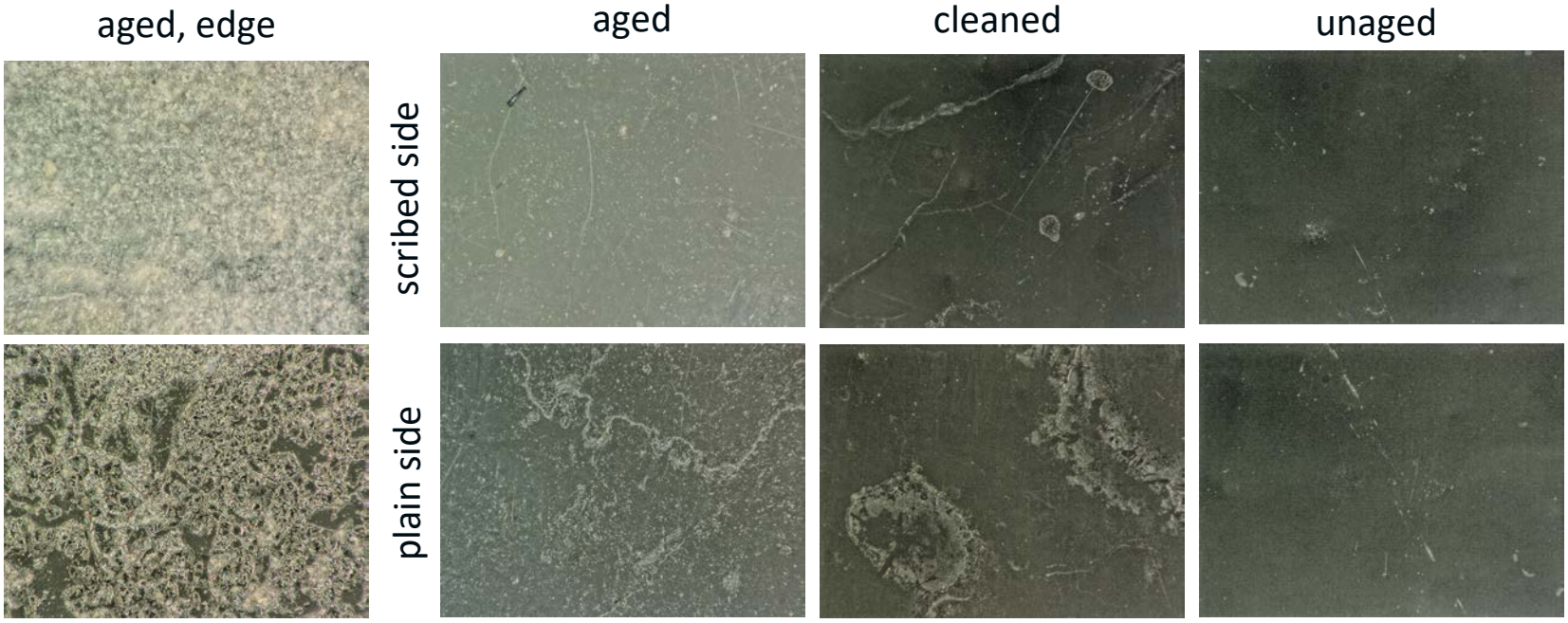

Representative microscope images, typically from the "mid" location.

Failure Analysis of DH4000: Optical Microscopy (Solite & EVA-3, 30x)

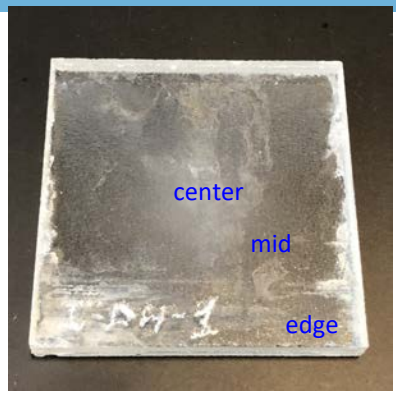

Example image locations shown for scribed (label) sample surface.

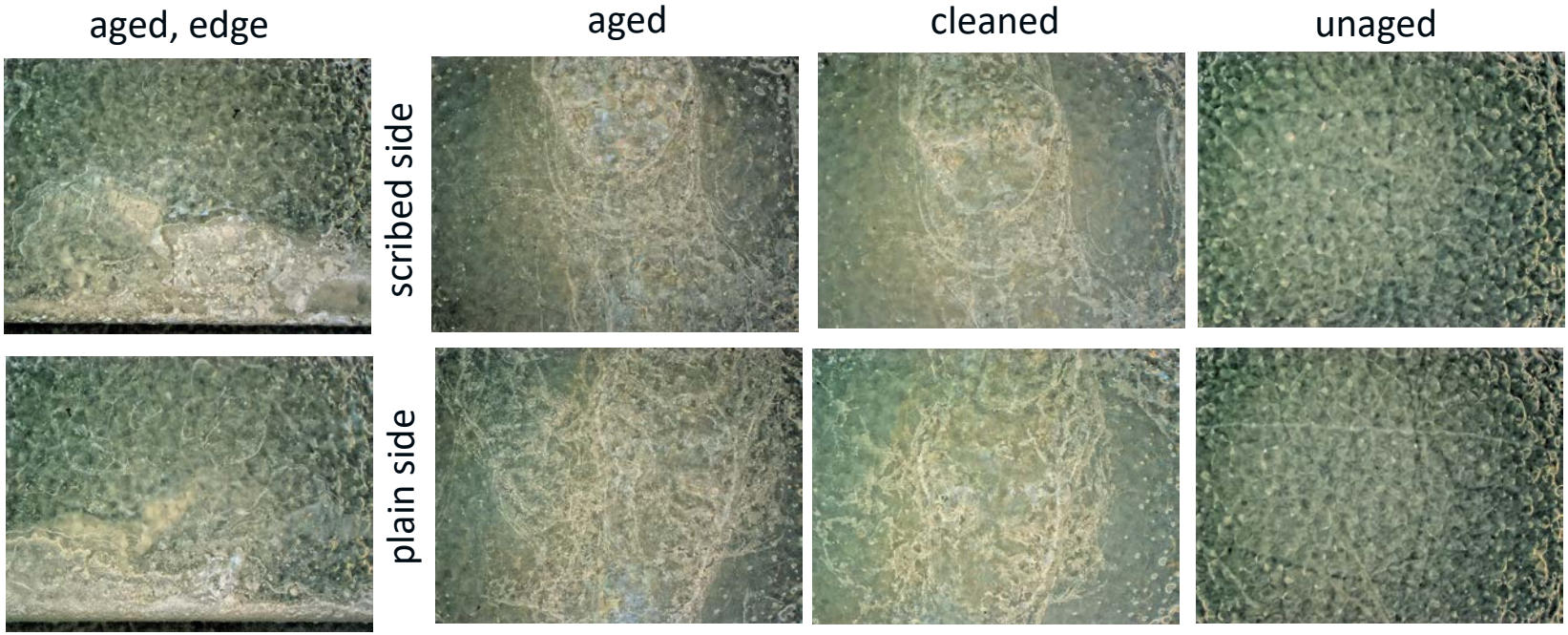

Representative microscope images, typically from the "center" location.

Failure Analysis of DH4000: Optical Microscopy (Solite & EVA-3, 200x)

- External glass corrosion confirmed for aged Solite glass.

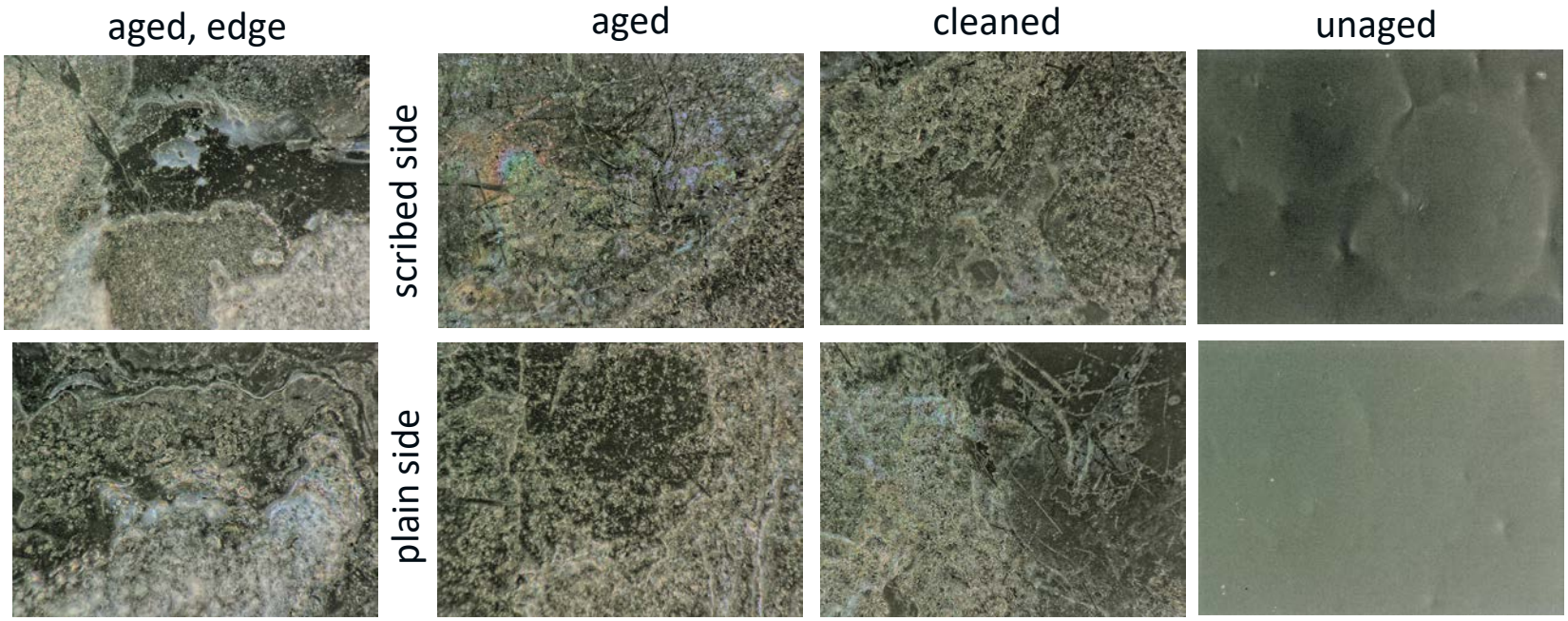

Representative microscope images, typically from the "center" location.

Failure Analysis of DH4000: External Optical Microscopy (silica & EVA-3, 30x)

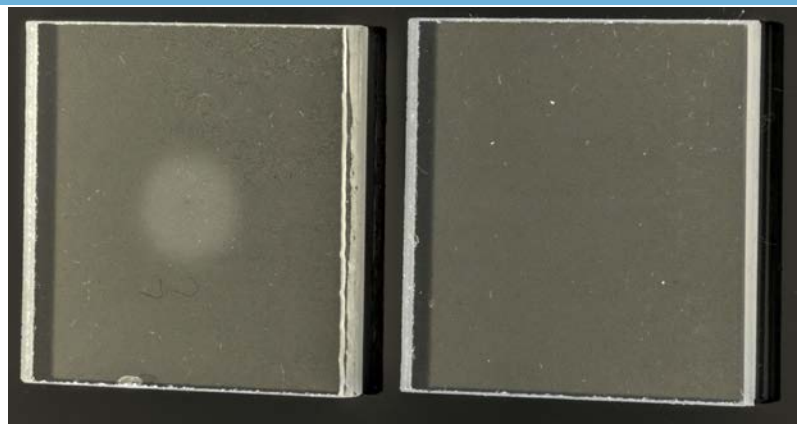

Camera photo (entire specimen).

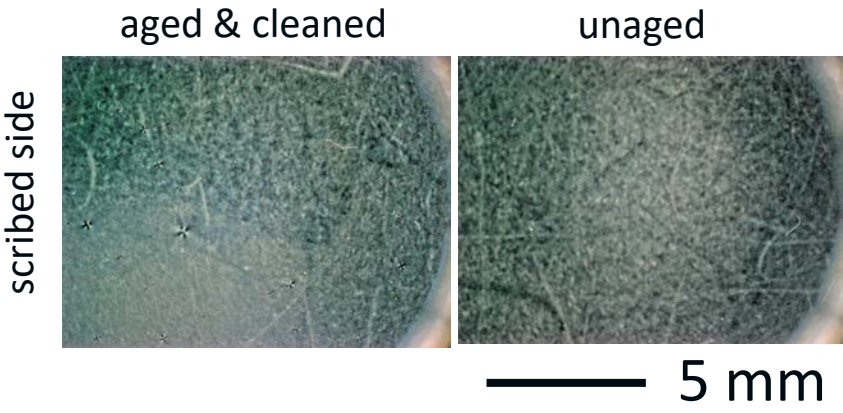

Representative microscope images, typically from the “center” location.

Failure Analysis of DH4000: External Optical Microscopy (silica & EVA-3, 200x)

- No external glass corrosion for silica glass.

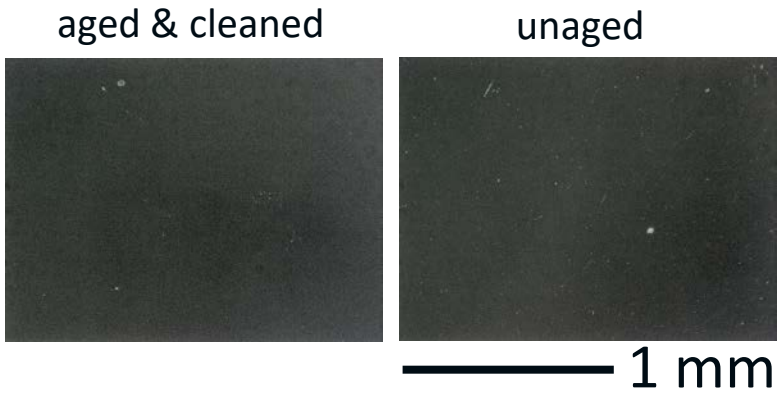

Representative microscope images, typically from the "center" location.

Failure Analysis of DH4000: External Optical Microscopy (Solite & TPO-3, 30x)

Camera photo (entire specimen).

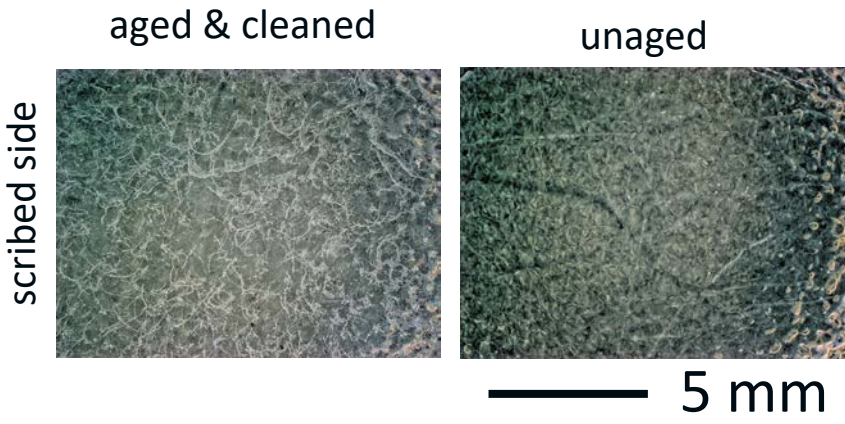

Representative microscope images, typically from the “center” location.

Failure Analysis of DH4000: External Optical Microscopy (Solite & TPO-3, 200x)

- External glass corrosion confirmed for aged Solite glass.

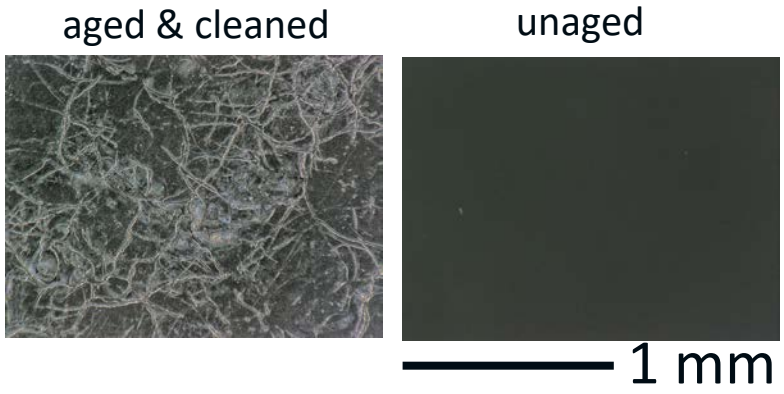

Representative microscope images, typically from the "center" location.

Microscopy of DH4000 Samples (At Encapsulant)

Samples were marked in irregular pattern on the scribed side of sample at periphery with Sharpies of 2 different colors, and then water jet diced to smaller sizes.
Insert tip of knife into encapsulant at middle of periphery facing edge to initiate delamination towards the center facing edge of the sample.
Insert edge of knife into periphery facing edge, see-saw to propagate delamination about 1/2 way into sample. stipple pattern will be visible from delamination and will extend in front of edge of knife.
Lay sample on flat surface and gently pry open with knife in place, using the knifer like a lever.
Finally pry apart sample with fingers .
“Label” side means the surface of the encapsulant in the direction of the scribed, Sharpied glass surface
“Plain” side means surface of the encapsulant in the direction of the unmarked glass surface

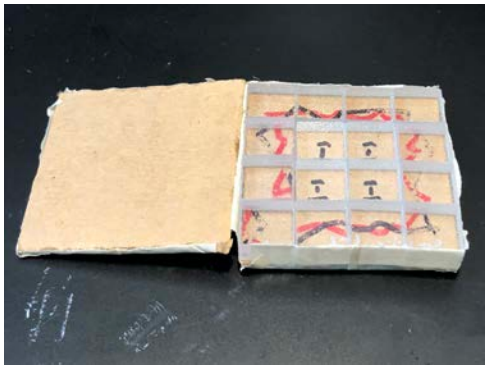

DH samples came apart with less force and smoother surface at interface.
“Crystals” (embedded glass, salt, or precipitate) at surface of interface on DH samples.

Limited topography of the stippled pattern on surface of EVA on DH samples.
Rounding of same crystal features observed after DI soak -> some water solubility

Unaged samples show plastic deformation of the EVA.
Lots of topography from stippled pattern of glass for unaged samples.

Similar surface texture observations observed for center & edge samples between DH and unaged samples.

Effect of optical polarization observed (EVA is bifringent) in only second session (DI soak & edge) for unaged EVA; DH samples did not show color though.
DI: sprayed/rinsed samples 5x at faucet temperature, then soaked over in 50 mL DI, at ambient T

All samples imaged with innermost facing edge along bottom of screen (bottom of the image, this is the core of the anaerobic region).

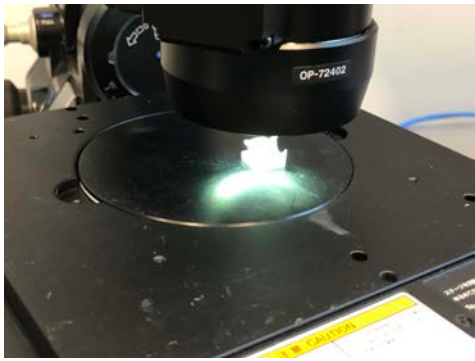

Failure Analysis of DH4000: Internal Optical Microscopy (Solite & EVA-A)

- Good adhesion (encapsulant/glass) from manual separation force for unaged; reduced adhesion for DH4000.
- Internal glass corrosion confirmed for aged Solite glass.
- Bits of glass lost from Solite, embedded in encapsulant.
- Comparing the same location, modestly water-soluble material at interface aged samples.

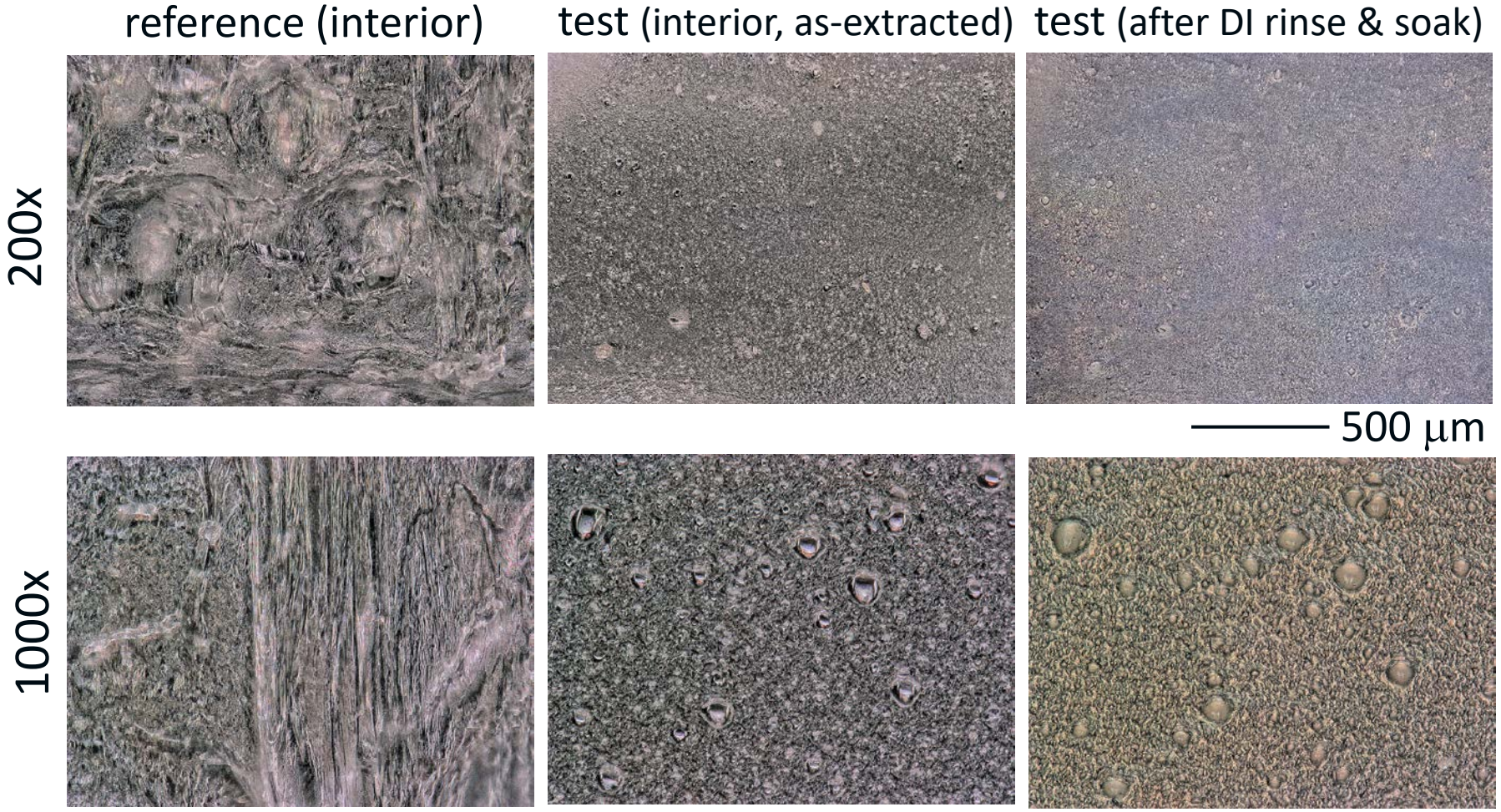

Representative microscope images, from unaged and DH aged coupons, from the "center" location.

Failure Analysis of DH4000: Internal Optical Microscopy (Solite & EVA-3)

- Good adhesion (encapsulant/glass) from manual separation force for unaged; reduced adhesion for DH4000.
- Internal glass corrosion confirmed for aged Solite glass.
- Bits of glass lost from Solite, embedded in encapsulant.
- Comparing the same location, modestly water-soluble material at interface aged samples.

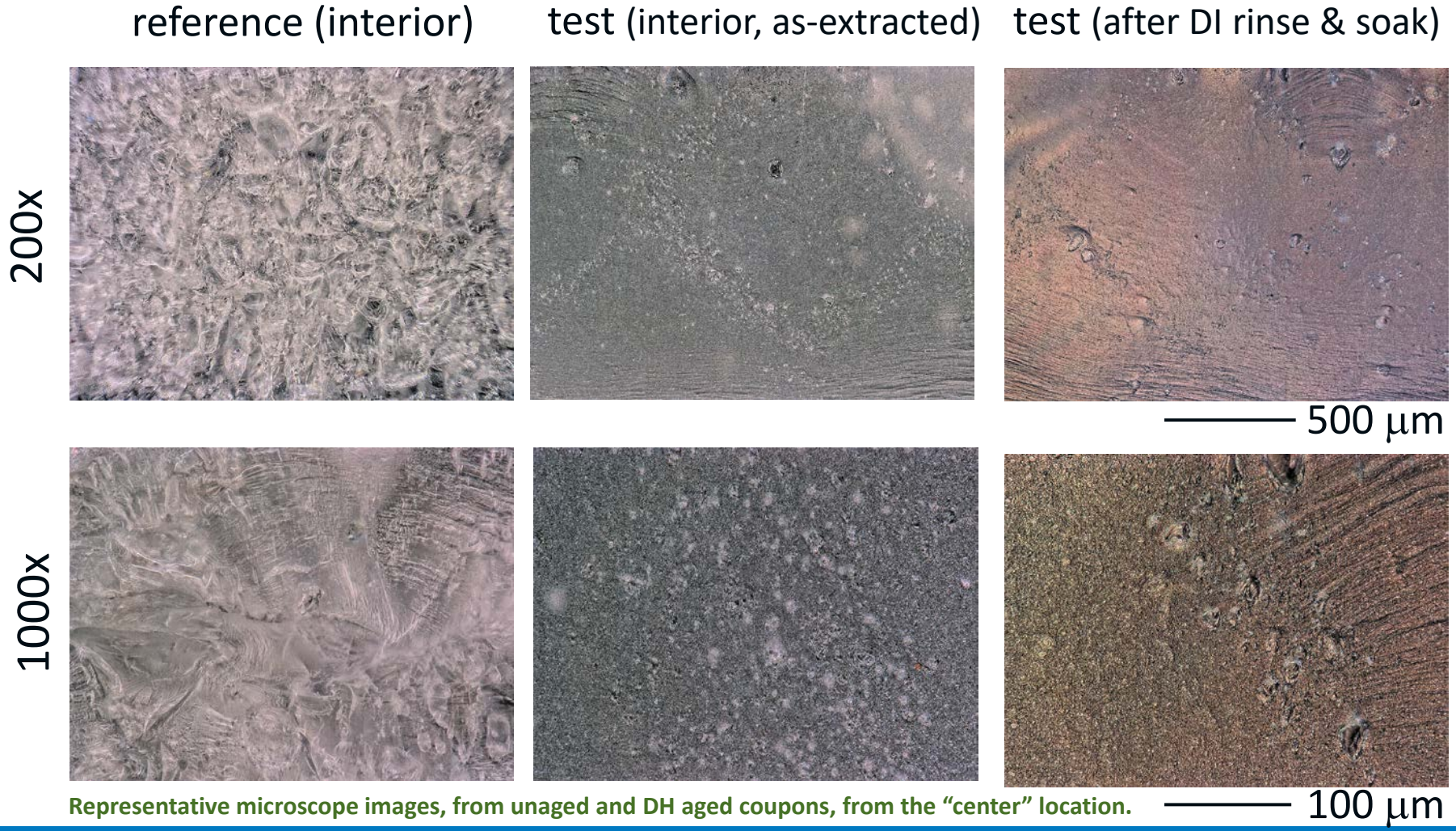

Representative microscope images, from unaged and DH aged coupons, from the "center" location.

Failure Analysis of DH4000: Internal Optical Microscopy (silica & “I” [EVA-3])

- Good adhesion (encapsulant/glass) for aged & unaged. Compare to CST study to identify which has best adhesion strength.
- Similar fractography for DH4000 sample suggests modest degradation has occurred at the interface.
- Comparison of Solite & silica: features and inelastic deformation for unaged EVA suggest geometry of rolled Solite glass affects failure.

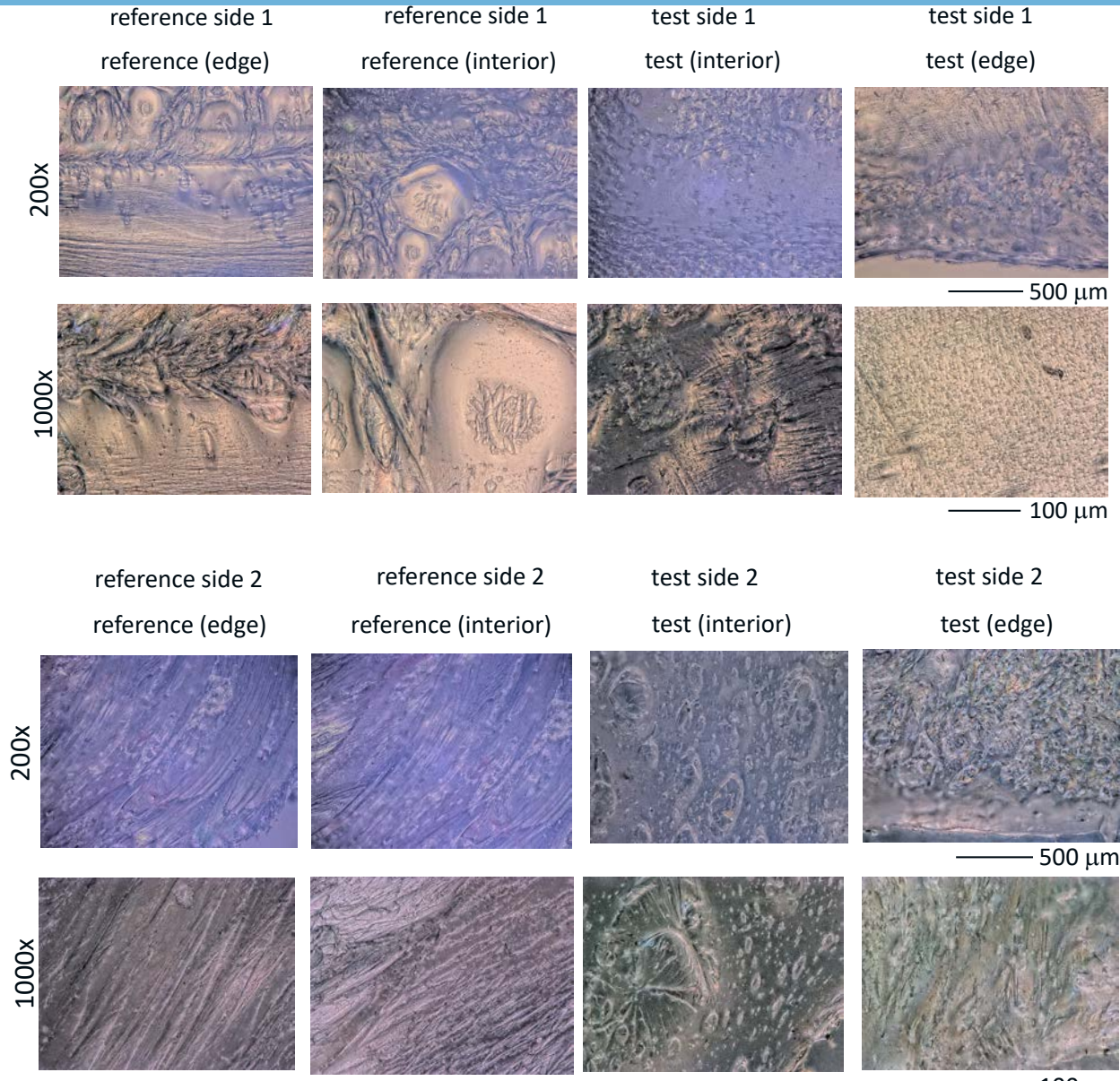

Representative microscope images, from unaged and DH aged coupons, from the “center” location.

Failure Analysis of DH4000: Internal Optical Microscopy (Solite & "D" [TPO-3])

- Limited adhesion (encapsulant/glass) during manual separation for aged & unaged. May reflect on the adhesion capability for the TPO material rather than the accelerated testing.
- Fractography is different for DH4000 sample (embedded glass) than unaged (includes inelastic deformation). Suggests notable degradation has occurred at the interface from DH.
- Is Solite less robust to DH than other makes of glass? The rolled surface seems prone to crumbling with DH.
- Comparison of EVA & TPO: greater loss of transmittance for EVA, suggests a reaction is occurring between by product of glass corrosion and encapsulant. Like acid/base reaction.

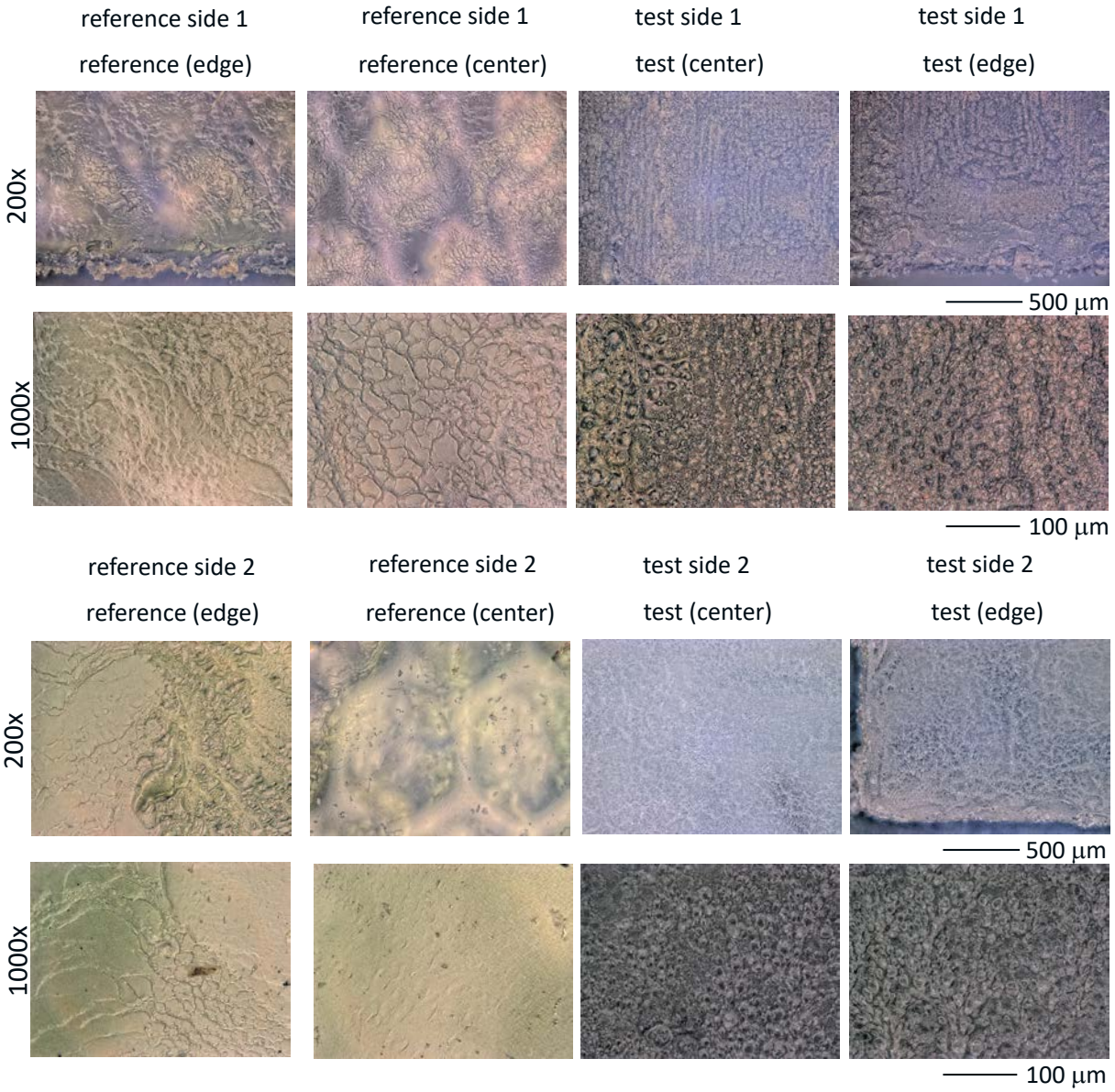

Representative microscope images, from unaged and DH aged coupons, from the "center" location.

OMI Verifies Specimen Recovery After Damp Heat

- Solite/EVA/Solite specimen characterized after 4000 h 85°C/ 85%RH.
- >20% τ_h loss confirmed on OMI.
  https://doi.org/10.1109/JPHOTOV.2021.3122925
- Precipitate formation, adhesion reduction observed at glass/encapsulant interface in destructive failure analysis.
- τ_h recovered in subsequent OMI examination!

Appearance of specimen G-DH-3 (Damp Heat aging).

2020/9 measurement

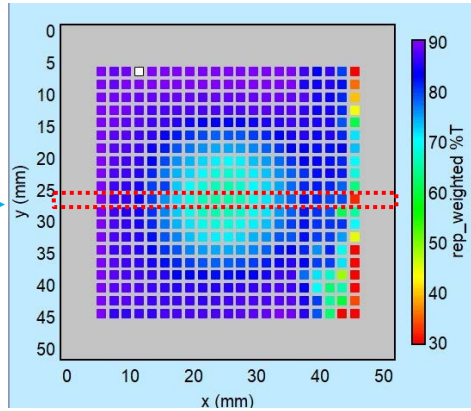

- τ_d (spectrophotometer, no integrating sphere) remains distinguished within recovered specimen.

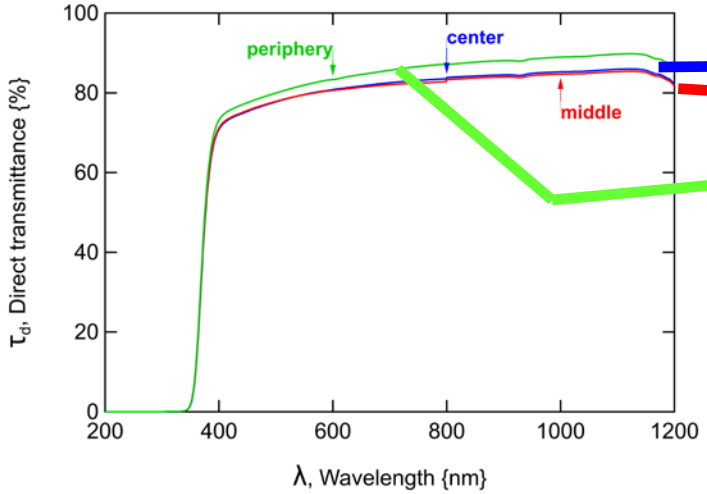

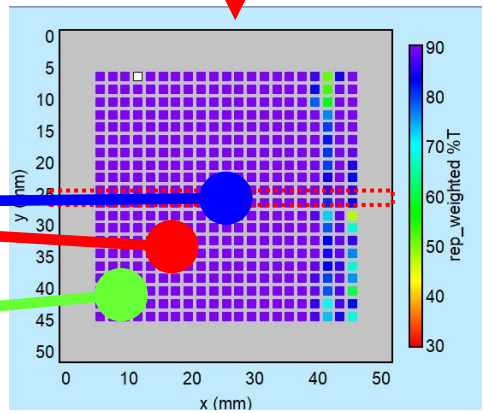

2022/4 measurement

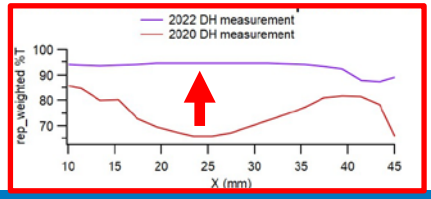

UV-VIS Fluorescence
(Comparing EVA-A in Glass Configurations for A3 Weathering)

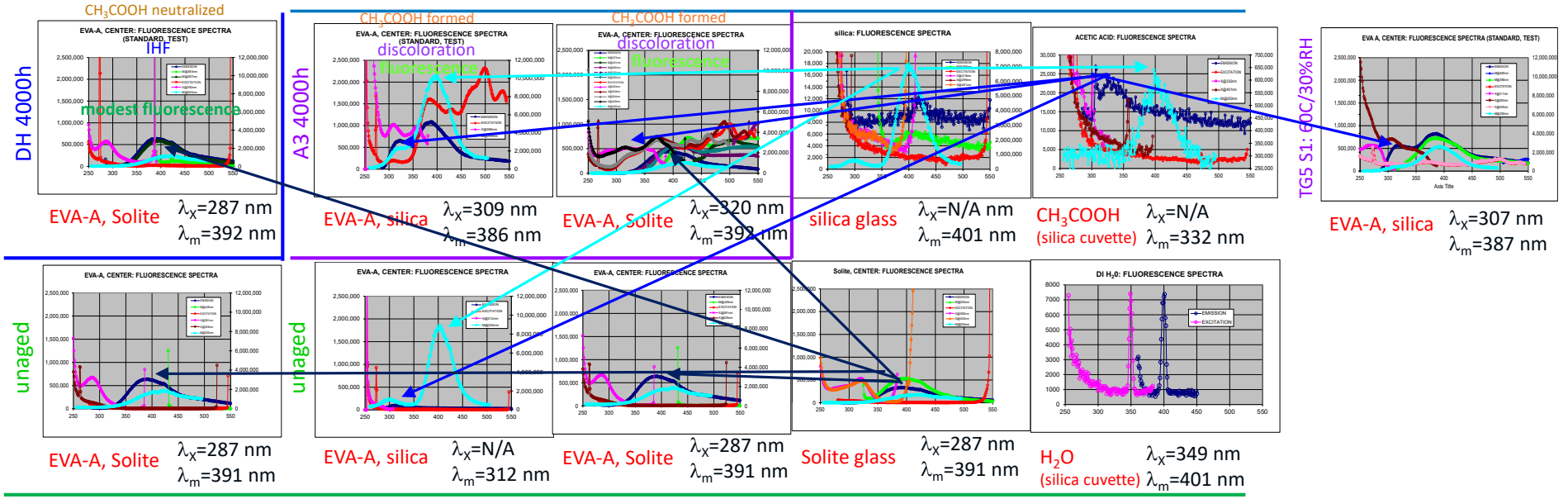

- Acetic acid: emission peak at 332 nm. Possible method to verify CH_3COOH. H_2O: emission peak at 401 nm.
- Solite glass: excitation and emission peaks may mask fluorophore species.
- Silica glass: emission at 401 nm.
- Similar spectra (peak locations) are observed in fluorescence spectroscopy between the DH aged EVA-A and EVA-3 coupons.
- Additional references: https://doi.org/10.1002/pip.3551, https://www.nrel.gov/docs/fy22osti/81505.pdf

UV-VIS Fluorescence
(Comparing EVA-3 in Glass Configurations for A3 Weathering)

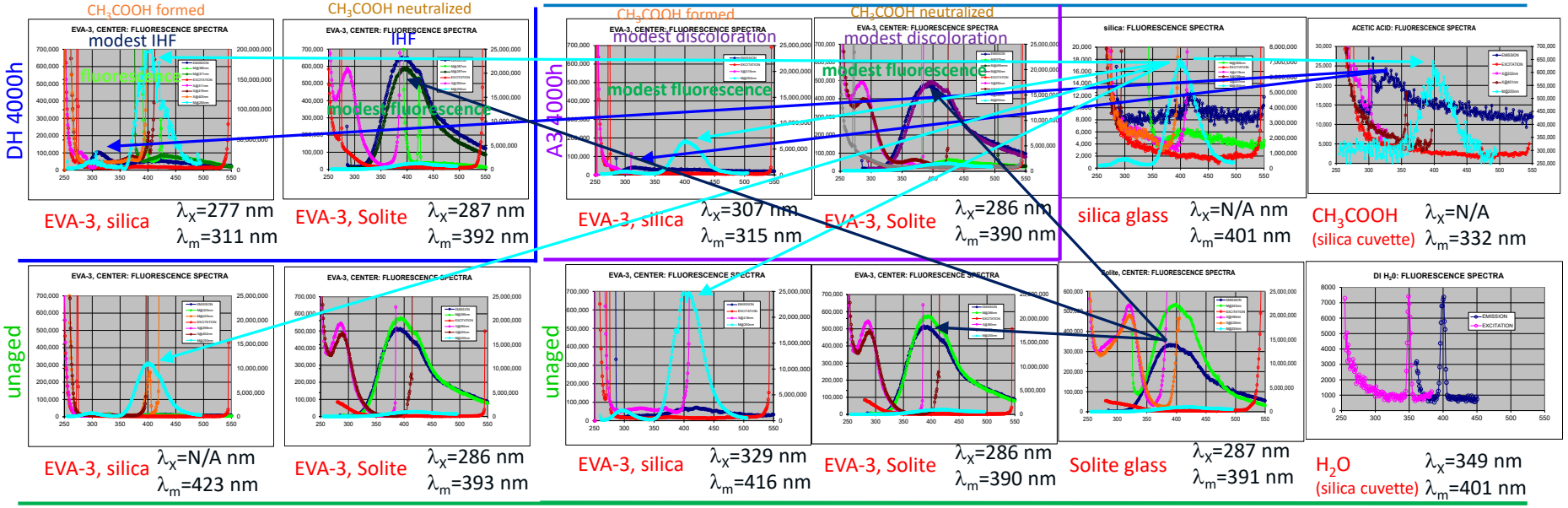

- The emission peak at 332 nm does seem inversely proportional to IHF for DH aging: it is present for silica glass, but absent (presumably neutralize) for Solite.
- Additional references: https://doi.org/10.1002/pip.3551, https://www.nrel.gov/docs/fy22osti/81505.pdf

Comparison of Fluorescence Spectra (Polyolefin Materials)

M (TPO-1, lower crystallinity, no UV absorber)

E (TPO-2, higher crystallinity, no UV absorber)

D (TPO-3, contemporary, with UV absorber)

J (POE-1, with UV absorber)

A (POE-2, no UV absorber)

A5

A4

A3

unaged

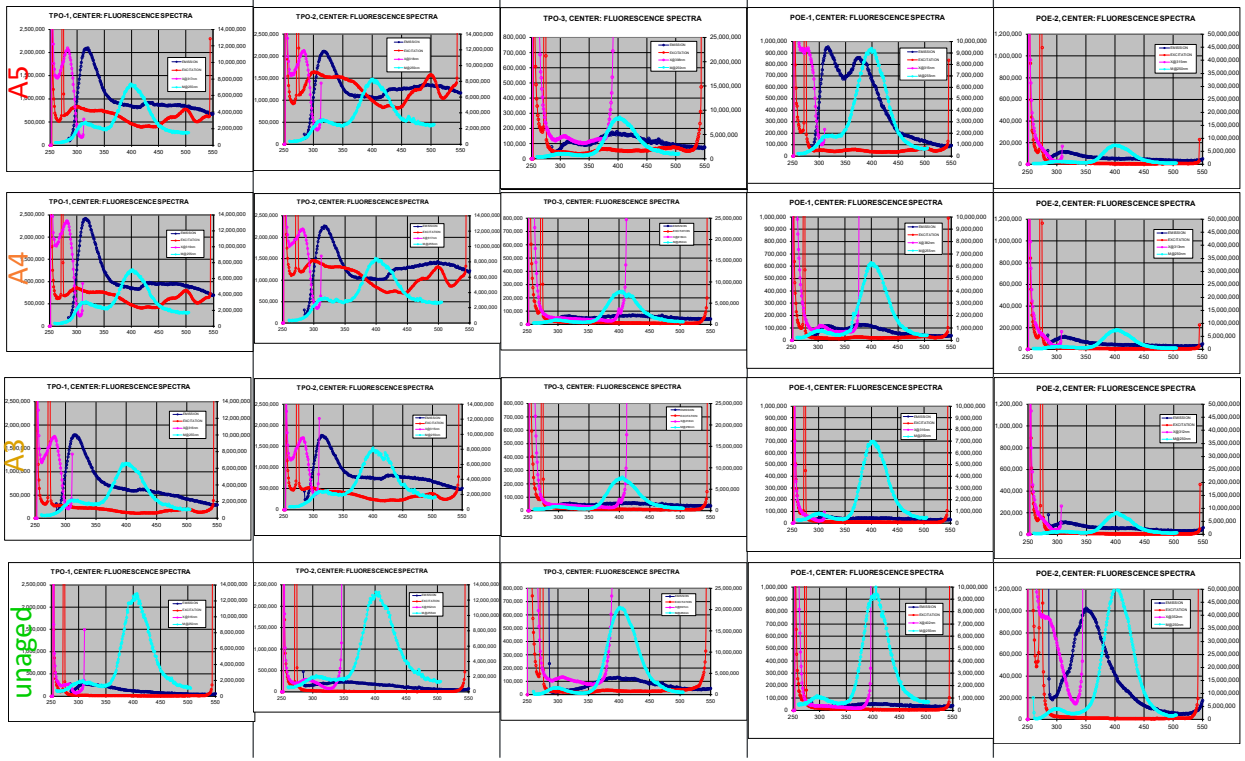

DH (Solite)

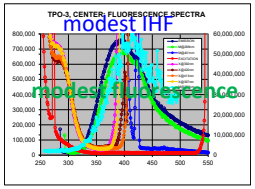

unaged (Solite)

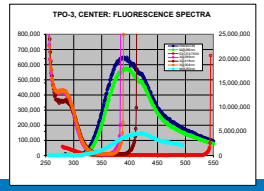

- Additional references: https://doi.org/10.1002/pip.3551, https://www.nrel.gov/docs/fy22osti/81505.pdf

Comprehensive Optical Analyses

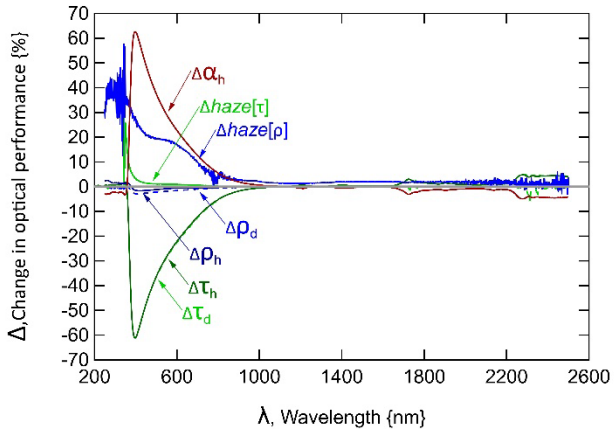

G (EVA-A) A5 4000h

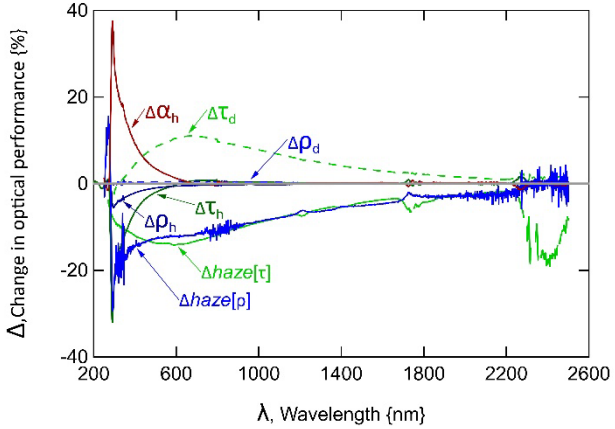

E (TPO-2) A5 4000h
most crystalline

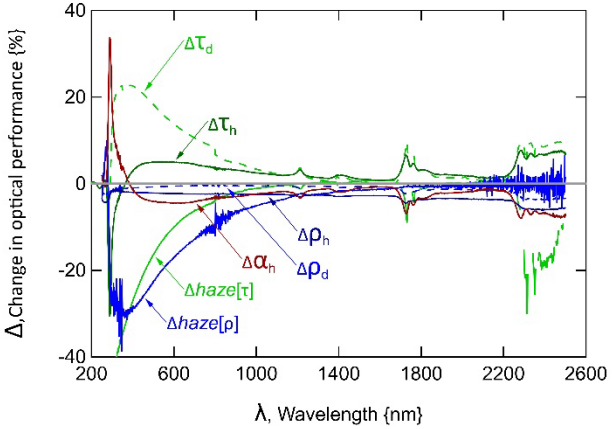

M (TPO-1) A5 4000h
less crystalline

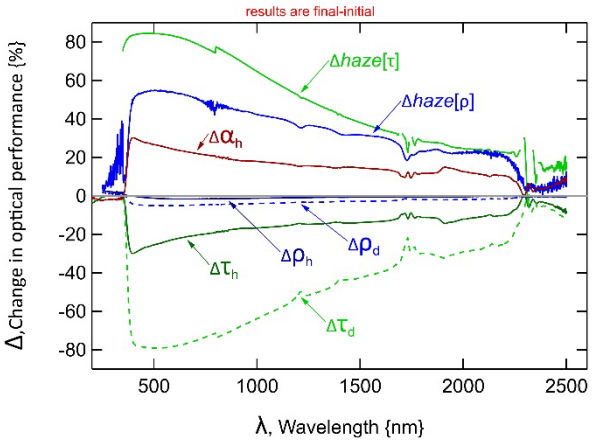

G (EVA-A) DH 4000h

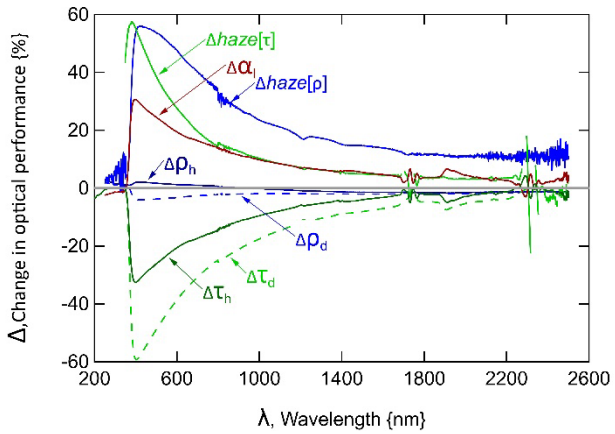

I (EVA-3) DH 4000h

- Glass corrosion gives both reflectance (reduced, AR effect) and absorptance (increased, scattering).
- Reflectance is minimal (ignore) for IHF, just absorptance (increased, scattering).
- Additional references: https://doi.org/10.1002/pip.3551, https://www.nrel.gov/docs/fy22osti/81505.pdf

Comparison of Reflectance of Unaged MiMo (EVA_b vs EVA_t)

ρ_{total} $\rho_{air/glass}$ $\rho_{glass/encapsulant}$ $\rho_{encapsulant/ARc/Si}$

$$F_r[\lambda] = \left(\left(\frac{\rho_{air/glass}}{100}\right) + \left(\left(1-\frac{\rho_{air/glass}}{100}\right)^2 \left(1-\frac{\alpha_{glass}}{100}\right)^2 \left(\frac{\rho_{glass/ecapsulant}}{100}\right)\right) + \left(\left(1-\frac{\rho_{air/glass}}{100}\right)^2 \left(1-\frac{\alpha_{glass}}{100}\right)^2 \left(1-\frac{\rho_{glass/ecapsulant}}{100}\right)^2 \left(1-\frac{\alpha_{encapsulant}}{100}\right)^2 \left(\frac{\rho_{E-AR_C-c}}{100}\right)\right)\right)$$
$$+\left(\left(1-\frac{\rho_{air/glass}}{100}\right)^2 \left(1-\frac{\alpha_{glass}}{100}\right)^2 \left(1-\frac{\rho_{glass/ecapsulant}}{100}\right)^2 \left(1-\frac{\alpha_{encapsulant}}{100}\right)^2 \left(1-\frac{\rho_{E-AR_C-c}}{100}\right)^2 \left(1-\frac{\alpha_{ARc}}{100}\right)^2 \left(1-\frac{\alpha_{Si}}{100}\right)^2 \left(\frac{\rho_{Si/Al}}{100}\right)\right)$$

ρ~0 $\rho_{Si/Al}$

$$F_{rT} = F_{r1} + F_{r2} + F_{r3} + F_{r4}$$

- A return function for the reflected light might be used to analyze measurements from a module or MiMo.
- Three terms dominate the initial reflection (single pass reflections only).
- A small band from ~300<λ<400 nm might be used to evaluate if encapsulant is UV blocking or transmitting or blocking. Distinction possible, may depend on cell type and using a reference.

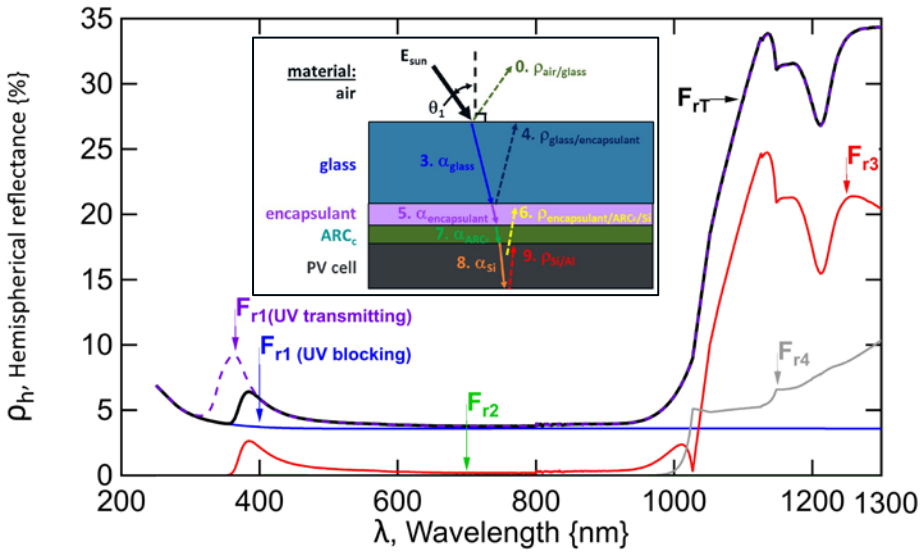

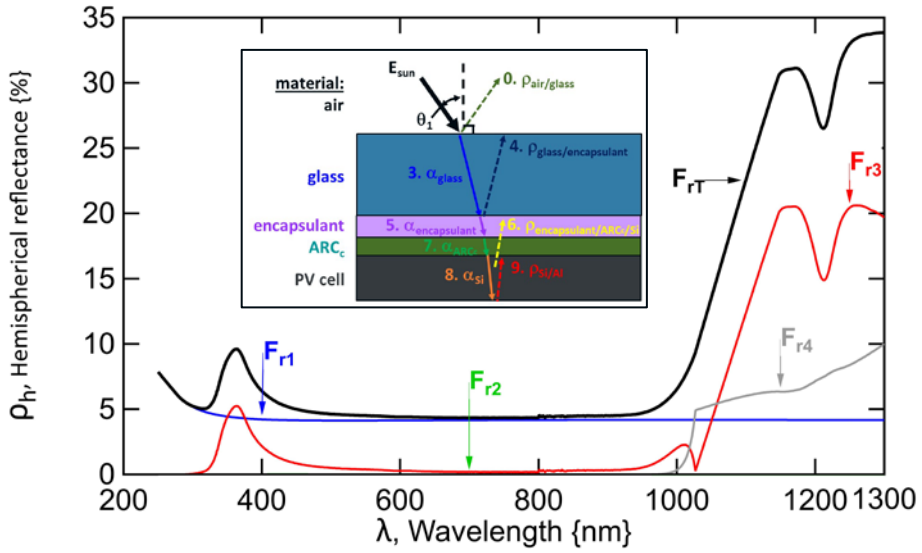

Overlay of spectra of reflectance components and the cumulative return function for MiMo with UV blocking EVA (left) and MiMo with UV transmitting EVA (right).

Reflectance of Contemporary PV Cells

- ρ of cells examined in this study was measured, both front (sun) & back (air) surface.
- Mostly contemporary cells examined (RJC, HJ, PERC, PERT) including mostly bifacial, few legacy cells (BSF).
- Difference in reflectance is expected for encapsulant/cell vs. air/cell configurations.
- Incident surface suggests localized performance improvement of SiN coating (with destructive interference) with the spectrum broadening effect of textured Si surface.
- Back surface reflectance is not as optimal (metallization and/or processing), including bifacial.

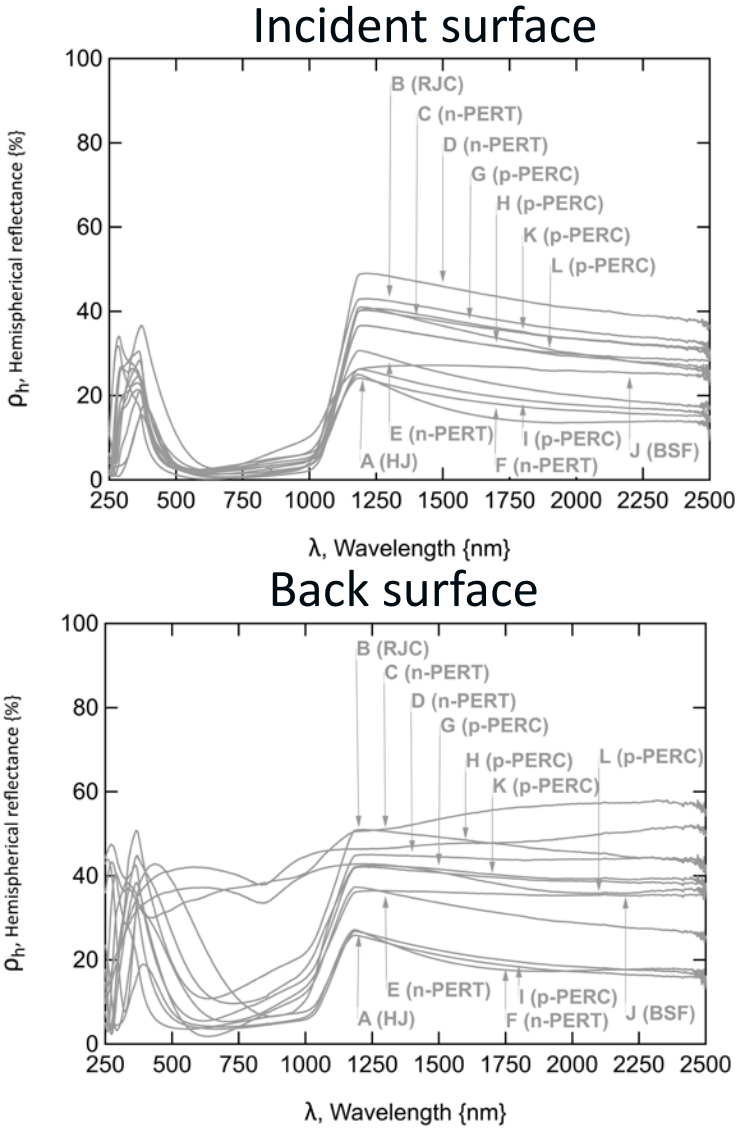

Measured reflectance (in air) for the cells used in the screen test for this project, including cell front (top) and cell back (bottom)

About Analysis to Solve for encapsulant/AR$_c$/cell

- Best resource for *n*, *k*: Palik et. al. Notable difference between measured & analyzed reflectance from silica/EVA$_t$/cell coupon for λ>975 nm for Schinke et. al.
  - -Smoothed *k* from Palik for $1028 \le \lambda \le 1051$ nm $\rightarrow$ $1028 \le \lambda \le 1147$ nm to avoid spurious spike, larger bump not observed in measurement.
  - -Subsequently smoothed EVA/SiN/Si $1028 \le \lambda \le 1051$ nm to remove spurious dip and $1051 \le \lambda \le 1147$ nm to match the measured reflectance.
- Fit appears to be good to $\lambda \le 1547$ nm for EVA/SiN/Si stack.
  - -Only -very- negative solutions $\lambda \le 250$ nm.
  - -α (aka f_{r4}) taken as $1 \cdot 10^{-12}$ for $\lambda \le 869$ nm. α_{Si} is ~100% at these wavelengths.
  - -Double root (or similar) solution for λ>1875 nm.
- Implication: reflection and multiple passes through Si are really intended/affect wavelengths near the band-edge at 1100 nm.

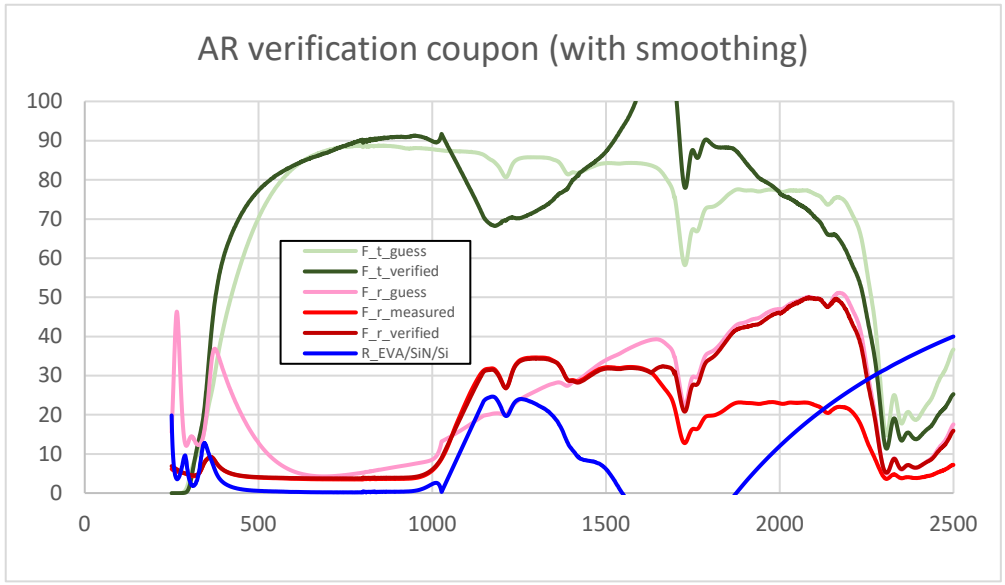

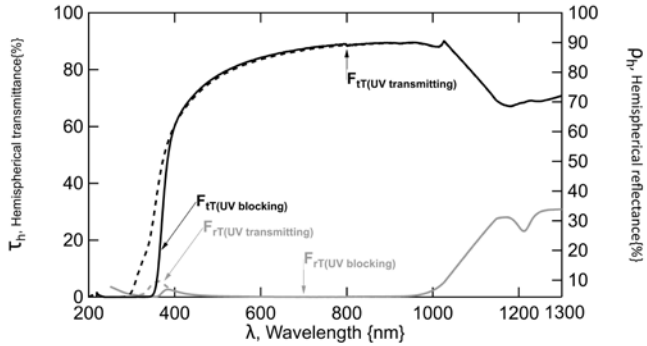

Overlay of spectra of the transfer and return functions for MiMo with UV blocking EVA or UV transmitting EVA.

Comparison of estimates (from complex refractive index only no graded index for multilayer stack), measured reflectance, and analysis (smoothed solution from 1028-1147 nm).

Implications of Degradation of the AR_c

- τ_h of 20% for $\rho_{EVAt/Si}$ explains why an AR_c is used on cells in today's PV industry.
- τ_h of 20% not observed on HV-/HV+ specimens in this study $\rightarrow$ much of the micro-scale surface texture and Si_xN_y ARc remain after accelerated testing.
- Identify and diagnose reduction in Si_xN_y thickness from decrease in λ of reflectance minima.
- Micro-scale surface texturing broadens and flattens the reflectance minima, making changes more difficult to observe.
- Substantive change in the micro-scale surface texture would require chemical process(es) that affect Si_xN_y then possibly also Si.

Microscopy: Morphology & Colorimetry of UV-LID Samples

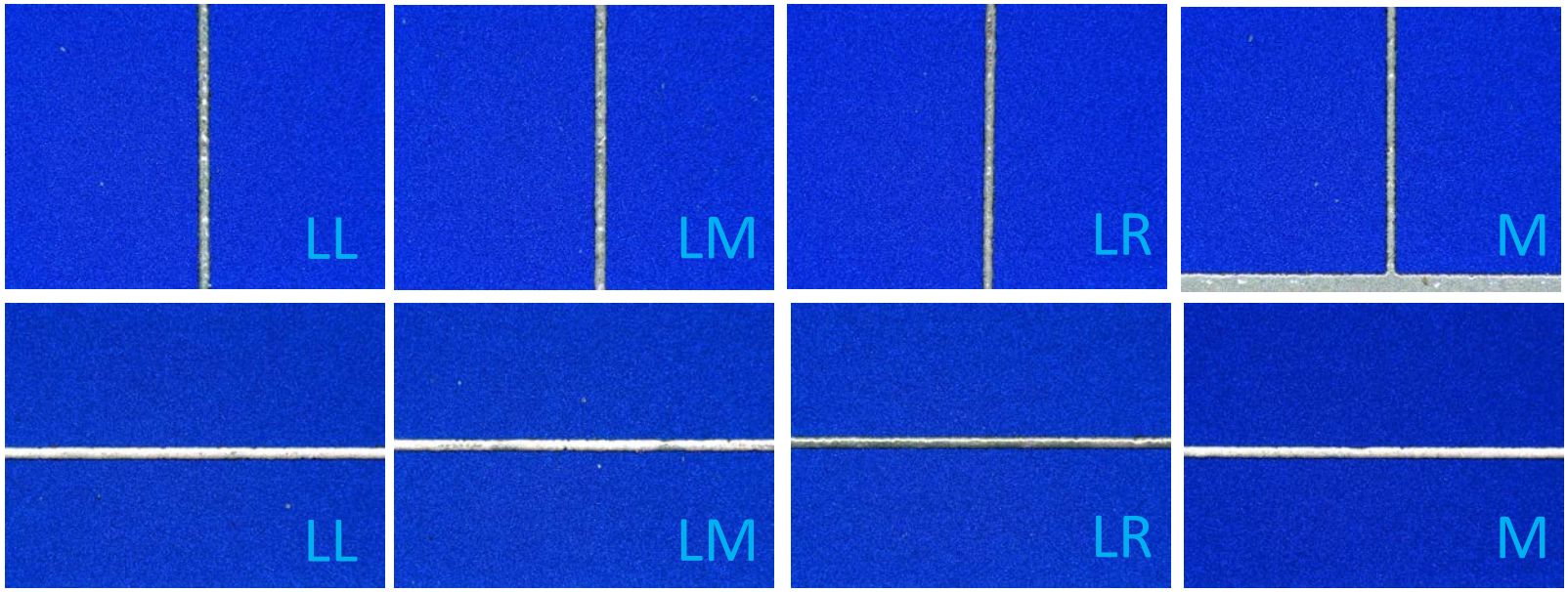

Measurement locations
(Keyence images at 30x, 200x):

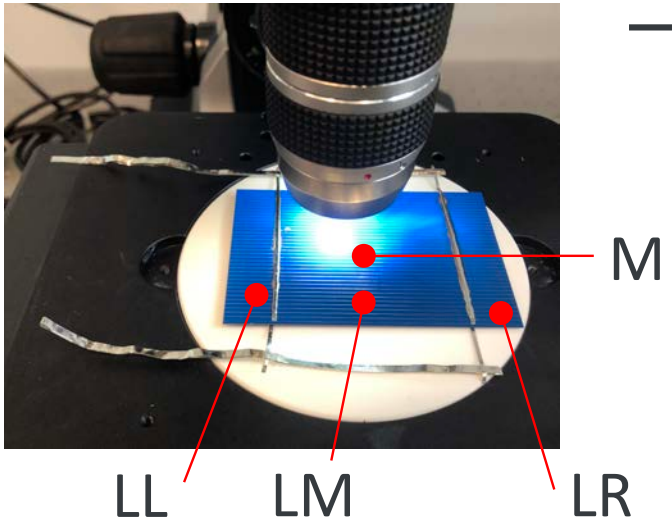

Microscopy: Morphology & Colorimetry of UV-LID Samples

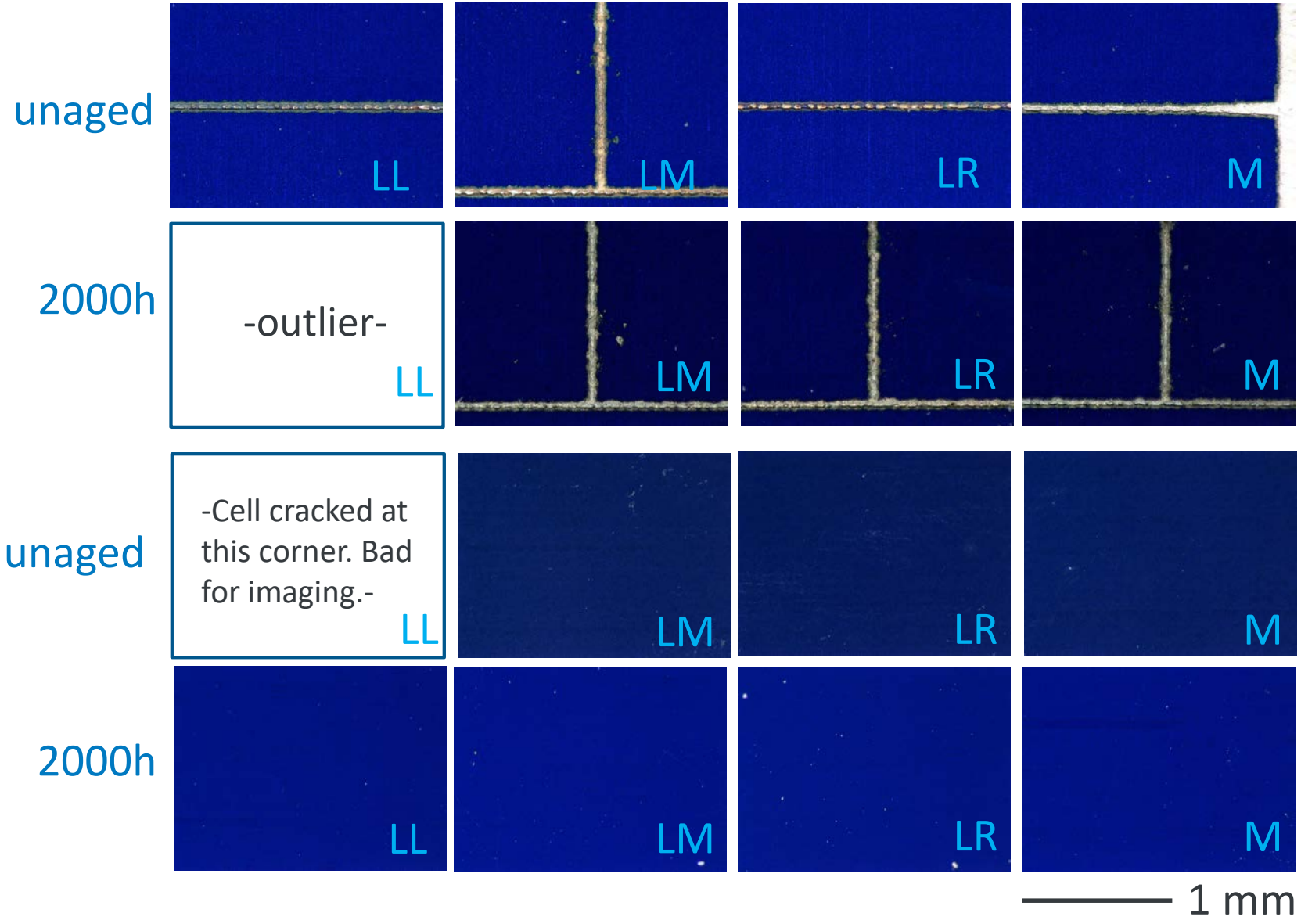

Subtle Differences Observed in Spectrophotometry

- Samples were measured test (UV screen test 1) then reference through each make, then repeated 3x inseries.
- Different areas of each specimen were examined in different scans.
- Subtle, not major changes observed.
- A systematic difference, believed to be an artifact of the measurement (detector + grating change at 800 nm) was observed for HJ.
- More unique differences that cannot be attributed to measurement artifacts (source change at 350 nm) observed for $\lambda < 500$ nm n-PERT and IBC.
- Unclear if any of the differences result from specimen variation (diced samples, not obtained from same cell).
- Anticorrelation observed between B (from RGB) and YI (negative YI value indicates blueness) for Keyence & Cary.
- Compare to past & future EQE measurements, especially n-PERT & IBC.
- Ship samples to SLAC for XPS?
- Does this help with UV-LID paper? Nemeth Si_xN_y AR sample more definitive?

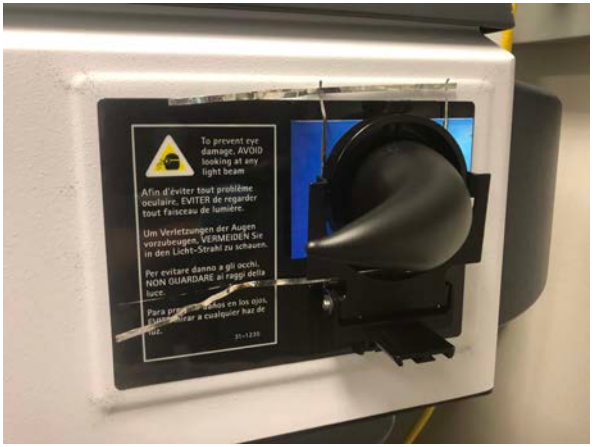

Test cell and light trap on the spectrophotometer.

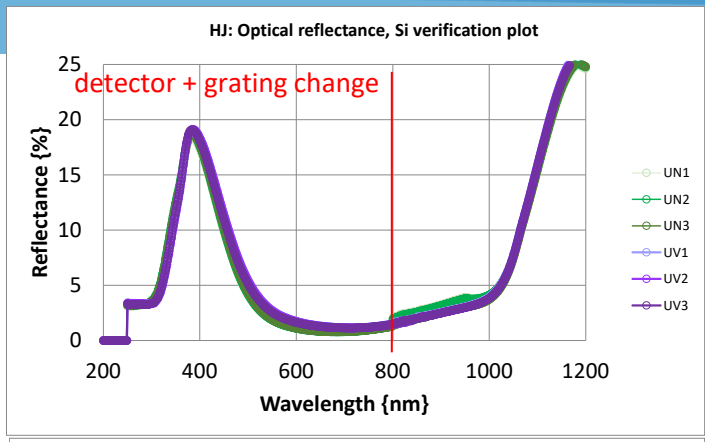

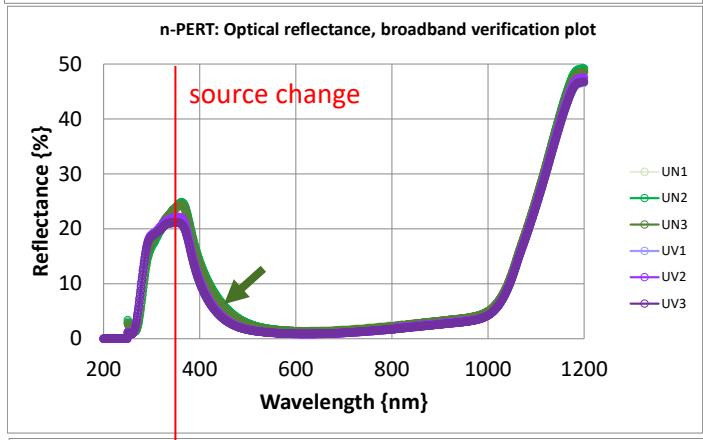

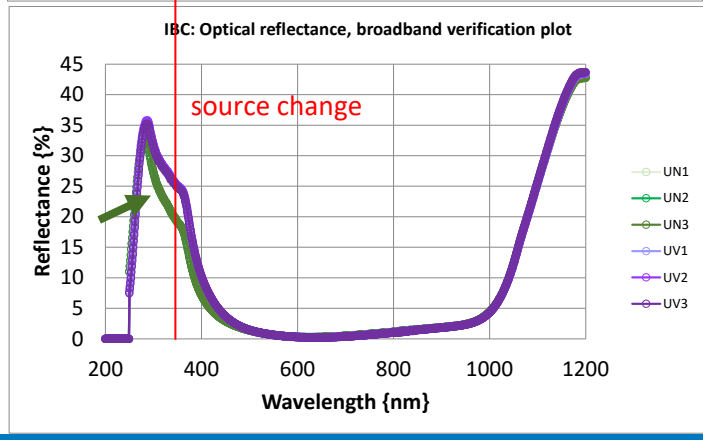

Microscopy: Morphology & Colorimetry of UV-LID Samples

- Microscope images taken on Keyence after white balancing and setting to same illumination mode and intensity.
- Comparing test and reference sample images: microscopy does not indicate coarse damage to AR or metal grid lines.

- RGB extracted with PhotoShop InkDrop tool from T, L, M, R, B of each 200x image (200x was more consistent brightness and contrast across samples than 30x).
- Differences were observed in color, exceeding 2 sigma variation, particularly for Blue.
  - -Cut samples not tracked relative to original cells. Samples could be from different cells.
  - -Could result from thickness/processing variation for the AR during manufacturing.
  - -May have been at slightly different angle during measurement (especially test cells with ribbon)

MAKE	CONDITION	READ POINT	R	G	B	ρ, solar weighted {%}	ρ, representative weighted {%}	YI, 1964
ASU	unaged	AVG	14±11	49±13	217±15	9.2±0.4	6.0±0.1	-333±4
ASU	UV suitcase 2000 h	AVG	10±9	53±19	197±22	9.2±0.2	6.3±0.2	-267±65
ASU		DELTA	-3	4	-20	0.0	0.3	65
PVGS	unaged	AVG	4±3	17±7	136±20	18.2±0.3	8.7±0.1	-224±17
PVGS	UV suitcase 2000 h	AVG	2±2	5±5	71±19	17.1±0.4	7.9±0.2	-228±22
PVGS		DELTA	-2	-12	-65	-1.0	-0.9	-5
SunPower	unaged	AVG	8±4	30±6	94±12	15.4±0.0	7.1±0.0	-320±4
SunPower	UV suitcase 2000 h	AVG	2±2	20±4	133±13	15.9±0.1	7.4±0.3	-398±15
SunPower		DELTA	-10	-17	29	0.5	0.3	-78

Estimated Impact of the HV-/HV+ Test

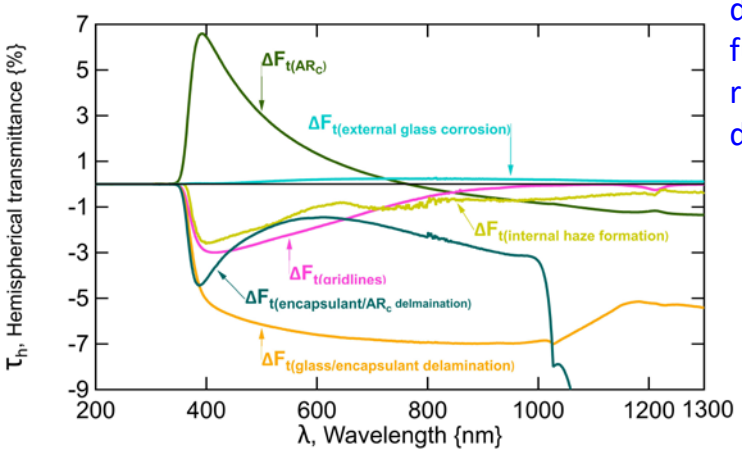

dF_t : change in transfer function, removing individual degradation modes

dF_r: change in return function, removing individual degradation modes.

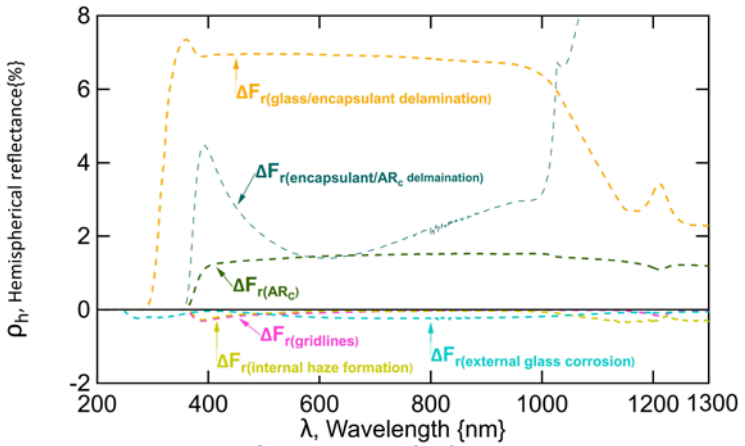

Observations:

- External glass corrosion increases the net transmittance (F_t) and decreases the net reflectance (F_r).
  - Small magnitude of effect, equal for F_t and F_r, centered at ~750 nm.
- Glass/encapsulant delamination decreases F_t, correspondingly increases F_r.
  - F_r affected at λ ~55 nm shorter than F_t (UV blocking encapsulant).
- IHF and gridline corrosion both decrease F_t and F_r by similar amounts, respectively.
  - Effect of each degradation mode is, however, an order of magnitude greater for F_t than F_r .
- Encapsulant/AR_c delamination decreases F_t, correspondingly increases F_r.
  - Below 1025 nm, net effect is less than at the glass/encapsulant interface.
- AR_c corrosion gives monotonic increase in F_r, with a more complex variation in F_t with wavelength.
- Rank order for F_t, (most reducing to most enhancing): c > f > e ~ d > a + b > g + h.
- Rank order for F_r, (most increasing to most reducing): c > f > g + h > e ~ d > a + b.
- Delamination (both glass/encapsulant and encapsulant/AR_c) and external glass corrosion give nearly equal and opposite effect on F_t and F_r, respectively.
- Combined effects of multiple modes distinguish delamination between the encapsulant surfaces: the net effect of combined modes relative to just the glass/encapsulant interface; the combined modes relative to just the encapsulant/AR_c interface.

Estimated Impact of the HV-/HV+ Test

Implications:

- External glass corrosion acts as AR layer: minor contributor for F_t, relatively more significant for F_r.
- $\Delta\lambda$ glass/encapsulant delamination: light reflects off surface of EVA_b for F_r passes through EVA_b in F_t.
- Estimates for IHF and gridline corrosion are taken for $\Delta\alpha$ only, not represented in model for F_r.
- Net effect of encapsulant/AR_c delamination reduced because of diminished solar intensity at longer λ's in addition to H_2O absorption band at ~1130 nm.
- F_r from AR_c corrosion results from smoothed corroded $\rho_{EVAb/ARc/Si}$ spectra. F_t depends on absorptance of Si_xN_y at short wavelengths and increased reflectance of corroded $\rho_{EVAb/ARc/Si}$ beyond 760 nm.
- Combined effect of degradation modes accentuates glass/encapsulant delamination relative to encapsulant/AR_c delamination, where F_r is reduced by the time it reaches the surface of the glass.
- Some degradation modes may occur during HV-/HV+ in addition to Damp Heat; others were only observed when an external voltage bias (HV+) was applied.

Estimated optical loss in F_t and F_r, for each degradation mode and the combined modes (with or without encapsulant delamination).

					HV-/HV+		
DEGRADATION MODE	LOCATION	MAY OCCUR DURING DAMP HEAT?	MAY OCCUR DURING HV-?	MAY OCCUR DURING HV+?	OCCURS IN TEST SPECIMEN (THIS STUDY)?	ΔF_t (300 nm -1250 nm) {%}	ΔF_r (300 nm -1250 nm) {%}
a + b: external glass corrosion	incident glass surface	y	y	y	y	0.2	-0.2
c. delamination	glass/encapsulant	n	?	y	n	-6.4	6.3
d. internal haze formation (immediately after aging)	glass/encapsulant	y	y	y	y	-1.0	-0.1
e: gridline corrosion + migration	encapsulant/AR_c	n	n	y	y	-1.1	-0.1
E: gridline corrosion + delamination (H_2 evolution)	gridline	n	y	n	n	N/A	N/A
f: delamination	encapsulant/AR_c	n	n	y	n	-4.5	3.8
g + h: AR_c corrosion	AR_c	n	n	y	y	0.6	1.4
1: a + b + c + d + e + g + h (including front delamination)	multiple	n	n	y	n	-7.7	7.6
2: a + b + d + e + f + g + h (including rear delamination)	multiple	n	n	y	n	-5.8	5.1
3: a + b + d + e + g + h (no delamination)	multiple	n	n	y	y	-1.3	1.4

Considering the Present Results…

- Comparing experiment and reference measurements suggests optical model is not complete (greater bandwidth for low ρ). AR_c likely includes pyramidal texturing.
- May also be tailored SiN thickness (vs. 80 nm); use of SiO_2- or black-Si-sublayers.

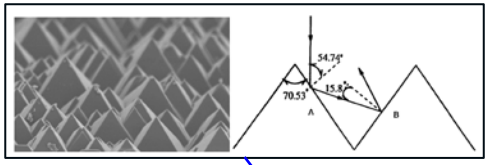

From S. Al-Turk, "Analytic Optimization Modeling of Antireflection Coatings for Solar Cells", MS Thesis, McMaster Univ., 2011.

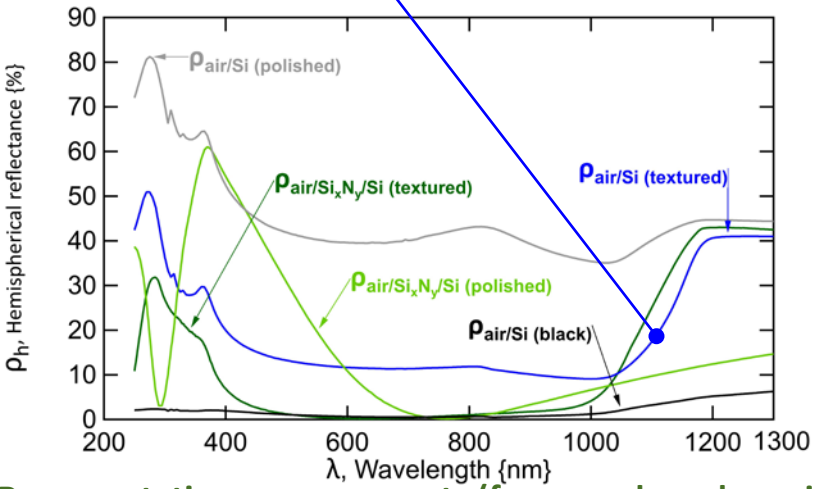

Representative measurements (for unpackaged specimens in air) showing the optical effects (reflectance) through the technological advancements in cell passivation.

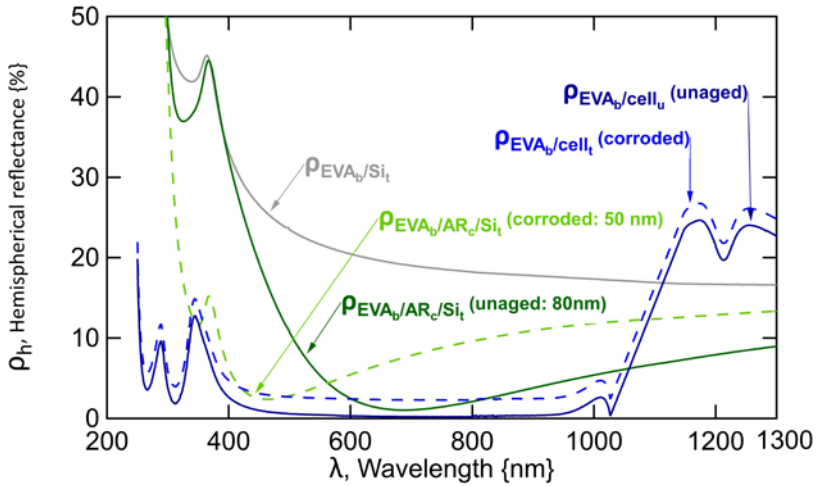

Spectra for packaged specimens (at interface with UV transmitting) showing the optical effects (reflectance) that might be encountered from degradation.

- Modeling effect of corrosion: an offset of 2.1% for $\rho_{EVAt/ARc/Si\text{-}textured}$ gives less red shift at 400 nm than $\rho_h = c_1 (\rho_{EVAt/ARc/Si\text{-}textured} - \rho_{EVAb//Si})$.

Regions in Voltage Degraded Sample Are Readily Distinguished in Reflectance Measurements

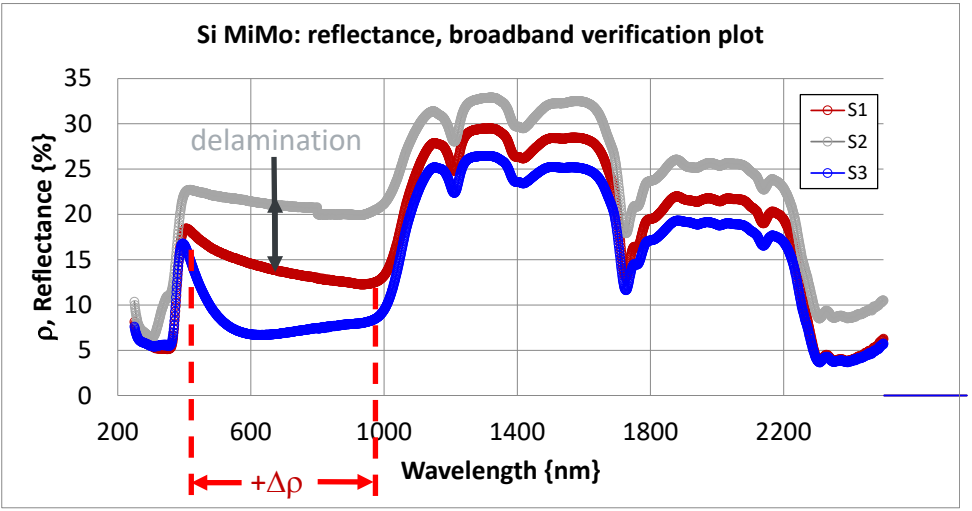

- Artificially weathered MiMo specimen (dark/85C/85% RH/+1000V).
- ~4% reflectance of delaminated region is immediately distinguished.
- Discoloration and loss of reflectance distinguished in visible region (400-1000 nm).
- Some loss of light likely from cracked (tempered) glass.
  (1 cm x 7 mm measurement area).
- Could compare to FL modules for validation. No shattered glass.

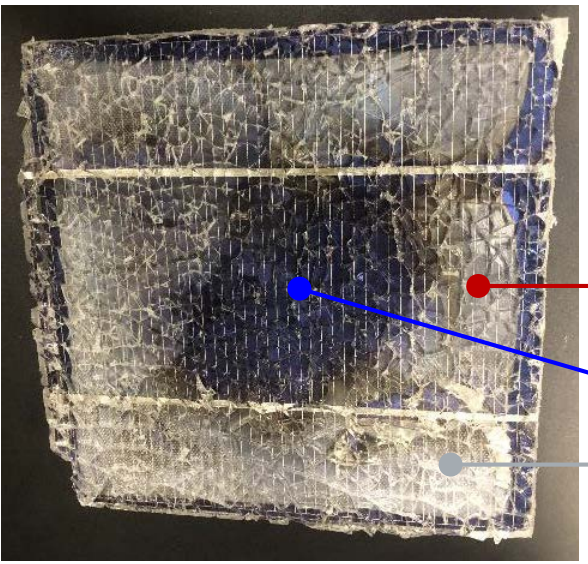

Si_xN_y discolored, no delamination

Si_xN_y not discolored, no delamination

Si_xN_y discolored, with delamination

Reference (for thickness of SiN from color): Henrie et. Al., Opt Exp., 2004.

Keyence Imaging Locations (Green #'s) for M1007-0059

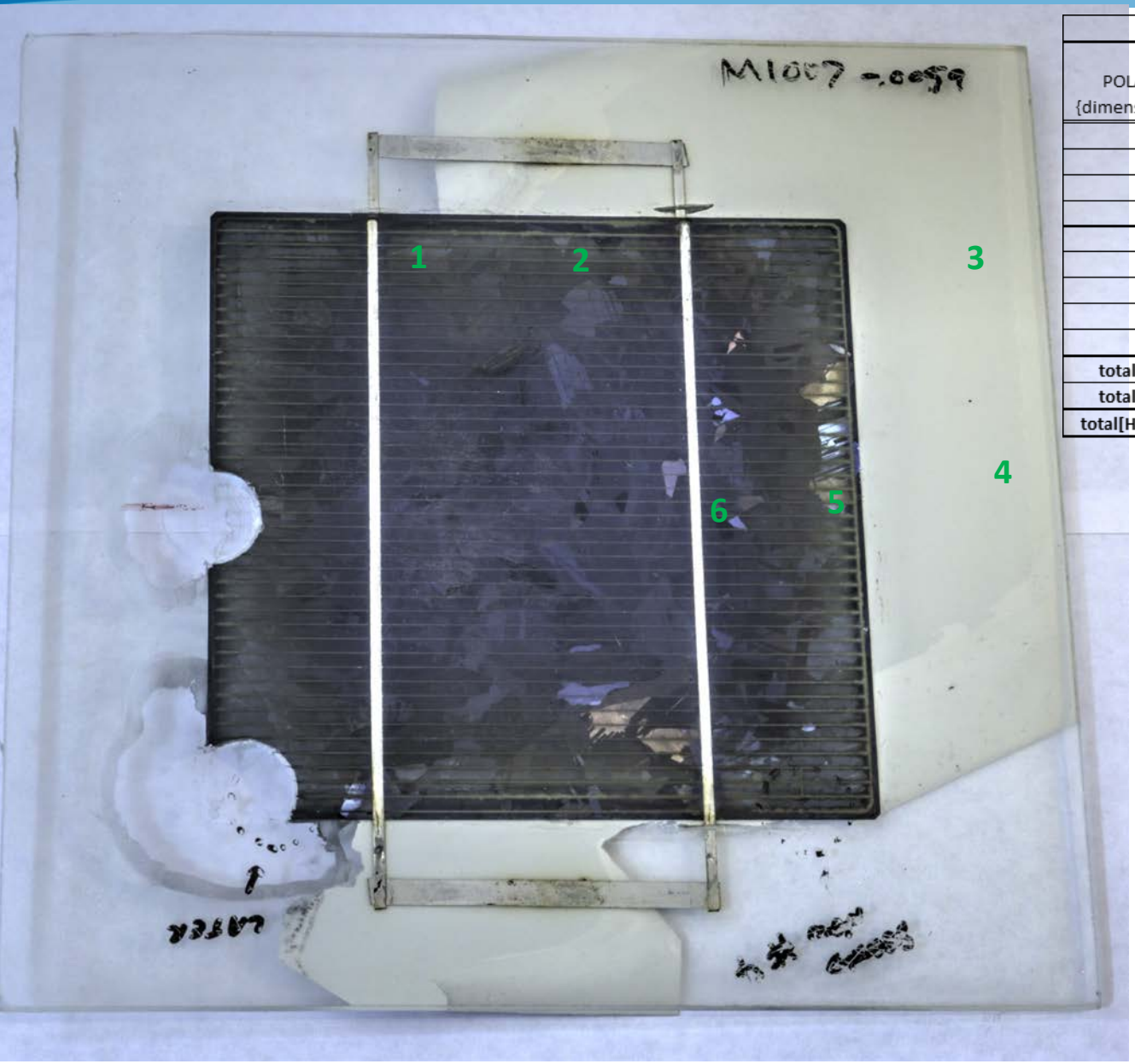

M1007-0059				
POLARITY {dimensionless}	NOMINAL DURATION {h}	EFFECTIVE DURATION {h}	ChT {°C}	ChRH {%}
-	28	1	45	30
-	195	10	50	50
+	195	10	50	50
-	219	28	60	50
+	166	21	60	60
-	195	49	70	70
+	170	43	70	70
-	169	169	85	85
+	168	168	85	85
total [HV-]	**806**	**256**		
total[HV+]	**699**	**241**		
total[HV-/HV+]	**1505**	**497**		

Keyence Imaging Locations (Green #'s) for M1007-0078

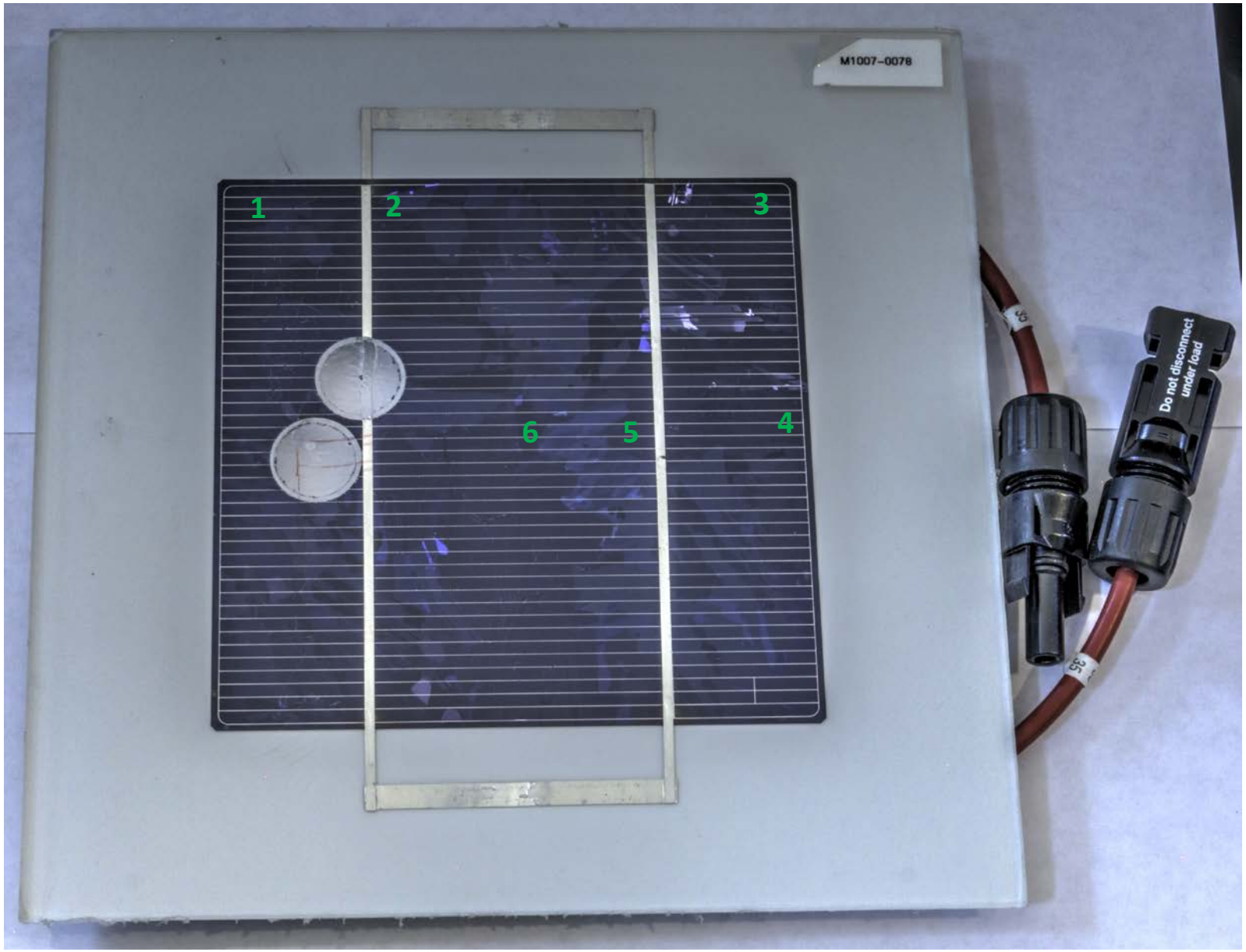

Microscopy of HV-/HV+ samples

M1007-0078
(unaged reference)

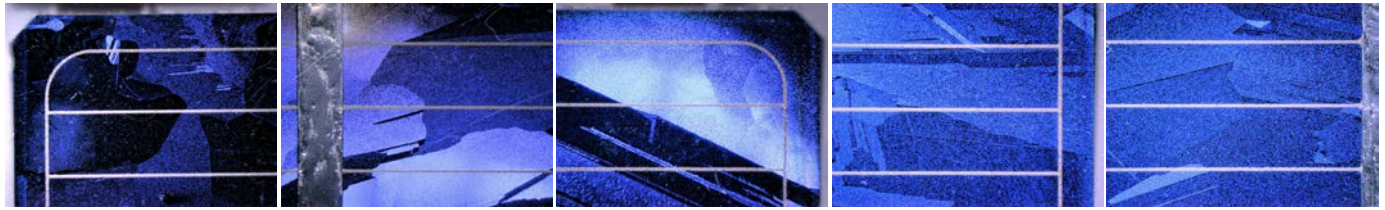

M1007-0059
(test HV-/HV+)

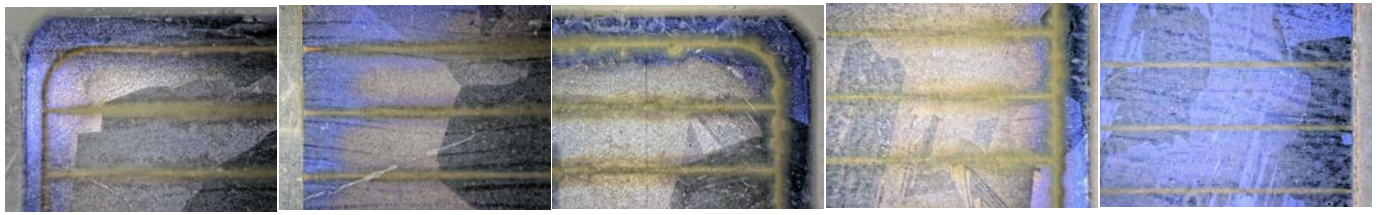

- Obvious differences between the color of the AR coating and grid lines for test and reference samples.
- Extent of effect (color as well as width of corroded gridline) varies with location on the test specimen.
- Range of additional affected area (space – delta width): 2% (middle) – 8% (corners).
  - -2% line width increase observed/representative of the interior of a cell.
  - -5-8% line width increase observed/representative of the corners of a cell.
  - -Greater corrosion at periphery: S or O_2 cannot transport through the center of the Si cell.
  - -While EL imaging shows reduced performance, gridline corrosion at cell corners may not solely limit PV current generation.

IBC Cell Measured to Determine Reflectance of Encapsulant/AR/Si Interface

- The reflectance of encapsulant/AR_c/Si (bulk/film/bulk) depends on proprietary design & manufacturing characteristics of the AR_c film → determine ρ empirically.
- Approach: back-calculate from known characteristics of glass, encapsulant, etc.
- Specimen geometry: silica (1/16”, 6” x 6”)/1x UV transparent EVA (STR 15585)/cell (IBC ~5”)/1x UV transparent EVA (STR 15585)/ TPE (Madico) backsheet.
- Good overlap observed between 6 replicate measurement profiles from coupon sample.
- No significant difference between corner measurement (with light trap) and middle measurements (no light trap).

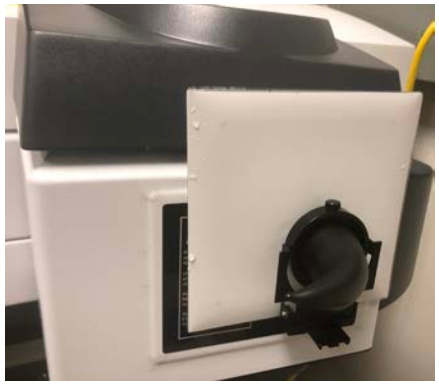

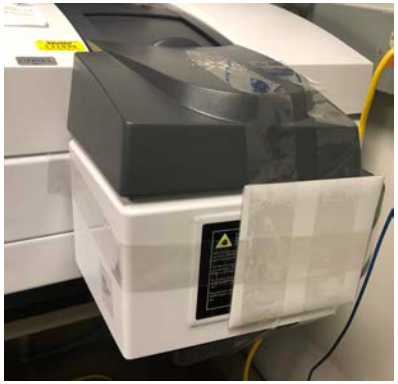

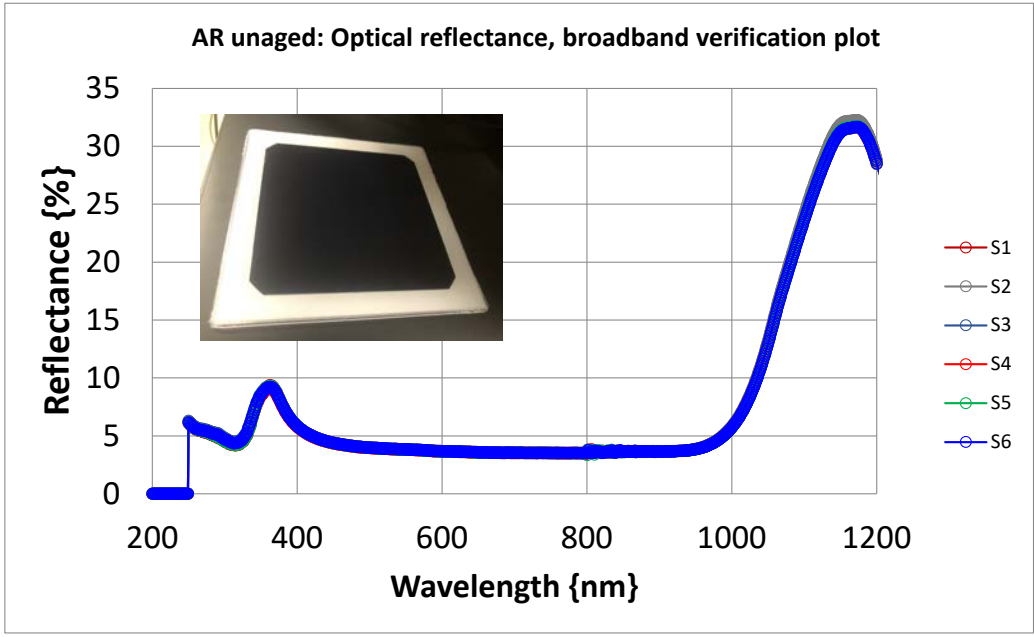

Configuration for middle measurement on spectrophotometer: (left) with and (right) without light trap.

Reflectance Measurement Locations for HV-/HV+ MiMos

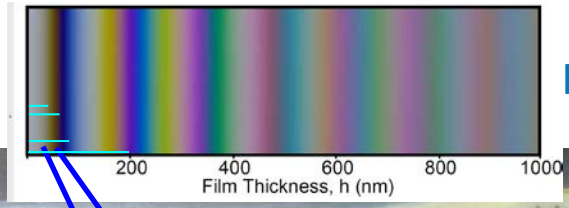

Henrie et. al, Opt. Exp, 2004.

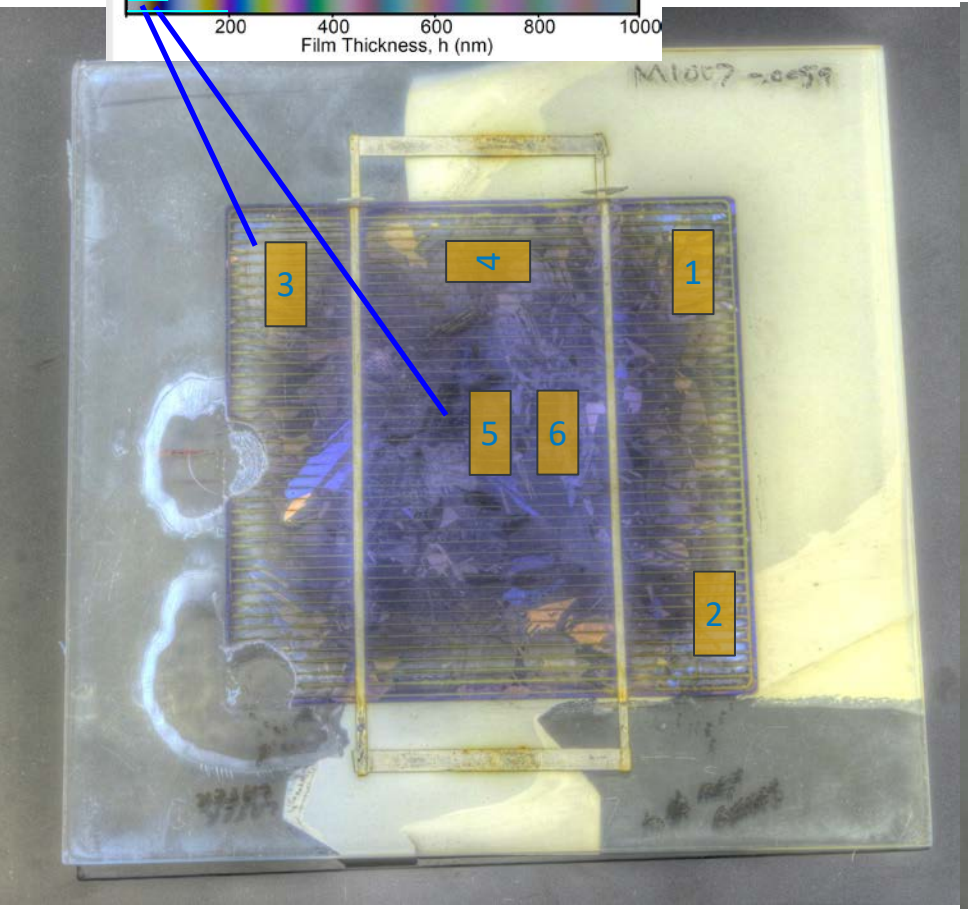

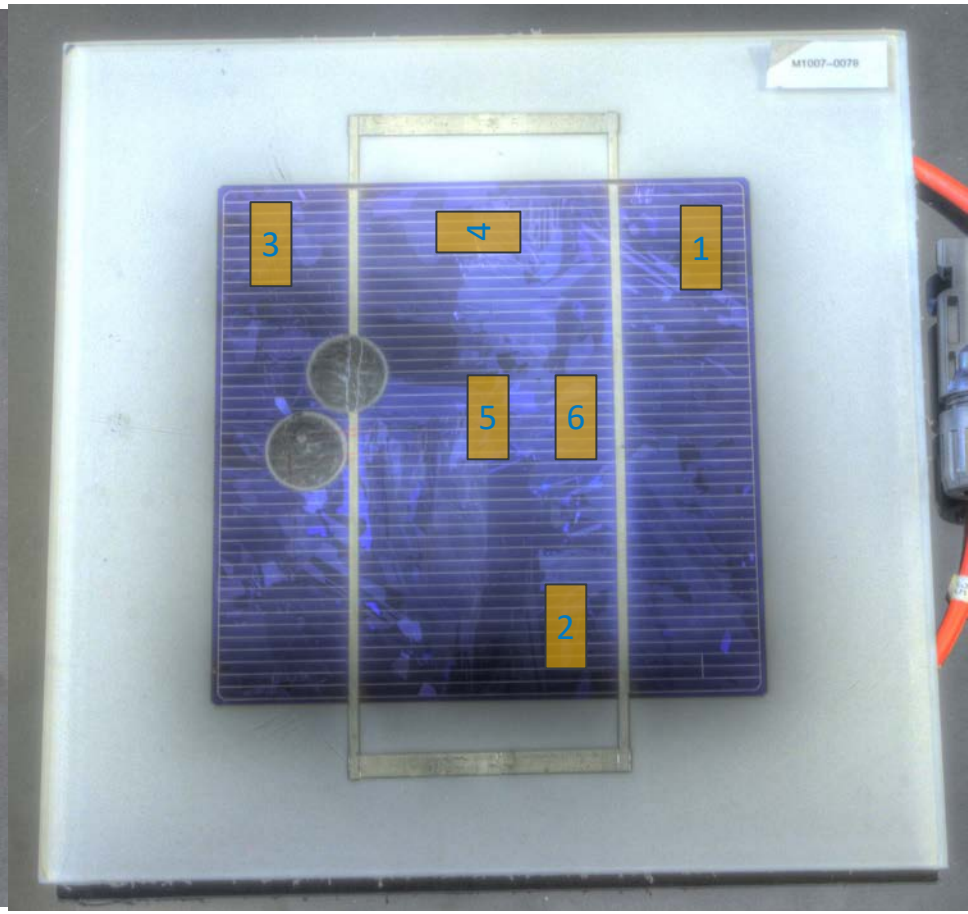

- No evidence of macro-delamination with 10x loupe. There may be micro-scale localized delamination, e.g., at gridlines. Could try to trigger delamination with TC test.

Test: M1007-0059

Unaged reference: M1007-0078

Reflectance Results for HV-/+ Samples

- Effects of AR_c discoloration (corrosion), gridline corrosion, internal haze formation (glass/encapsulant) clearly observed on HV-/+ test specimen M1007-0059.
- External glass corrosion expected for StarPhire glass after DH (from coupon experiments).
- A range of spectra-specific effects observed for test specimen: ρ increased ~600 nm + 1150 nm, ρ decreased 400 nm.

- Spectra from M1007-0059 show similarity to MiMos in HV+ experiment.
- Is it possible to verify MiMos relative to full size module from a tropical location?
- Color of AR suggests thickness of AR 60 - 80 nm (blue), with reduction to 40 to 50 nm (gray).
  -Unclear if just thickness or also composition changed.
- Encapsulant layer of BS may be discolored; no strong discoloration of encapsulant.
- Spectra at center of test sample that is similar to reference may simply be attenuated only by the haze… not corrosion of AR. TBD.

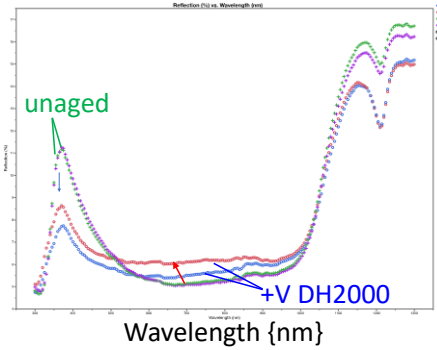

Other (HV+) MiMo specimens

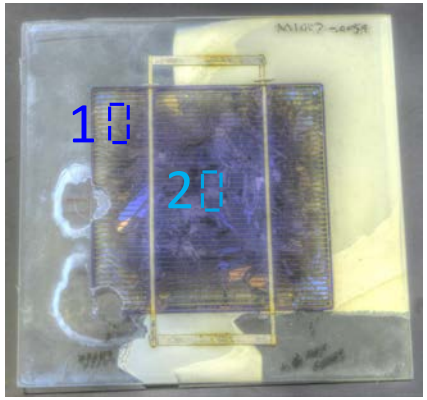

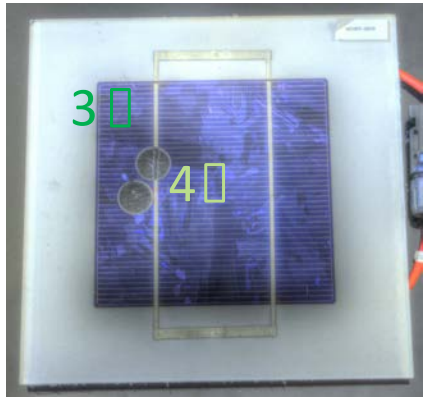

Measurement locations with approximate spot size & geometry on (left) test and (right) reference specimens.

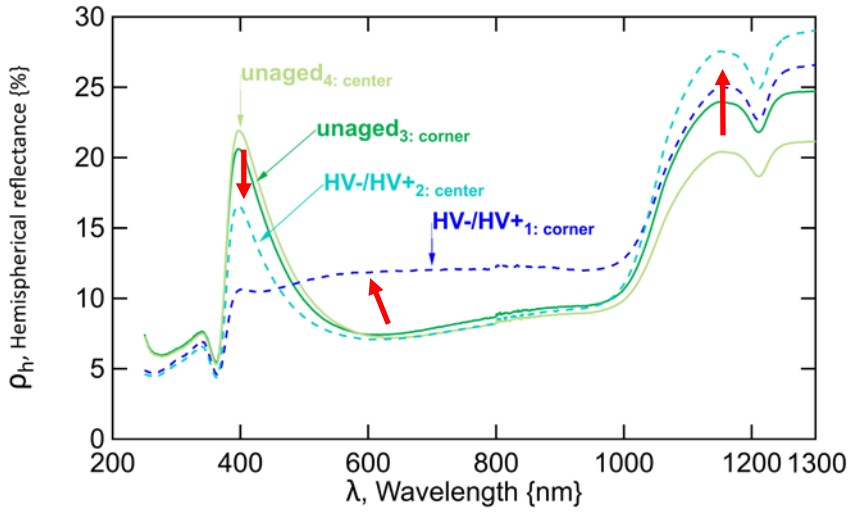

Discussion (1)

Glass corrosion:

- Optical- and electron-microscopy verified that extended DH aging (up to 8000 h) gave greater damage on Sn-poor side of float glass.
- Rolled Solite glass, which more resembles the front glass used in PV modules, was used as the example for external surface corrosion to subsequently differentiate from IHF.
- StarPhire float glass, which is more prone to glass corrosion, was instead used in the HV-/HV+ specimen.
- Degradation would be reduced perhaps similar to a PV module for the HV-/HV+ specimen if the Sn-rich surface of its StarPhire glass was conventionally made to be external facing, reducing external glass corrosion.
- Degradation, however, would be increased relative to a PV module for the HV-/HV+ specimen if its more vulnerable Sn-poor surface was internal facing, enabling IHF.
- Future: recommend to quantify degradation on MiMos/modules using same BoM before & after HV-/HV+.

Internal haze formation:

- Moisture saturation was observed for silica/encapsulant/silica coupons after DH, occurring in addition to the chemical reaction deduced from the destructive failure analysis in this study.
- While prolonged storage in a desiccator should have removed excess moisture from the sample coupons, water will be present immediately after extended DH testing of coupon or module specimens.
- An E_a was assumed to give an equivalent aging duration at 85°C/85% RH, current leakage and the rate limiting kinetics for the acid/base interaction suspected in IHF may have a different thermal activation.
- It is unclear if the internal glass corrosion thought to facilitate IHF may be activated by the voltage potential or interact with the PID occurring in a PV module.
- The use of textured glass and inability to perform transmittance measurements make it difficult to confirm and quantify IHF in a PV module.
- Future: recommend to quantify degradation on MiMos/modules using same BoM before & after HV-/HV+.

Discussion (2)

Gridline corrosion:

- Representation based on EVA discoloration, which results from absorption of light in chromophore species.
- Crystallites of corroded Ag may instead favor optical scattering, giving a different dependence with wavelength, particularly if the optical response varies with oxide crystal-size or -shape.
- Area affected by gridline corrosion (e.g., 6% of sun side), is subject to the accuracy of estimation including the optical efficacy (where the size of the attenuating region is assumed to match the visually discolored region).
- External glass corrosion, gridline corrosion, and AR_c corrosion are all heterogeneous, which may limit the accuracy of a general representation.
- Variation within a cell (greatest at corners for gridline corrosion) and within a module (proximity to a metal edge frame) will affect the effective magnitude of degradation.
- Variation between cells may further affect the electrical performance of cells in series and circuits in parallel.
- Future: verify morphology of corrosion product(s) to give greater confidence in their optical effect.
- Quantify size of the effected region as well as the variation of damage within a cell to aid optical analysis.

Antireflective coating (cell) corrosion:

- Coating thickness is estimated based on color, the integrity of the underlying Si is surmised from reflectance spectra; it remains to directly verify loss of thickness and/or change in chemistry of the Si_xN_y AR_c layer.
- Degradation mode(s) should be known to apply the appropriate model: analytic representation of a multi-layer stack or comprehensive ray tracing analysis of a thin film on a textured surface.
- F_t at the cell strongly depends on the absorptance of light through the Si_xN_y layer.
- Because of its absorptance, the corrosion of the AR_c may be the most optically significant HV-/HV+ degradation after delamination of the encapsulant interfaces.
- Future: verify degradation mode(s) to confirm the approach for more accurate optical modeling and provide essential details (e.g., layer thickness and surface texture geometry) for analysis.

Discussion (3)

Optical and PV performance:

- Relative to 6.3% loss in I_{sc}, the HV-/HV+ specimen showed a 13.5% loss in open circuit voltage and 24.7% loss in maximum power by the end of the experiment.
- Change in performance identifies that much of damage in the HV-/HV+ experiment occured at the cell, including PID and other modes affecting the PV junction.
- Relative to the 1505 h duration HV-/HV+ test, the IEC 62804-1 PID test is applied for 96 h.
- Relative to HV-/HV+ test, a wide variety of conditions occur in outdoor PV use, which may favor degradation of optical performance relative to cell degradation over years of time.
- Degradation modes in this study may occur in DH and PID accelerated testing and may be favored in hot & humid outdoor locations as well as bills of material allowing elevated leakage current.
- While the optical return and transfer are of lesser importance in the HV-/HV+ experiment, their significance remains to be determined in industry standard tests as well as through field use.

Acknowledgements

☞Thanks also to William NEMETH, Paul NDIONE (NREL), Brenor BROPHY (First Solar), and Ralf LEUTZ (Leopil)

This work was supported by the U.S. Department of Energy under Contract No. DE-AC36-08-GO28308 with the National Renewable Energy Laboratory. This material is based upon work supported by the U.S. Department of Energy's Office of Energy Efficiency and Renewable Energy (EERE) under the Solar Energy Technologies Office (SETO) office.

NREL STM campus, Dennis Schroeder

✋Your questions and feedback are much appreciated! Please help me to cover the important details & perspectives.

NREL/PR-5K00-82324